Reko Kemppainen

ECG Parameters in Short-Term Prediction of Ventricular Arrhythmias

Faculty of Information and Natural Sciences

Thesis submitted for examination for the degree of Master of Science in Technology.

Espoo, Finland 27.5.2012

Thesis supervisor:

Prof. Risto Ilmoniemi

Thesis instructor:

M.Sc. Mikko Kaski

Aalto University
School of Science
and Technology

Aalto yliopisto

diplomityön
tiivistelmä

Tekijä: Reko Kemppainen

Työn nimi: EKG-parametrien käyttö kammioperäisten rytmihäiriöiden lyhyen aikavälin ennustamisessa

Päivämäärä: 27.5.2012 Kieli: Englanti Sivumäärä:9+75

Informaatio- ja luonnontieteiden tiedekunta

Lääketieteellisen tekniikan ja laskennallisen tieteen laitos

Professuuri: Lääketieteellinen tekniikka Koodi: Tfy-99

Valvoja: Prof. Risto Ilmoniemi

Ohjaaja: FM Mikko Kaski

Malignit kammioperäiset rytmihäiriöt, kuten kammiotakykardia ja kammiovärinä, ovat yleisimpiä syitä sydänperäiseen äkkikuolemaan sekä sairaalassa että sen ulkopuolella. Sairaalassa kuten sen ulkopuolellakin tällaiset rytmihäiriöt ovat aina hengenvaarallisia ja pitkittyessään vähentynyt tai pysähtynyt hapenkuljetus elimistöön pienentää todennäköisyyttä selviytyä. Huolimatta viimeaikaisista ponnisteluista viiveettömän ja tehokkaamman elvytyksen eteen, sairaalassa tapahtuvien sydänkohtausten ennuste on pysynyt huonona. Tämä johtuu lähinnä viiveestä elvytyksen aloittamisessa ja monitoroinnin puutteesta, joten oleellisinta ennusteen parantamisen kannalta olisi jatkuva rytmihäiriöriskin kvantitatiivinen arviointi potilasmonitoroinnilla. Näin useat rytmihäiriöt voitaisiin estää ja alkaviin voitaisiin reagoida nopeammin. Nykyisin potilasmonitorointi on kuitenkin keskittynyt jo alkaneiden rytmihäiriöiden tunnistamiseen eikä ennustavia ratkaisuja ole tarjolla. Äkillistä sydänkohtausta edeltävien ilmiöiden tutkiminen ja rytmihäiriöriskin määrittäminen kajoamattomalla potilasmonitoroinnilla ovat ensisijaisen tärkeitä, mikäli rytmihäiriöpotilaiden ennustetta halutaan parantaa sairaalaympäristössä. Tässä opinnäytteessä tutkitaan rytmihäiriöitä edeltäviä muutoksia EKG-signaalista mitattavissa parametreissa eri potilasryhmissä ja yksittäisillä potilailla. Esittelemme algoritmin, joka arvioi EKG.sta mitatuista parametreista yksittäisen potilaan riskiä rytmihäiriön käynnistymiseen. Valitsemamme lähestymistapa poikkeaa täysin olemassa olevista eikä vastaavia tuloksia ole aikaisemmin julkaistu. Algoritmin kehityksessä hyödynnetään laajasti olemassa olevaa tutkimustietoa rytmihäiriöiden käynnistymisestä ja ylläpidosta. Olemassa olevat menetelmät on esitelty laajassa kirjallisuuskatsauksessa. Opinnäytetyön lopussa algoritmin kliinistä hyödyllisyyttä ja tulevia kehitysnäkymiä on arvioitu saavutettujen tulosten valossa.

Avainsanat: Elektrokardiografia (EKG), äkillinen sydänkuolema, epänormaali repolarisaatio, ennustavat algoritmit sydänmonitoroinnissa, spontaanit kammioarytmiat, T-aallon morfologia

Aalto University

abstract of the
master's thesis

Author: Reko Kemppainen

Title: ECG Parameters in Short-Term Prediction of Ventricular Arrhythmias

Date: 27.5.2012 Language: English Number of pages:9+75

Faculty of Information and Natural Sciences

Department of Biomedical Engineering and Computational Sciences

Professorship: Biomedical Engineering Code: Tfy-99

Supervisor: Prof. Risto Ilmoniemi

Instructor: M.Sc. Mikko Kaski

Malignant spontaneous ventricular arrhythmias, such as ventricular tachycardia (VT) and ventricular fibrillation (VF), are the most common trigger of sudden cardiac death (SCD) in and out of hospital. For a hospitalized patient, occurrence of such arrhythmia is a struggle of life and death where every second of oxygen deprivation, resulting from reduced blood flow, decreases chances of survival. Despite recent advances in resuscitation strategies, survival rates in in-hospital cardiac arrests remain unacceptably low. Main factors contributing to the poor prognosis are lack of patient monitoring and delay in the initiation of resuscitation. Thus, in order to increase the likelihood of successful resuscitation, or prevent the arrhythmia from happening in the first place, continuous and quantitative risk of arrhythmia assessment is required. Currently, however, cardiac monitoring is utilized to detect the onset of life threatening cardiac episodes only. Thus, development of risk indices and the study of precursors of lethal arrhythmias have great clinical value and will lead to better cardiac monitoring.

In this thesis, changes in ECG signal preceding lethal cardiac arrhythmias are studied both in different patient groups and in individual patients. Furthermore, an algorithm predicting imminent ventricular tachyarrhythmias is presented. Current knowledge of underlying mechanisms of onset of ventricular arrhythmias is used to assess the risk of arrhythmia continuously during cardiac monitoring of a patient. Our approach is novel and similar assessment of such algorithm has not been published previously. A review of existing methods and applications for risk assessment of SCD with discussion of future trends and possibilities is also given.

Keywords: Electrocardiography (ECG), In-hospital sudden cardiac death, Abnormal repolarization, Predictive monitoring, Spontaneous ventricular tachyarrhythmias, T wave morphology

Preface

This thesis was written at General Electric Healthcare Finland Oy. It is part of broader trend in GE towards more predictive non-invasive monitoring of human hemodynamics in critical care. I want to thank the company and engineering manager Jouni Erkkilä for providing me this great opportunity to work in this project. I also thank my supervisor, professor Risto Ilmoniemi, for his valuable comments.

I want to express my gratitude to my encouraging and inspiring instructor Mikko Kaski. He has given me all the freedom needed but still devoted to my thesis when I needed more guidance and someone to discuss with. Special thanks to chief hospital physicist and my current boss, Kari Tahvanainen. I would like to thank him for reading the draft and giving remarks on spelling, structure and subject matter. In addition, I want to thank cardiologist Seppo Utriainen and anesthesiologist Seppo Hovilehto for clinical perspective and discussions.

I would like to thank my mentor Anne Ahkola-Lehtinen. Numerous encounters gave me perspective and helped to see things in wider context. Finally, I would like to thank my family and friends, especially Sanna, for the support during the process and Ville, Antti and Jukka-Pekka for proofreading the text.

Lappeenranta, 27.5.2012

Reko Antti Kemppainen

Contents

Symbols and Abbreviations

Symbols

$\mathbf{A}$	Matrix
$\mathbf{a}$	Column vector
a	Scalar
$\mathbf{A}^T$	Matrix transpose
$\mathbf{A}^{-1}$	Matrix inverse
$\mathbf{A}^\dagger$	Moore-Penrose pseudoinverse
$\|\|\mathbf{a}\|\|_2$	Euclidean norm of a vector

Abbreviations

ANS	Autonomic nervous system
AMI	Acute myocardial infarction
AP	Angina pectoris
APD	Action potential duration
AV	Atrioventricular
ASY	Asystole
CA	Cardiopulmonary arrest
CAD	Coronary artery disease
CCU	Coronary care unit
CNS	Central nervous system
CV	Conduction velocity
DCM	Dilated cardiomyopathy
FER	Fitting error ratio
HCM	Hypertrophic cardiomyopathy
HF	Heart failure
HTR	Heart rate turbulence
HRV	Heart rate variability
ICD	Implantable cardioverter defibrillator
ICU	Intensive care unit
IHCA	In-hospital cardiopulmonary arrest
LTCA	Life threatening cardiac arrhythmia
NPV	Negative predictive value
OLC	Optimal linear combination
OR	Operating room
PPV	Positive predictive value
PVC	Premature ventricular complex
SA	Sinoatrial
SCD	Sudden cardiac death
TDP	Torsade-de-pointes
TWA	T wave alternans
VF	Ventricular fibrillation
VT	Ventricular tachycardia
VTA	Ventricular tachyarrhythmia
WCD	Wearable cardioverter defibrillator

1 Introduction

Sudden cardiac death (SCD), i.e. death caused by abrupt failure of heart for some reason, is a major cause of death in the industrialised western world. Malignant spontaneous ventricular tachyarrhythmias (VTAs), such as ventricular tachycardia (VT) and ventricular fibrillation (VF), are assumed to be the most common triggers of sudden cardiac death [22]. In clinical setting, e.g. coronary care unit (CCU) or intensive care unit (ICU), with electrocardiography (ECG) monitoring such arrhythmias are diagnosed almost instantaneously and immediate actions are taken to prevent arrhythmia from causing any further damage or SCD. In many cases, however, preventive actions could be performed to prevent arrhythmia from occurring if quantitative measure of risk of arrhythmia was available before the onset of arrhythmia [69].

There are multiple scenarios in which short-term prediction could be a valuable tool. For the hospitalized patients, identification of imminent arrhythmia could lead to introduction of prophylactic techniques such as antiarrhythmic drugs and prediction of a VTA would increase alertness of the staff decreasing the delay of care and enabling administration of preventive medication. Decreased delay in the initiation of cardiopulmonary resuscitation (CPR) could make a dramatic difference in the likelihood of survival for these patients [59, 75].

A major unanswered question in SCD is what is the immediate precipitating event that causes the SCD at a specific time in an otherwise stable patient. Understanding the trigger acting on the receptive substrate, which most likely may be different in different patients and may involve very small changes in conduction, refractoriness, and the like, is a major goal of SCD research [76]. Especially, multiple changes in repolarization characteristics of the heart can be associated with risk of ventricular arrhythmia and it is believed that changes in repolarization are the key in short-term prediction of arrhythmias (see e.g. [72, 45, 38, 66, 65]). In this thesis ECG parameters related to repolarization and their variability are studied, and their usefulness in prediction of VTAs is discussed in detail.

Numerous recent studies have tried to identify parameters that change before an imminent VTA episode with contradictory results. The focus in these studies has been in trends averaged over all arrhythmia patients and little attention has been paid to what happens before an event in individual patients. Thus, we introduce a completely novel idea of predicting VTA episodes based on detection of specific fast changes that are supposed to reflect changes in the cardiac state of a patient. In order to quantitatively evaluate the usefulness of different ECG parameters in VTA prediction, an algorithm predicting imminent episodes is developed. The algorithm is tested and predictive performance is assessed by using a data set of 61 patients (37 controls, 14 sustaine arrhythmias and 9 non-sustained). The database was recorded at a coronary care unit (CCU). The database is divided into training and validation sets in order to learn predictors of VTAs and confirm their usefulness. Based on our results, it seems that predictive algorithm that achieves clinically useful sensitivity and specificity could be achievable using parameters extracted from an ECG signal.

2 Background

The heart is an essential part of the human cardiovascular system providing all the mechanical energy needed for the circulation. Should the heart fail in its vital task, it would have fatal consequences. The failure can happen, for example, as a consequence of malignant ventricular arrhythmias. Continuous evaluation of performance and condition of the heart is essential in clinical monitoring, e.g., in intensive care unit (ICU) or coronary care unit (CCU). Among all the available methods for cardiac monitoring, electrocardiography (ECG) is the most widely used due to its relative ease of recording and analysing in a non-invasive manner.

In this chapter a short description of the heart and ECG are given. In addition, phenomena underlying heart failure are discussed to justify the selection of parameters, measuring risk of SCD explained in the next chapter.

2.1 Electrophysiology and the Heart

ECG is a non-invasive measure of electrical potential at the surface of the body. Essentially, it measures the potential difference between pairs of points on the body as a function of time. The potential is generated by the myocardial cells in the heart. To understand ECG one has to understand the depolarization and repolarization cycle of a single cell, how the electrical activity is propagated and how synchronous activity of all the cells in the heart produce measurable potential at the surface of the body (i.e. forward model of ECG).

2.1.1 Heart and Cardiovascular System

The heart is located in the mediastinum, a mass of tissue that extends from the sternum to the vertebral column between the lungs. It is surrounded by supportive and protective membrane called pericardium. Pericardium is separated from the outermost layer of the heart, epicardium, by the pericardial cavity containing liquid that reduces friction as the heart beats. Majority of the heart's mass is comprised of the myocardium (i.e cardiac muscle), that is responsible for the pumping action. The myocardium is bounded by connective epi- and endocardium tissue layers that are the outer and inner surfaces of the heart, respectively.

The heart has four chambers, two atria and two ventricles. Oxygenated blood circulates from the lungs to the left atrium and through the mitral valve to the left ventricle. The left ventricle ejects blood into the aorta. From the aorta, blood is delivered to all organs throughout the body via arteries (except for the alveoli of the lungs). Deoxygenated blood returns to the right atrium through the superior and inferior vena cava and passes through the tricuspid valve to the right ventricle. Then, blood passes through the pulmonary valve into the pulmonary trunk and back to the lungs. The two atria are separated by the interatrial septum and the ventricles by interventricular septum. In addition to cardiac muscle tissue, the heart

wall includes a dense connective tissue that forms the fibrous skeleton of the heart. The fiborous skeleton acts as an insulator between the atria and ventricles and forms a structural foundation for the heart valves. The myocardium has its own network of blood vessels, coronary circulation, that ensures nutrition and oxygen delivery to the pumping heart muscle. See Fig. 1 for the illustration of the anatomy and conduction system of the heart. [77]

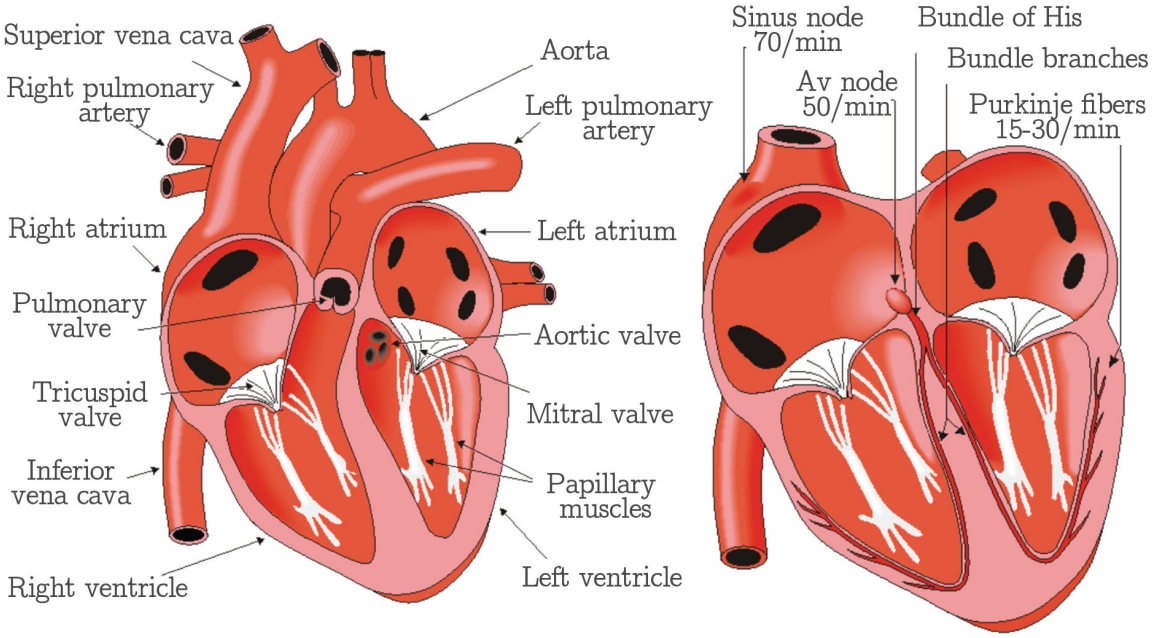

Figure 1: ***Left:*** *The anatomy of the heart.* ***Right:*** *The conduction system of the heart and intrinsic excitation rates in different regions along the conduction system. [39]*

2.1.2 Electrophysiology of the Myocardial Cells

At rest, non-automatic myocardial cells have stable negative membrane potential. For myocardial cells, cytosol is negatively charged with respect to the extracellular fluid so that the resting membrane potential is about -90 mV. The negative potential is established and maintained by an active, i.e. energy consuming, exchange of ions across the cell membrane in the direction of the concentration gradient. Ions responsible for the resting membrane potential are sodium (Na^+) and potassium (K^+). At rest sodium concentration is substantially greater outside of the cell than in cytosol. The opposite applies for the potassium concentration. [30]

Action potential is a short-lasting event during which the electrical membrane potential of a cell rapidly rises and falls. The action potential of non pacemaking

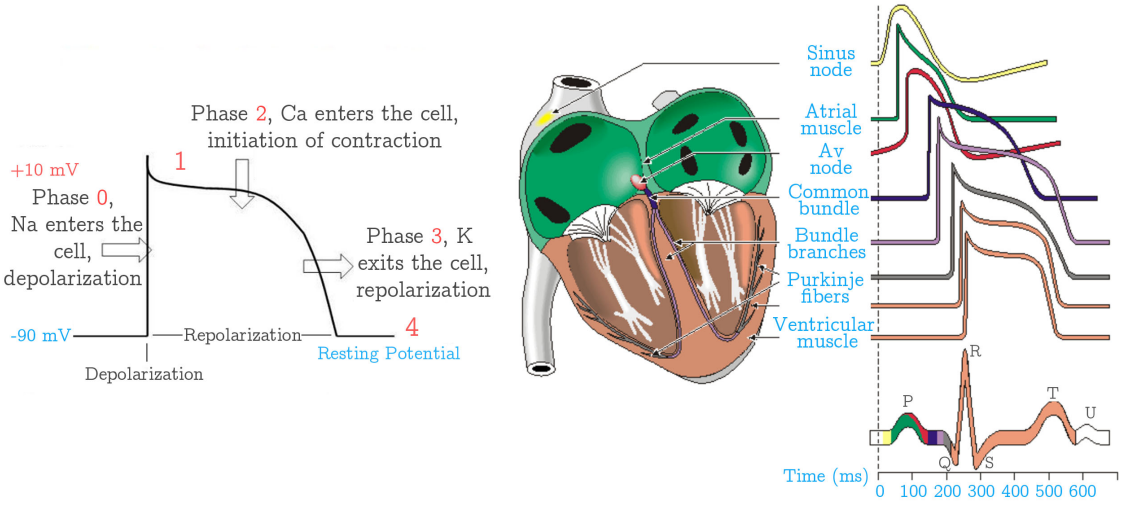

Figure 2: ***Left:*** *Five phases of cardiac action potential.* ***Right:*** *The propagation of the action potential. The shape of the action potential in individual cells has distinct characteristics in different regions of the heart.*

myocardial cells has five distinct phases (see Fig. 2). When the membrane potential is increased due to changes in the membrane potential of neighbouring cells, the cell reaches a threshold level of approximately -65 mV which opens fast Na^+ channels. The influx of positive Na^+-ions is driven by an electro-chemical gradient which depolarizes the cell rapidly ($\approx$ 1-2 ms) to approximately +20 mV. The fast depolarization, phase 0, is immediately followed by a rapid repolarization, phase 1. The rapid repolarization is caused by the inactivation of Na^+ channels and increased permeability for K^+-ions. The outflow of positively charged potassium repolarizes the cell. This outflow, however, is active only for a very short period of time and the cell remains polarized at the end of phase 1.

The third step (phase 2) is called the action potential plateau. The two dominant currents are the inward calcium current and the delayed rectifier potassium outward current. The changes in membrane potential depend on the balance between inward and outward currents and varies as a function of location in the myocardium. Inactivation of the calcium channels leads to the end of the plateau. Since outflow of positive potassium-ions dominates, the cell repolarizes rapidly to the resting potential (phase 3). At rest, phase 4, the cell membrane is permeable only to potassium, thus the inward rectifier potassium current is largely responsible for setting the resting membrane potential.

Following the phase 0, there is a parallel set of cellular and molecular processes called excitation-contraction coupling which links electrical functionality of a cardiac cell to mechanic contraction. The triggering mechanism in this coupling is the inflow of calcium (Ca^{2+}), which in turn unlocks the contraction mechanism of the cell

(through a conformational change of the troponin protein complex) [10].

2.1.3 Propagation of the Action Potential

Once an action potential is initiated, it will propagate along the cell membrane until the entire cell is depolarized. Furthermore, myocardial cells have unique property of transmitting action potentials from cell to cell by means of direct electrical coupling, called gap junction. These intercellular low-resistance connections allow direct and fast change of ions between neighbouring cells. Thus, an impulse originating anywhere in the myocardium will propagate throughout the heart, resulting in a coordinated mechanical contraction.

A small portion of the cardiac cells make up a conduction system that is specialized on fast transmission of electrical impulses. Efficient and coordinated pumping of the myocardial muscle tissue is enabled by this specific conduction system that allows fast propagation of electric impulse and coordinated contraction of the muscles. These cells are autorhythmic and depolarize repeatedly and independently at cell specific rate. Since the cells in the sinoatrial (SA) node, located in the right atrium, possesses the fastest intrinsic rate of depolarization, each normal (sinus) beat is initiated there. Also, the SA node, His bundle and Purkinje fiber network contain pacemaker cells. However, the SA node remains the dominant pacer due to fastest intrinsic excitation frequency and phenomena called overdrive suppression [40].

From the SA node, the activation propagates through the atria along atrial muscle fibers and reaches the atrioventricular (AV) node. The AV node is located between atria and ventricles and is the only location through which an action potential enters the ventricles in a structurally normal heart. From the AV node the action potential enters the bundle of His. From there the propagating action potential is conducted through the right and left bundle branches to the Purkinje fibers that rapidly conduct the action potential to the ventricular myocardium. Depolarization of the myocardial muscle cells is followed by a coordinated contraction leading to efficient pumping of blood. After approximately 0.3 seconds from the depolarization, cells repolarize and return to the resting state.

2.1.4 Electrocardiography

As a result of the electrical activity of the heart, measurable potential difference is established on the surface of the torso. An action potential propagating through a single cell makes intracellular fluid positively charged for the depolarized part of the cell while rest of the cell remains negatively charged. The distribution and movement of charged particles in the cell makes up a macroscopic (current) dipole. Furthermore, since action potential spreads in the myocardium as a continuous wave boundary [30], the surface corresponding to the boundary between depolarized and polarized tissue may be represented by a layer of dipoles (see Figure 3). The vector sum of these microscopic dipoles is called the heart vector and is an important

concept in ECG analysis and interpretation.

At cell level, repolarization gives rise to a microscopic dipole with opposite polarity compared to depolarization. Similarly to depolarization, repolarization can be thought to make up a dynamic dipole layer. However, for repolarization, it is not as straightforward because it is not a conduction phenomena. Since repolarization is of special interest in this thesis, more detailed discussion is given below.

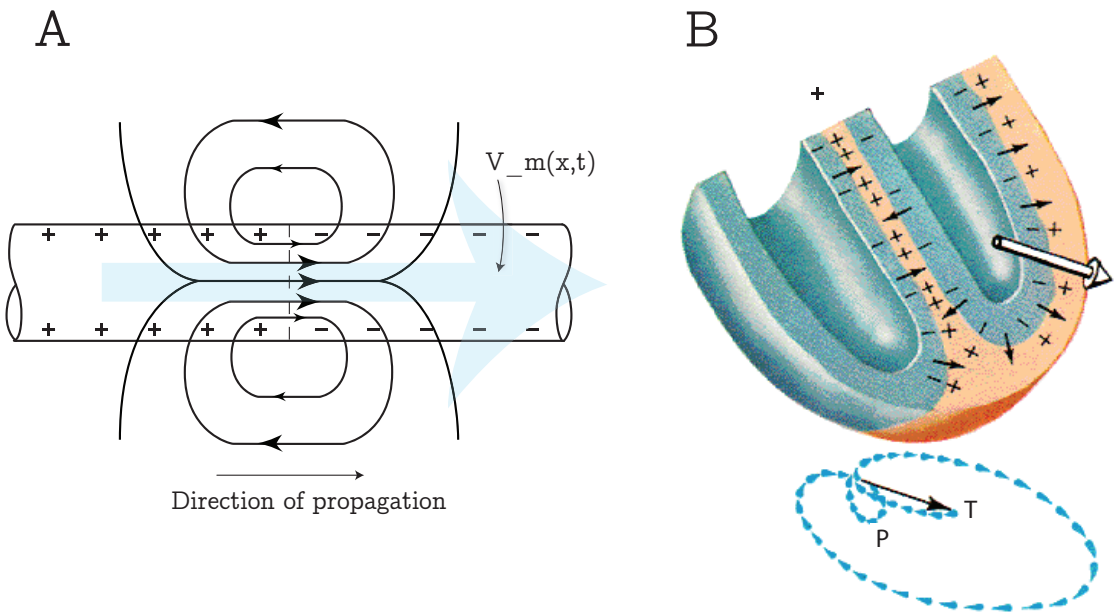

Figure 3: ***Left:*** *Propagating action potential is a dipole.* ***Right:*** *Propagating action potential in the heart can be modelled as a layer of current dipoles.*

For a known current and charge distribution, geometry and conduction values of the torso, potential at surface of the torso can be calculated by Maxwell's equations [39]. In practise, however, certain approximation are usually made. Usually, the torso is approximated as linear, isotropic and homogeneous conductor and quasi-static approximation is supposed to hold for the Maxwell's equations. With these simplifying assumptions the potential at the surface of the torso is given by the Laplace's equation [39].

The normal electrocardiogram (Fig. 4 and 5), is a signal generated by a normal heart without any conduction abnormalities or defects. The first observable oscillation in ECG signal (the P wave) is a result of atrial depolarization. The P wave is followed by an isoelectric period caused by a delay at the AV node. As the wave of depolarization spreads to the septum, a small deflection may be seen (the Q wave) when the polarization wave propagates from left to right between the ventricles. Subsequently, the wave of polarization spreads to the ventricles. The ventricles polarize from endo- to epicardium. During the ventricular depolarization, the direction of the heart vector is dominated by the left ventricle due to its bigger size compared to the right ventricle. The depolarization of the left ventricle causes

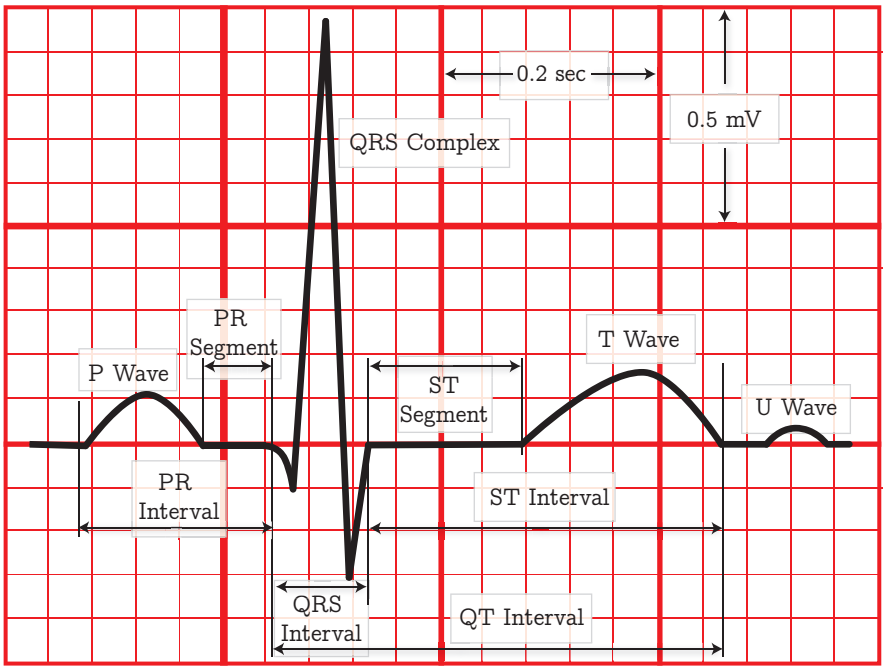

Figure 4: *Intervals and wave names of the normal ECG.*

greatest deflection in ECG signal (the R and S waves). Ventricular depolarization is followed by an isoelectric period, called ST segment, which results from the long plateau period of the myocardial cells. Finally, the individual cells start to repolarize and another wave of charge passes through the heart. Normally, it appears as if repolarization waves were propagating from epi- to endocardium with reversed polarity compared to depolarization phase [39]. As a result, repolarization waves (the T wave) on the ECG usually have the same polarity as depolarization waves. Additionally, the U wave may appear after the T wave. Currently, it is known that the U wave is a mechanoelectric phenomena but all the details underlying the U wave are not known [54].

2.1.5 Ventricular Repolarization and T wave Morphology

The shape of the T wave is determined by the excitation sequence and the distribution of action potential duration (APD) in the myocardium. It is highly susceptible to all kinds of influences, both cardiac and non cardiac (e.g. hormonal, neurologic), and is therefore highly variable in its appearance [13]. In clinical practise, investiga-

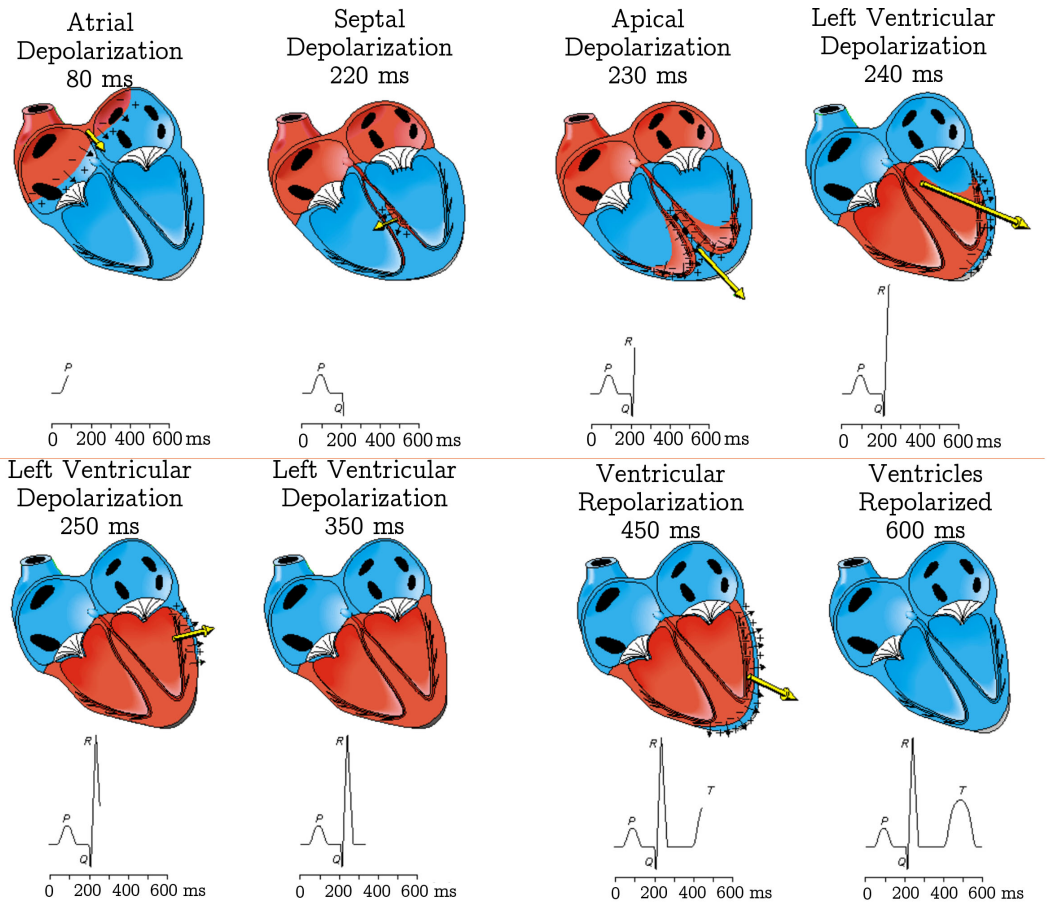

Figure 5: *The relation of normal ECG signal to the heart cycle. [39]*

tion of the normalcy of repolarization is an important diagnostic tool. It is used, for example, to diagnose ischemic heart disease and myocardial infarction [23]. Lately, the idea that proarrhythmic changes in the cardiac cells are seen on the T wave of ECG has gained increased interest among researchers (see e.g. [81, 83]). This intriguing idea is also under investigation in this thesis.

If all the cells in the heart had identical action potential the wave of repolarization would just follow the wave of depolarization. However, this is not the case. Unlike depolarization, repolarization is not a propagating phenomenon. Instead, repolarization occurs in each cell after the plateau phase, the duration of which is not homogenous throughout the myocardium and is not necessarily the same in neighbouring cells. Of course, the myocardial cells located in the same area are likely to have approximately similar repolarization characteristics. As a consequence, it may seem that repolarization propagates from cell to cell like depolarization. [39]

In a healthy heart, measurable repolarization signal can be approximated to arise from a propagating dipole layer with reversed polarity compared to depolarization. However, with certain pathologies, the cell level properties of repolarization may be altered locally resulting to discontinuous "wave propagation". The local changes are

also seen on surface ECG since the T wave morphology is believed to be determined by the differences in the action potential morphology and synchronization in different anatomical regions of the ventricles. [39]

Phenomena underlying the changes in the morphology of the T wave may be categorized as primary and secondary repolarization abnormalities [54]. Abnormalities in the ST segment and T wave, which are the result of changes in the shape and/or duration of the repolarization phases of the transmembrane action potential and occur in the absence of changes in depolarization, are called the primary repolarization abnormalities. Conversely, abnormalities in the ST segment and T wave that occur as a direct result of changes in the sequence and/or duration of ventricular depolarization, manifested electrocardiographically as changes in QRS complex shape and/or duration, are referred to as the secondary repolarization abnormalities. In other words, the secondary changes do not require changes in the shape or duration of phases 2 and 3 of ventricular action potential of individual cells but primary changes do. If an investigator is interested to track the changes of action potentials of the cells, like in this thesis, distinction between the two types of abnormalities is essential.

Primary changes may be localized or diffuse and may be caused by variety of events which may be arrhythmogenic. These include ischemia, myocarditis, drugs, toxins, and electrolyte abnormalities, particularly abnormalities of serum calcium and potassium concentration. In addition, an abrupt change in heart rate, sympathetic stimulation and change in the body position can also cause primary repolarization abnormalities. Secondary repolarization abnormalities appear when changes in depolarization sequence alter the repolarization sequence. Conduction blocks, such as left and right bundle-branch block (LBBB and RBBB), premature ventricular contraction (PVC), and paced ventricular complexes are examples of secondary repolarization abnormalities. [54]

As heart rate changes, both primary and secondary repolarization abnormalities take place. Increased heart rate shortens action potential duration (APD) and repolarization time of individual cells (primary). Additionally, conduction properties change as a function of heart rate, which results to secondary repolarization changes [13]. Conditions causing the primary changes can also affect conduction properties and change the depolarization properties. Thus, the two repolarization alterations are commonly seen concurrently and cannot always be separated. Consequently, one can classify a repolarization change to be primary with any certainty only in the complete absence of depolarization changes.

2.1.6 Measurement of ECG

The electrocardiogram is a measure of the potential difference between electrodes attached to the surface of the body. In principle, the potential is measurable from arbitrary body positions. However, to standardise the measurement, only certain lead configurations are used. The most common measurement configuration is the

12-lead ECG system (or subset of it), which is also used to obtain the data in this thesis. Other commonly used lead configurations, such as, the vectocardiographic lead system and more complicated system are not used nor described in this thesis. For more detailed information of alternative ECG lead systems, see e.g. [39] and [23].

The first clinically important ECG measuring system was used in 1908 by Einthoven [39]. The Einthoven limb leads are still part of the modern 12-lead ECG system. They are defined as potential differences between arms and left foot. In particular, lead I is the difference between left and right arms, lead II is the difference between left foot and right arm and, finally, lead III is the difference between left foot and left arm, see Fig. 6. The three limb leads are used to define the so-called Wilson central terminal. The Wilson central terminal is formed by connecting a resistor from each terminal of the limb leads to a common point. The potential differences between the central terminal and body extremities are used to get more signals. The so-called augmented leads aVL, aVF and aVR are formed by linear combinations of potentials at the body extremities. Furthermore, six electrodes are placed around the torso in the horizontal plane. The precordial leads, V1-V6, are potential differences between the chest leads and the central terminal, see Fig. 6. Note that there are only 8 independent signals in the standard 12-lead system since only two of the leads I- III are independent and the augmented leads are fully redundant with respect to the limb leads. [39]

To understand the link between the heart vector, resulting from the cell level cardiac activity, and surface potential (i.e. ECG) the following simplifications are usually made: the source is thought to be purely dipolar, the body is approximated as a linear, isotropic, homogenous, and spherical conductor. The source is modelled as a slowly time-varying single current dipole located at the center of the spherical conductor. In addition, the quasi-static approximation to Maxwell's equations is assumed to hold. Thus, the static electric field, current density, and electric potential everywhere are non-dynamically related to the heart vector. In this simplified forward model, it can be shown that signals in the leads are projections of the heart vector to predefined angles (see Fig. 7). [10, 39]

2.1.7 Autonomic Nervous System – The Role of Regulation

Without any external influences the SA node would initiate a heart beat about 100 times per minute. However, the consumption of oxygen and nutrients vary as function of activity of the body and cardiac output must be regulated accordingly. The most important regulator of the heart is the autonomic nervous system (ANS) via signalling transmitter molecules and chemical modulation via hormones. Several experimental and clinical observations support the observation that the ANS and the neurohuomoral signalling have a role in the genesis of fatal cardiac arrhythmias [37].

The center of cardiac modulation is located in the medulla oblongata in the brain

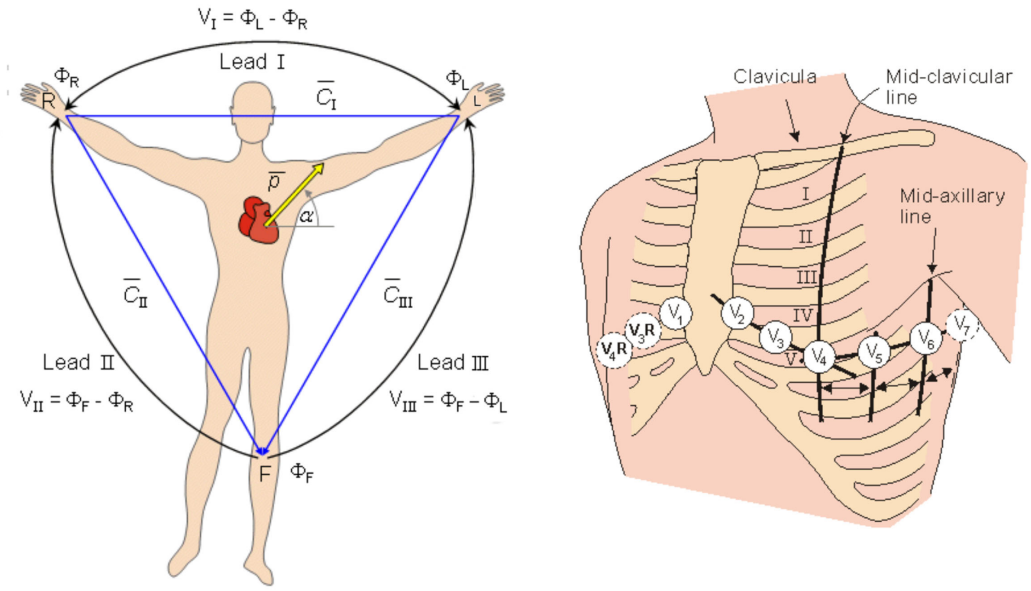

Figure 6: ***Left:*** *The positions of the limb leads.* ***Right:*** *The positions of the precordial leads. [39]*

stem and the hypothalamus. The cardiovascular center receives afferent connections from a variety of sensory receptors, such as chemoreseptors and baroreceptors, and from higher brain areas and has efferent neuronal connections to various parts of the heart (see Figure 8). The innervation can be divided into the sympathetic and the parasympathetic branches which are the two compelling components of the ANS. [77]

The sympathetic efferent neurons innervate the SA node, AV node and the most part of the myocardium (see Fig. 8). Activation of these neurons releases norepinephrine which increases the firing rate of the SA node, increases the propagation speed of the depolarization wavefront through the AV node and increases the strength of contraction in the atria and ventricles. The sympathetic neurons innervate the adrenal gland, which releases adrenaline in blood. Parasympathetic nervous system modulates the heart via the vagus nerve. It innervates the SA and AV nodes and, when activated, releases acetylcholine. Conversely to the sympathetic branch, the parasympathetic nerve impulses decrease the firing rate of the SA node and decrease action potential propagation through the AV node. The two branches of cardiac ANS operate at different time-scales – parasympathetic changes take effect in orders of a few seconds, while for the sympathetic branch it takes up to 15 seconds to accelerate the cardiac functions. [77]

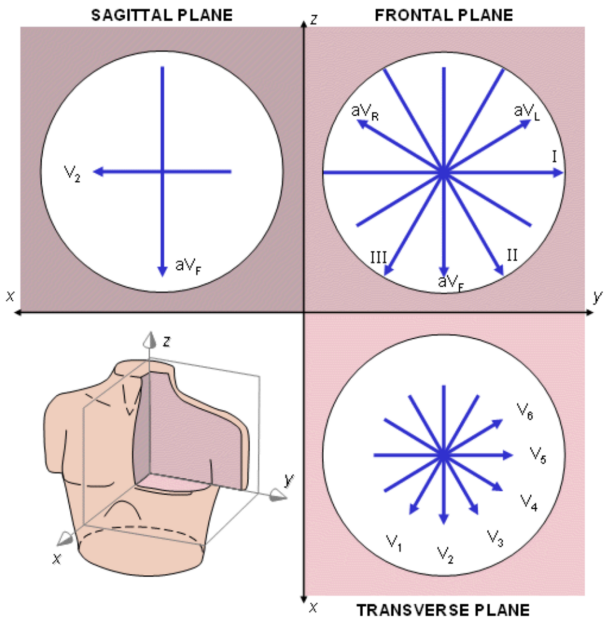

Figure 7: ***Left:*** *Projection angles of frontal plane limb leads.* ***Right:*** *Projection angles of transverse plane. [39]*

2.2 Ventricular Arrhythmias and Sudden Cardiac Death

Cardiovascular diseases are the single most common cause of natural death in the developed nations. SCD is estimated to account for approximately 50 percent of these deaths. Due to the enormous and incalculable socioeconomic burden [70], researchers' efforts to uncover the underlying mechanisms, identify the people who are at high risk, and develop methods to decrease the incidence of SCD have been substantial. In the context of this thesis, only the onset and the last 48-24 hours before SCD is under investigation.

Ventricular arrhythmias are thought to be the most common primary cause of SCD. The onset and maintenance mechanisms of these arrhythmias are well studied but poorly understood processes. It is known, that ventricular arrhythmias hardly ever occur in a healthy heart. In majority of the cases an underlying cardiac disease can be found, which causes a heart failure (HF), i.e. a medical condition defined as inability of the heart to supply sufficient blood flow to meet the body's needs. Various cardiac diseases, however, change the cardiac function differently. [76, 25, 56, 58]

2.2.1 Time Scale and Risk of Sudden Cardiac Death

For majority of the SCD occurrences, death is the first and last manifestation of the underlying cardiac illness. However, this does not mean that the illness itself

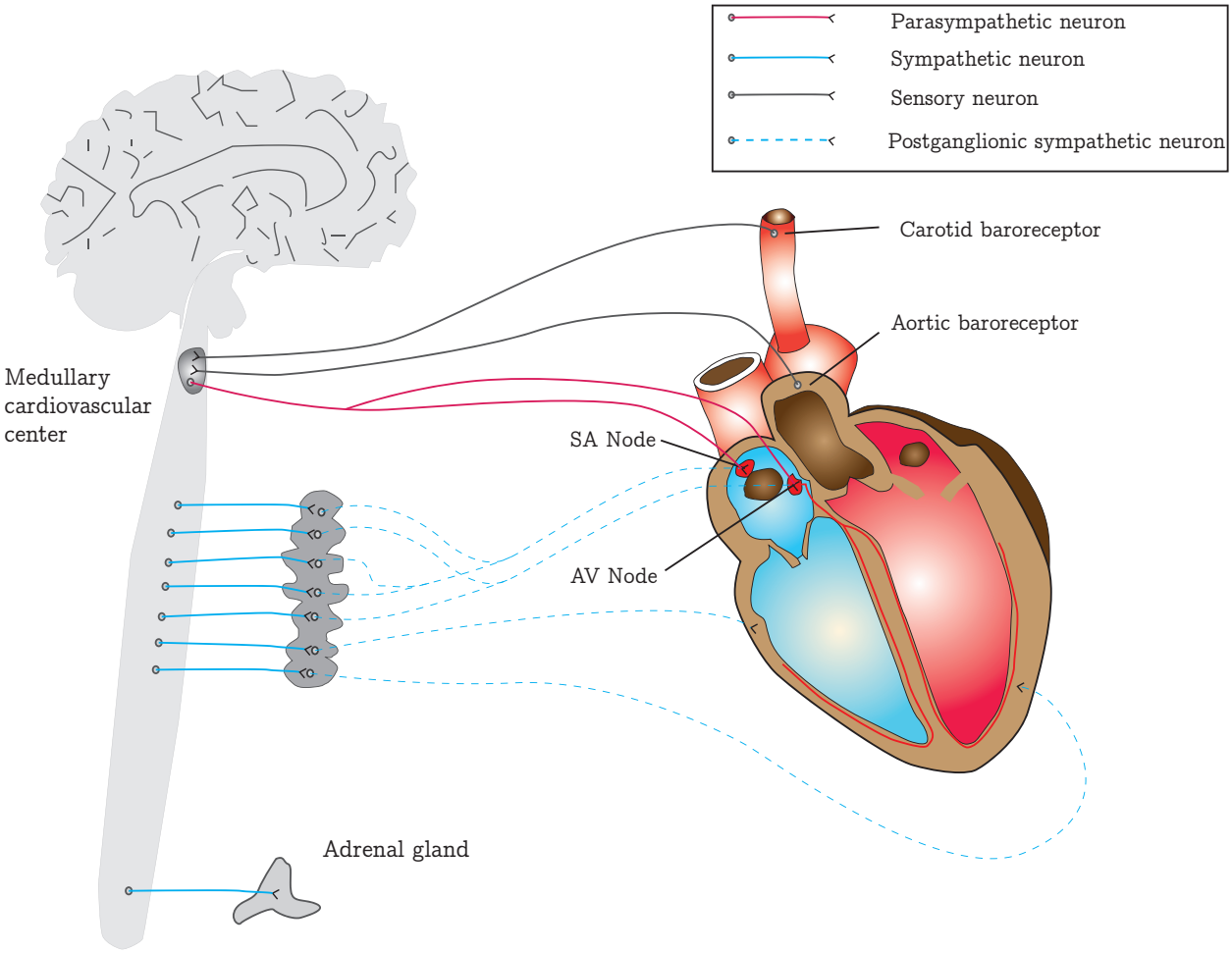

Figure 8: *The center of cardiac modulation receives afferent connections from various sensory receptors and from higher brain areas. The parasympathetic and sympathetic branches innervate the SA node, AV node and myocardium enabling the control of cardiac output.*

develops rapidly. On the contrary, it may take years or decades for the disease to advance with complex processes where the way of life and genome have an important role [22].

Only 5 – 10 % of the SCD can not be explained to be caused by a disease. Thus, for approximately 90 –95 %, a cardiac disease, such as coronary disease, infarct or cardiomyopathy, and its effect on the cardiovascular system are said to make up a substrate for the SCD. The risk of SCD is increased by the substrate but to destabilize the heart the cardiac state must be altered by some "exposing factor". These factors affect usually in the time-scale of days to hours and include e.g. transient ischaemia, electrolyte disturbances, neurocardiovascular influences, and hemodynamic fluctuations. Particularly, acute myocardial ischemia is considered to be the most common factor triggering fatal arrhythmias [25]. In addition, sometimes a

triggering event, such as premature ventricular contractions (PVCs), are present which onsets a malignant cardiac event such as an arrhythmia. The division to these different time-scales and corresponding agents is illustrated in Fig. 9. [22]

In this viewpoint spontaneous occurrence of ventricular tachyarrhythmia VTA may be regarded as a stochastic event that arises from complex interactions between relatively fixed anatomic and functional substrates and transient triggering event. In this thesis proarrhythmic factors that alter the cardiac state minutes to hours before arrhythmias are investigated. Some of these are discussed with details below in section 2.2.6.

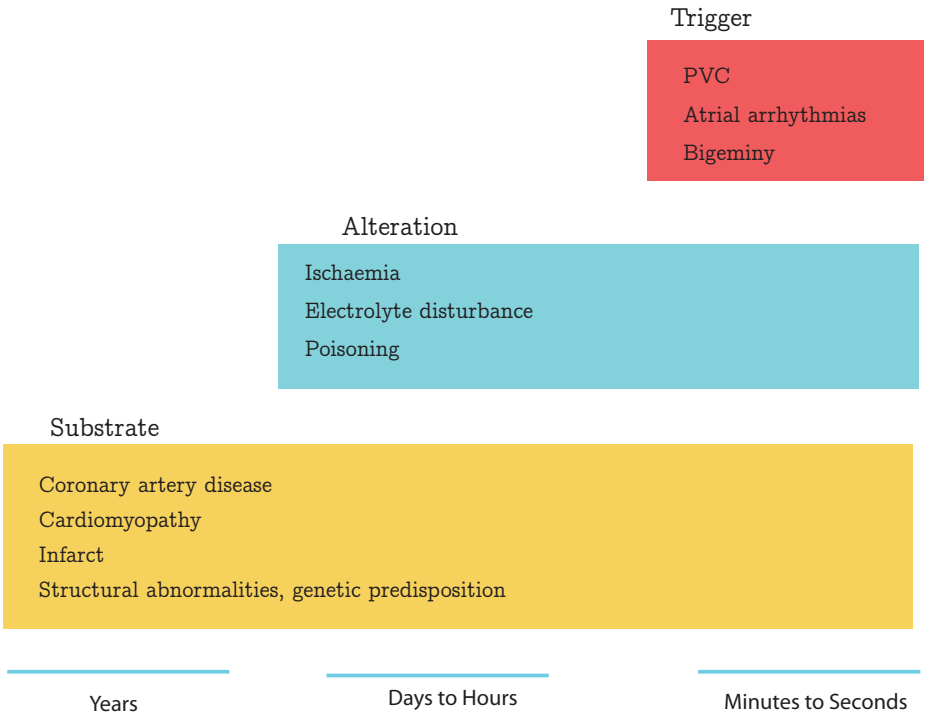

Figure 9: Three levels of assessing the of risk of sudden cardiac death with different time scales.

2.2.2 SCD in General and Specific Populations

The most important unanswered question in the study of SCD is: who is prone to it. Effective measures of increased risk of SCD have been found for specific patient populations but not for general population [22, 70]. The problem is that majority of the SCDs occur among patients who do not have any symptoms before the occurrence. In this general population, incidence of SCD is only about 1/1000 per year [25]. Thus, it is almost impossible to identify high-risk cases from this population where death is the first and last manifestation of the underlying cardiac illness. See Fig. 10 for illustration and more details.

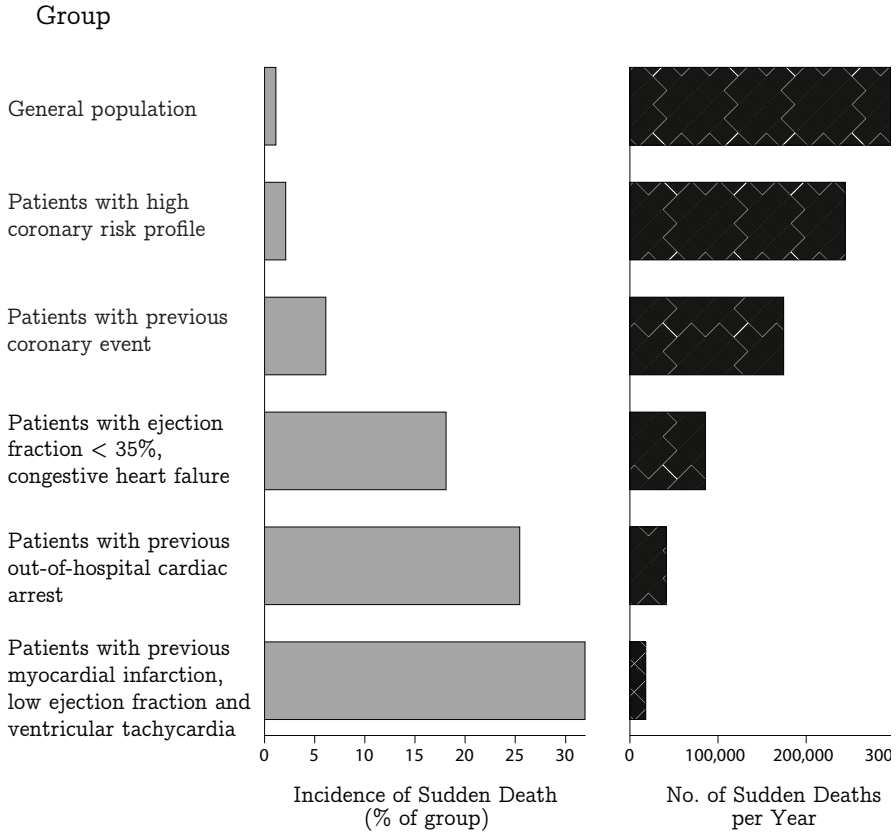

Figure 10: *The incidence of SCD in specific populations and annual numbers of sudden deaths in these populations. [25]*

2.2.3 Classification of Ventricular Arrhythmias

Cardiac arrhythmias exist in various forms and underlying mechanisms. Some of them may be relatively harmless, like atrial and junctional arrhythmias, whereas others, such as ventricular fibrillation, are life threatening [22]. In this thesis, we are only interested on malignant arrhythmias that are caused by short-term time varying changes in the cardiac state. These include ventricular tachycardia (VT), ventricular fibrillation (VF) and asystole (ASY).

In ventricular arrhythmias the electrical activation does not originate from the AV node and/or does not propagate in the ventricles the normal way. If a single beat originates from ventricles prematurely early during a sinus rhythm it is called a premature ventricular contraction (PVC). PVCs usually have wider QRS complexes due to abnormal conduction. If PVC and supraventricular (i.e. SA node triggered) beats alternate so that every other is of ventricular origin the rhythm is called bigeminy. [9]

Figure 11: *Examples of ventricular arrhythmias. A: Premature ventricular contraction (PVC). B: Ventricular tachycardia (VT). C: Ventricular fibrillation (VF).*

Ventricular tachycardia (VT) is a fast rhythm of more than 3 consecutive beats originating from the ventricles at rate more than 100 beats per minute [9]. VT that lasts longer than 30 seconds is called sustained. Furthermore, monomorphic VT has only one repeating QRS morphology, whereas polymorphic VT exist with multiple morphologies and beat origins. Torsade-de-pointes (TDP) is a special form of VT which is characterized by irregular rates of 200-250/min with marked variability in amplitude and direction of the QRS wave that seems to twist around the isoelectric baseline. TDP is closely related to prolonged QT interval [22]. Ventricular fibrillation (VF) is a rhythm characterized by chaotic activation of ventricles. The ECG signal recorded during a VF is typically undulation without identifiable QRS complexes. VF causes immediate cessation of blood circulation and degenerates further into pulseless electrical activity or asystole, a flat ECG indicating no cardiac electrical activity. See Fig. 11 for illustration of different rhythms.

2.2.4 Mechanisms of Ventricular Arrhythmias

The ultimate cause of ventricular arrhythmias is a critical alteration in the electrical properties of the myocytes. The four known arrhythmogenic mechanisms are altered automaticity, triggered activity, sodium dependent reentry, and calcium dependent reentry [40]. These mechanisms are illustrated in Fig. 12.

Altered abnormal automaticity is caused by altered phase 4 depolarization. This kind of automaticity is a property of all pathologically depressed myocardial cells making them to act as pacemakers. Consequently, abnormal automaticity may trigger an action potential virtually anywhere in the heart. Altered automaticity causes, for example PVCs and both junctional and ventricular tachycardias. Note, that automaticity that causes ventricular escape beats (i.e. normal automaticity), for example, is a normal property of cardiac cells of the conduction system. [40, 9]

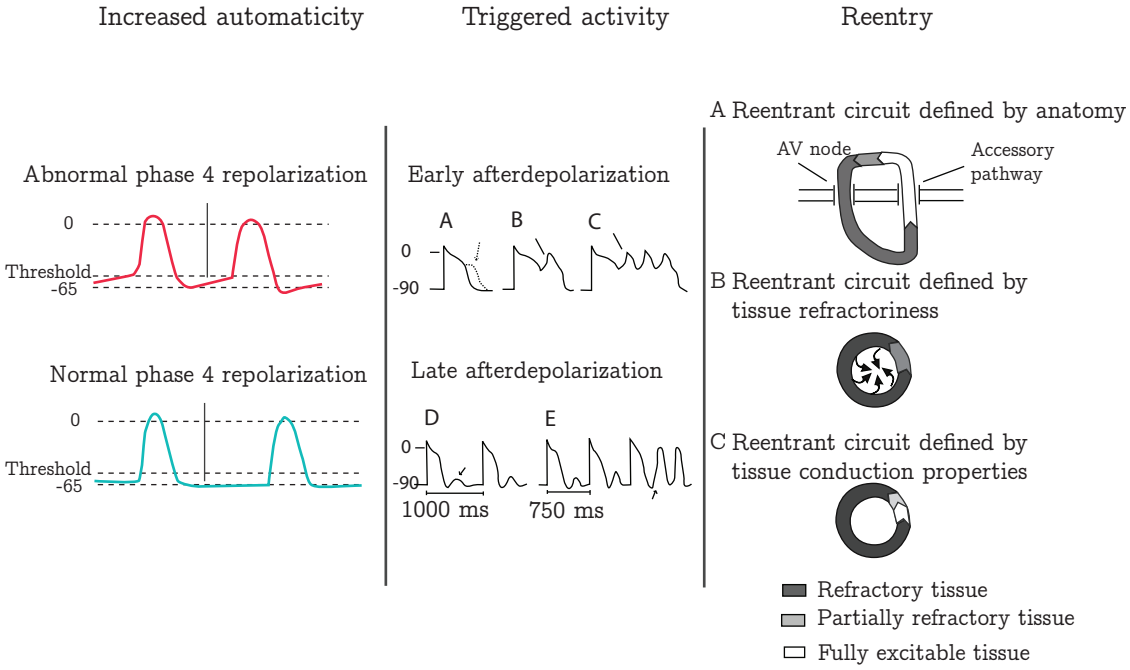

Figure 12: *The main mechanisms behind ventricular arrhythmias.* ***Increased automaticity****: resting potential increases during phase 4 triggering action potential in a normally nonautomatic cell.* ***Triggered activity****: Early afterdepolarization is an upward oscillation of the membrane potential during phase 2 causing no action triggered impulses (A), one extra impulse (B) or series of triggered impulses (C). Late afterdepolarization causes an abnormal upstroke of membrane potential during phase 3 causing no triggered activity during lower heart rate (D) and series of triggered activity during higher stimulus rate (E).* ***Reentry****: Reentry circuit can be facilitated by anatomy (A) tissue refractoriness (B) or tissue conduction properties (C). [9]*

Depolarization of a cell membrane abnormally after or during repolarization (phase

3 of action potential) is called delayed afterdepolarization (DAD) or early afterdepolarization (EAD). If the afterdepolarization reaches a threshold potential, it triggers an action potential, which may propagate to the surrounding cardiac cells causing the whole heart to depolarize abnormally [9]. Both EAD and DAD are related to abnormal repolarization. For example, TDP is thought to be caused by EAD and DAD is thought to cause some forms of VT [40].

Re-entry is a conduction process, where an impulse propagates through a tissue already depolarized by the same impulse. Furthermore, re-entry is circulatory movement around an obstacle, that can be anatomic or functional, leading to repetitive excitation at a frequency that depends on the conduction velocity of the impulse and the dimensions of the obstacle. In addition to the circuit, an unidirectional block and the presence of slow conduction are needed for re-entrant arrhythmia to take place. In fact, the great majority of clinical tachycardias have a re-entrant mechanism. Clinical tachycardias are caused by abnormalities in propagation of the electrical impulse through cardiac tissue rather than abnormalities in activation of individual cells [9].

Anatomical re-entry may be established on congenital circulatory pathways, like Wolf-Parkinson-White syndrome (WPW), or acquired anatomical obstacles, such as scar resulting from a myocardial infarct. Conversely, functional re-entry occurs in the absence of a predetermined structural circuit [9]. It is postulated that the functional re-entry occurs as a propagating wave turns back on its own refractory tail [40]. It is also suggested, that spiralling wave, causing ventricular fibrillation, may maintain themselves through re-entrant mechanisms [9].

2.2.5 Diseases Behind Sudden Cardiac Death

Coronary artery disease (CAD) or atherosclerotic heart disease is the end result of the accumulation of atheromatous plaques within the walls of the coronary arteries that supply the myocardium with oxygen and nutrients. CAD is found to be the most common cause of sudden cardiac death (SCD) accounting for approx. 80 % of the cases [22]. In addition to lethal arrhythmias, CAD can cause the death by rupture, hemorrhage and thrombosis. Most often, CAD causes ischemic heart disease that is known to cause arrhythmias by two mechanisms: VT triggered by acute myocardial ischemia with or without preexisting myocardial scarring and VT related to anatomical substrate from previous infarction without active ischemia [25]. Another major disease behind SCD is the cardiomyopathy, which causes gradual deterioration of the function of the myocardium. Dilated and hypertrophic cardiomyopathies account for approx. 10–15 % of the cases. In addition, various uncommon causes, such as congenital heart disease and known genetically determined ion channel anomalies [56], e.g., Brugada and long-QT syndrome, are responsible for the remaining 5 % of the cases. These rare congenital diseases are well studied and documented in literature and will not be studied in this thesis. Although the risk factors behind these diseases are known, it is unclear how to assess the risk of arrhythmias caused by these diseases. [25]

Arrhythmias are thought to cause vast majority of SCDs. However, there is usually no specific anatomic pathology of sudden cardiac death [58]. The only reliable way of diagnosing cardiac rhythm is ECG. Thus, statistics are based on ECG recordings of hospitalized patients suffering SCD and generalization to SCDs occurring out of hospital is uncertain [22].The most common arrhythmic event causing SCD (63 %) is ventricular tachycardia (VT) degenerating to ventricular fibrillation (VF) and, later, to asystole, see Fig. 13. Different forms of bradyarrhythmias, particularly in patients with advanced heart disease, make up the second largest primary cause of SCD accounting for 17 % of the cases [25]). Furthermore, torsade-de-pointes (TDP) is the cause of SCD in 13 % and primary VF is the cause of SCD in 7 % of the cases. [22]

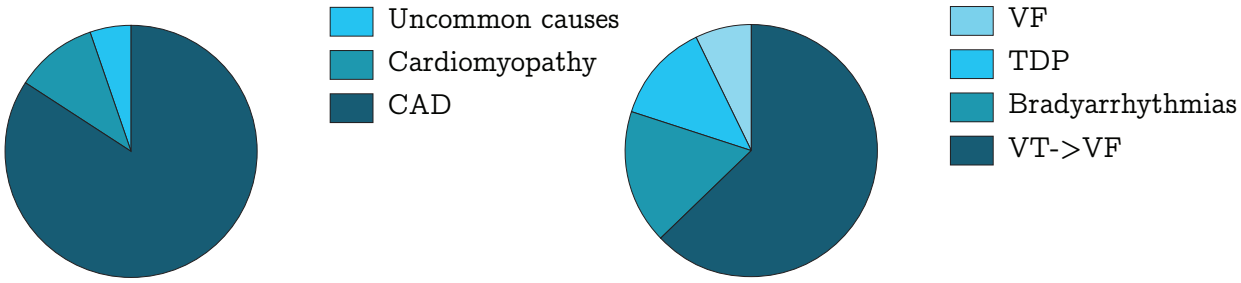

Figure 13: ***Left:*** *Diseases behind SCD.* ***Right:*** *Cardiac arrhythmias behind SCD. [25]*

2.2.6 Arrhythmogenic Mechanisms in Heart Failure

Advancing heart failure (HF) causes substantial changes in the heart, spanning from cell/molecular to organ-system levels [31]. These changes promote the prolongation of the action potential, the enhancement of spatio-temporal gradients of repolarization, the formation of calcium-mediated triggers and conduction abnormalities, all of which combine to form an electrophysiological substrate that is ripe for the genesis of lethal arrhythmias and sudden cardiac death. Although increased transmural dispersion of repolarization is suggested as potential unifying mechanism for arrhythmias associated with various diseases, it is unclear whether these changes are directly linked to the onset of arrhythmias [31].

Myocardial ischemia alters both active and passive conduction properties of the heart [8]. The former occurs between 5 and 7 minutes after arrest of myocardial perfusion and is manifested as a change in ion transportation properties across the cell membrane. In particular, the fast depolarizing sodium current is reduced and the resting potential becomes less negative [40]. The latter occurs between 20 and 30 minutes after the arrest of perfusion and is manifested as decoupling of the myocardial cells, i.e. the amount of inter-cell gap junctions decrease. All of these changes lead to increased electrical resistivity and decreased conduction velocity, which is sometimes observed in ischemia triggered arrhythmias [8]. Further degeneration of

conduction properties will eventually lead to a conduction block, which is a prerequisite for a reentrant arrhythmia [40, 2]. In fact, decreased conduction velocity is documented as a general property of a failing ventricle [31]. The decrease in the conduction velocity (CV) is seen as a widening of the QRS complex.

Changes in ionic currents during ischemia are not restricted to the depolarization phase. In fact, both plateau and repolarization phases are very sensitive to changes in the cardiac state [56]. Prolonged action potential duration (APD) is a common finding in a failing heart and is seen as a prolongation of the QT interval in the surface ECG [31]. The three key changes behind the changes are a downregulation of repolarizing potassium current, an increase in late Na^+ current and changes in intracellular calsium (Ca^{2+}) handling [31]. In addition, these changes occur heterogeneously in different cardiac cell layers affecting mid-myocardial and endocardial muscle layers more than the epicardium, which increases repolarization heterogeneity [2].

Increased abnormal automaticity and triggered activity are well documented phenomena in a failing heart. They act as triggers of arrhythmia in a vulnerable tissue substrate [2]. Especially, intracellular calcium (Ca^{2+}) cycling abnormalities are thought to be responsible for multiple arrhythmogenic changes, such as early and late afterdepolarizations and extraction-contraction decoupling [56, 61]. Abnormal calcium handling may cause beat by beat alternation in action potential duration (APD) that can be seen as T wave alternans in the surface ECG [66].

Cardiac diseases, such as ischemic heart disease and cardiomyopathies, cause reinnervation of the heart and, in autopsy specimen, an increased density and spatial heterogeneity of sympathetic nerves were associated with previous history of ventricular tachyarrhythmia (VTA) [76]. Consequently, increased sympathetic tone is likely to increase transmural dispersion of repolarization and regional heterogeneity of the other electrophysiological properties, such as action potential duration and conduction properties, in a failing heart [31].

2.2.7 In-hospital Cardiopulmonary Arrest and Sudden Cardiac Death

The application area of the predictive algorithm described in this thesis is cardiac monitoring. Thus, it is useful to review the need and applicability of the algorithm in real clinical settings. The questions addressed will be the following: What is the meaning of time and monitoring in cardiac resuscitation? Who would benefit from the predictive algorithm? How much earlier the prediction would be needed to be useful? How the anticipatory data would change the way we treat the in-hospital cardiopulmonary arrests (IHCAs)?

Currently, the resuscitation guideline to treat IHCA is described by the concept of "chain of survival", which includes early recognition, cardiopulmonary resuscitation (CPR), defibrillation and advanced care [49, 48]. Despite wide-spread appliance of the concept, the IHCA mortality remains unacceptably high, around 80 % [33, 50]. Multiple factors, such as the first monitored rhythm, the delay before initiation of

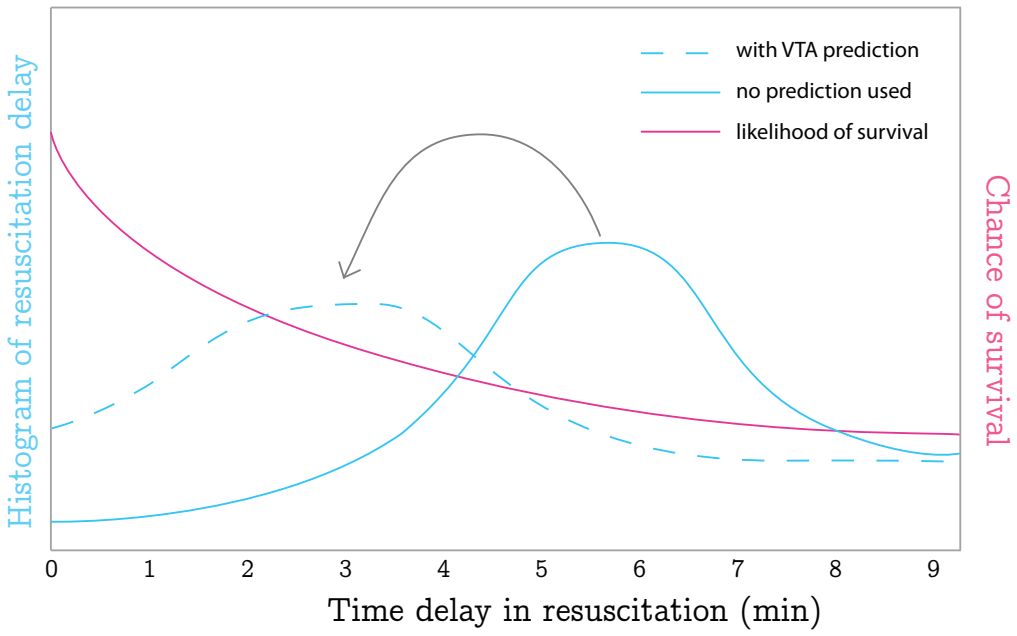

Figure 14: *Percentage of patients and probability of survival as a function of time delay from the onset of VTA to the beginning of CPR. Probability of survival decreases by 7-10% with every minute of delay [53]. (Image not in scale)*

CPR and the unit where the patient is admitted, affect the survival rate substantially [60].

Cardiac arrhythmia is classified into "shockable" versus "non-shockable", based on the underlying rhythm. The two shockable rhythms are ventricular fibrillation and ventricular tachycardia while the two non-shockable rhythms are asystole and pulseless electrical activity (PEA) [50]. This division refers to whether particular class of arrhythmia is treatable using defibrillation. It has been reported that about in 25–30 % of IHCAs the first documented rhythm is VF/VT, PEA and asystole account for 35 % each [33]. The statistics are found to be the same between heart failure (HF) and non-HF patients [50]. Thus, only one third of the cardiac arrests (CAs) are caused by a shockable arrhythmia. The likelihood of survival is substantially higher for shockable rhythms than for other arrhythmias. Survival rates range from 18 % to 64 % for VF/VT and from 1.2 % to 14 % for non-shockable rhythms [60].

The time from the onset of IHCA to the beginning of CPR is found to be a critical predictor of survival in multiple studies [60]. The only effective treatment for ventricular fibrillation is prompt defibrillation, as the probability of survival decreases by 7-10 % with every minute of delay [22, 68]. Resuscitation guidelines suggest that emergency care for cardiac arrest should include defibrillation within 3 minutes in a hospital setting, and within 5 minutes elsewhere. Furthermore, Spearpoint et al. claim that CPR should be initiated within 1 or 2 min [71]. Consequently, patients suffering an IHCA in the ICU or CCU present a better prognosis despite their more severe underlying conditions [59] and it may be assumed that patients

may die unnecessarily due to sudden cardiac arrest if proper in-hospital resuscitation programmes are not available [18]. The difference in the location dependent survival rates can be explained by alertness of the staff, cardiac and other monitoring [75] of the patients and the higher proportion of shockable rhythms in ICU/CCU [60].

Two main patient groups that would benefit from the predictive algorithm can be distinguished. The groups are set apart by the first monitored rhythm, location, whether the cause of arrhythmia is primarily heart related, time course and progression of deterioration [48]. The first group is usually located in a monitored area in the hospital (such as ICU/CCU), the onset of CA is caused primarily by a cardiac cause, usually ischemia, deterioration is likely to be fast and the first monitored rhythm is VT/VF that can be defibrillated fairly often and the patient is likely to discharge alive. In comparison, the patients in the second group are usually located in a general ward, not actively monitored and a slow non-cardiac physiological deterioration leads to cardiac arrest with the underlying rhythms of PEA/ASY with very poor chance of survival to hospital discharge. Since IHCA is more likely to be avoidable in the non-cardiac group and CPR is more likely to succeed in the cardiac group [24], different strategies are needed when handling and preventing IHCA in these groups. Majority of the IHCAs are non shockable thus for these prevention would be the only way to increase likelihood of survival substantially. For shockable rhythms, both shorter delay to defibrillation and prevention would lead to better results.

The reported incidence of IHCA is relatively low, 0.175 events/bed annually including all hospital areas [60] or in-hospital incidence of attempted CPR of 0.0591 attempts/bed per year [68].

Incidence of in-hospital VT/VF is difficult to estimate. Some studies estimate that the incidence among VT/VF patients is around 1-5 % [29]. In selected in-hospital cohorts comprising high percentage of patients with cardiac ischemia, the prevalence of VF/VT is high and exceeds 50 % [60]. Consequently, CCU patient selection criteria have significant effect on the incidence rate.

2.2.8 Prediction of In-Hospital Cardiac Arrest

Despite recent advances in the understanding of the pathophysiological mechanisms leading to cardiac arrest, and considerable efforts to spread the knowledge of basic life support (BLS), the mortality of patients with cardiac arrest remains high and many survivors suffer from devastating neurological sequelae. Most in-hospital cardiac arrests are preceded by events that often go overlooked and whose correct interpretation could be associated with a reduced mortality rate. However, because many factors can delay cardiopulmonary resuscitation (CPR), it appears that the prevention rather than the treatment of cardiac arrest would be a major factor in reducing the subsequent heavy burden of death and disabilities [7]. Since only a minority of IHCA patients survive and failed resuscitations consume substantial healthcare resources and identification of potential survivors from pre-arrest factors

is very complicated [33], the prevention would be highly desirable.

Independent investigators have demonstrated that in many instances cardiac arrest occurring in a theoretically protected environment such as a hospital cannot really be considered sudden and unexpected because it can be preceded by anticipating events, which, in a post-hoc analysis, could be regarded as warning signs [7]. Evidence of deterioration during the 8 h before the arrest has been reported in up to 84 % of cases, the most common findings being respiratory problems, deterioration of mental status and haemodynamic instability [60]. In addition, Berlot et al. reported that in 86.4 % of patients the nurse or medical records reported the appearance of new symptoms or the deterioration of the underlying condition during the 6 h preceding the cardiac arrest [7]. Another recent study identified failing respiratory, cardiovascular, and nervous systems and abnormalities of heart rate, blood pressure, respiratory rate, and conscious level as a common signs that precede IHCA [49].

In many cases, it is not clear if the IHCA simply represents the biologic conclusion of the patients affected by multiple severe underlying diseases or a truly unexpected event that, if successfully prevented, might not have caused the death of the subject [7]. However, potentially 61.9 % of IHCAs are avoidable and the likelihood for potentially avoidable cardiac arrest is estimated to be higher for patients in general ward than in critical care areas (77.8 % and 40.5 %, respectively) [24]. Potentially reversible causes for cardiac arrest include hypovolemia, hypoxia, electrolyte disturbance, particularly hyper- or hypokalemia, acidosis, tension pneumothorax, cardiac tamponade, acute coronary syndrome, pulmonary embolus, hypothermia or poisoning [84]. Even when cardiac arrest is unavoidable, predictive algorithm is useful since it reduces the delay to the onset of CPR or defibrillation. This would increase, for example, the prognosis of patient with acute myocardial infarction since of those patients that survive defibrillation of VF to hospital discharge, one-year mortality is not increased compared to patients with uncomplicated infarcts [9] and early defibrillation increases the likelihood of the discharge.

From the above, it is clear that in most cases an in-hospital sudden and unexpected death is neither sudden nor unexpected. The current policy of training hospital professionals CPR and early defibrillation does not even consider that IHCA can be foreseen and in many cases prevented. Observers have suggested that avoidable arrest results from a failure to act on clinical information rather than a lack of information. Problems include information gaps and delay between nurses and doctors, inexperience and lack of education, failure in monitoring oxygen saturation and respiratory rate losses [24]. These problems could be tackled by increased automated monitoring of high risk patients. Monitoring of basic biosignals should be possible and cost-effective beyond critical care areas and should be promoted as a part of systemic approach to the prevention of in-hospital cardiac arrests.

An interesting question is, could ECG be used to monitor anticipatory events beyond electrical activity of the heart. For example, respiratory and function and tone of autonomic nervous system (ANS) can be monitored from ECG signal [10]. Thus, it is obvious that patients in the general ward would also benefit from (cardiac)

monitoring, which would increase the usability of monitoring beyond ICU and CCU. However, as not all important vital signs are, or can be, monitored continuously in general ward areas, the ability of these systems to predict cardiac arrest remains unconfirmed [48].

3 Review of Risk Assessment of Ventricular Tachyarrhythmias

Mechanism of ventricular tachyarrhythmias (VTAs), i.e. what makes an arrhythmogenic substrate (see the previous chapter), are known and well studied. The onset, however, is the mystery. It may be assumed, if the onset is not random, that mechanoelectric properties of the myocardium are altered prior to the onset. These changes may be measurable or small and invisible in surface ECG or occur too slowly to be detected. The assumption in this thesis, however, is that some arrhythmias are preceded by a transient change in the heart and that they are measurable with surface electrodes.

In recent years, the focus of research has been on discovering prognostic parameters that discriminate SCD cases from a high-risk population in follow-up studies. These studies have demonstrated relatively good predictive performance among some patient groups [37, 27, 51, 25, 12]. Advances in measurement and storing of ECG signals have enabled recording of long high resolution ECG signals prior to VTAs, which makes it possible to investigate mechanism responsible for the onset of VTAs. In this chapter, ECG parameters and methods, used for short-term prediction are reviewed.

3.1 Morphology Related Parameters

Majority of the arrhythmogenic changes in the cardiac state, such as ischemia [38] and drugs [4], manifest themselves as changes in the repolarization phase of individual myocardial cells. This may be observed as a change of the morphology of the T wave. Especially, optical action potential mapping and patch clamp techniques have identified changes in the early and late phases of repolarization in failing hearts [2]. QT interval prolongation is a well studied parameter (see e.g. [35]), mostly because of its relation to the long QT syndrome and Torsade-de-pointes (TDP). Recently, also the change of the shape [32] and amplitude oscillations [20, 47] of the T wave have been found to have a prognostic value. These parameters are thought to reflect spatio-temporal repolarization heterogeneity or altered repolarization sequence and instability, which are known to cause arrhythmias [37, 2].

3.1.1 T Wave Morphology

Atypical T wave morphology may reflect abnormalities of the ventricular repolarization process and mean, for example, increased repolarization heterogeneity, i.e. dispersed spatial distribution of repolarization, in the myocardium. However, the link between these abnormalities and the onset of VTAs is unclear [31]. Changes in T wave morphology prior to the onset of VTA are relatively poorly studied. Existing research is limited to drug induced effects and invasively measured data using implantable cardioverter defibrillators (ICDs). Recent computer simulations

of repolarization have demonstrated the exploitability of T wave morphology as a measure of repolarization sequence [14], ventricular repolarization heterogeneity [78, 81] and specific ion channel properties [82].

Xue et al. have studied a set of new T wave morphology parameters as an improvement to cardiac safety trials currently relying on QT interval measurements only [4]. The parameters are targeted to detect changes caused by the fast potassium current IKr that is the most common factor behind drug induced repolarization changes and arrhythmias [3, 82]. The T wave morphology parameters, symmetry, flatness, and notch, are described b Xue et al. in [83]. In addition, certain antiarrhythmic [32] and antidepressant [67] drugs are known to predispose to malignant VTAs. Kurokawa et al. [32] studied the effect of antiarrhythmic drug bepridil on T wave morphology in a recent follow-up study that tried to identify distinguishing TU-morphology changes that predispose to VTA episodes. After multivariate analysis, the only differentiating parameter studied was increased proportion of negative T waves. All these studies suggest that T wave morphology is an important feature when assessing the risk of drug induced arrhythmia. However, meaningful measurement of these parameters presuppose stable state during the measurement. Thus, they are not useful, for example, during acute myocardial ischemia due to substantial ST changes and non-stationarity [54, 38].

Maury et al. [42] studied T wave morphology prior to the onset of VTA using intracardiac electrocardiograms stored in ICDs. The group investigated eleven morphology parameters prior to the onset and compared these to control recordings sharing comparable QRS and T wave morphology and similar heart rate in the same patient. Significant differences were found only in T wave amplitude (higher before VTAs) and slopes (steeper before VTAs). Durations and timings of the different parts of the T wave did not change significantly. This study implicates that T wave amplitude and slope related parameters could also demonstrate changes in surface ECG prior to VTA onset. Shusterman et al. [65], in contrast, found that the peak and the mean amplitude of the T wave, as well as the area under the T wave, did not show a statistically significant change before an onset.

The most significant conceptual challenges in using T wave morphology parameters for short-term arrhythmia prediction is inter-subject variability and non-specificity. The former means that T wave parameters are not comparable inter subjectively. They are useful only when their change is investigated as a function of time and when ECG signal is stationary. If the same parameter is measured from another patient it is not guaranteed to measure the same cell level phenomena or, conversely, the same change in the cardiac state can cause completely different change in the ECGs of the two individuals. The latter means that two different cell level changes can cause similar changes in the surface ECG. In addition, in subjects with advanced heart disease or conduction defects, T wave is ambiguously defined and sometimes impossible to quantify automatically, T wave morphology changes as a function of heart rate [13] and gender [45, 19]. These complicate things further and mean additional technical and conceptual challenges.

3.1.2 QT interval

Measurement of the duration of the QT interval has become a standard procedure in many commercial devices during the past years [37]. Despite its wide spread application in long term risk assessment, its clinical usability as a risk factor of imminent VTA episodes in general population is yet to be demonstrated. QT variability (QTV) is a measure of changes in QT interval morphology and duration with non-alternans characteristics. QTV is closely related to the T wave alternans (TWA) and often called complex T wave variation or T wave lability.

Beat-to-beat changes in repolarization are known to increase heterogeneity of repolarization throughout myocardium which predispose to initiation and maintenance of reentry arrhythmias [85]. Both shortening, with shortened cycle lengths, and prolongation of QT interval seems to increase the risk of arrhythmia in patients with [17] and without [37, 85] a structural heart disease. Abrupt changes in HR, frequently observed before VTA episodes, has motivated Zareba et al. [85] to suggest misadaptation of QT to rapid changes in heart rate to be the most likely reason for increased number of beats showing substantial QT prolongation in patients with arrhythmic events when compared to controls. In addition, it has been shown that QT dynamicity, expressed as QT/RR slopes, is related to haemodynamic status and bears some prognostic value [37].

Several research groups have studied the dynamics of QT interval prior to the onset of an arrhythmia. However, major discrepancies exist among the results. Lewicke et al. [35] measured QT intervals of beats preceding a spontaneous initiation of a VTA using data stored in wearable cardioverter defibrillators (WCDs). Comparison between the pre-onset and a control period with the same heart rate showed no statistically significant change in the QT interval duration. Similar results were obtained by Shusterman et al. using Holter ECGs [65] and Sachdev et al. [57] using long-term surface ECG recorded from patients in ICU. By contrast, Diem et al. [15] used ICD data to demonstrate a significant prolongation of the QT and corrected QT (QTc) times before the onset of a VTA episode as compared to a baseline reference values in patients with structural heart disease and Fei et al. [17] observed significant shortening of the QT interval prior to the onset of VTA in patients without structural heart disease.

The discrepancies between the results may be, for example, due to the absence of inclusion of heart rate independent factors, like sex, haemodynamic state, drugs, autonomic nervous system tone, time of the day, age etc. [37, 85]. Another confounding factor may be the difficulty of defining and measuring T wave in some cases. Namely, computerised methods work well in the presence of good quality ECG and monophasic T waves, but unfortunately this is not true for abnormal electrocardiograms with the T wave not clearly defined morphologically or characterised by irregular morphologies. Furthermore, if the dynamic variation of QT interval to heart rate is evaluated on beat-by-beat basis, as is the case in many published reports, the QT/RR relation will probably mix up the two phenomena of QT adaptation and QT dynamicity, since steady-state cannot be reached after a

single RR interval [37].

3.2 Variability Parameters

In this subsection parameters that are related to the alterations and variability of the heart beats are reviewed. These parameters are well studied and understood in the context of long-term risk of cardiac arrhythmia ratification. However, in the context of short-term prediction, existing studies have more contradictory results.

3.2.1 Heart Rate Variability and RR Dynamics

As mentioned above (see Ch. 2.1.7), the risk of sudden cardiac death is known to vary during a day, being highest in the morning and evening and lowest during the night [22]. This, and other findings, strongly suggests that autonomic nervous system (ANS) has a role in SCD and arrhythmia onset. Especially, a variety of experimental and clinical data supports the hypothesis that increased vagal tone reduces the risk of malignant VTAs, whereas sympathetic stimulation enhances it [37]. In addition, an increase in heart rate has been observed preceding the onset of ventricular tachyarrhythmias (VT) in the majority of patients in whom spontaneous initiation has been recorded, which suggests elevated sympathetic and/or diminished parasympathetic activity. [64]. Findings are controversial, however, and there is no consensus whether different branches of ANS have a significant role in the initiation of VTAs. Since the ANS is the most significant modulator of the heart, especially sinoatrial (SA) node and, consequently, heart rate, the idea in heart rate variability (HRV) measurement is to quantify short- and long-term variation of the HR. With some limitations, these oscillations reflect changes in the relative balance between the sympathetic and parasympathetic branches of the ANS, i.e. the sympathovagal balance [10, 37].

Based on the physiology of the ANS, the activity of the two branches is generally thought to be seen as oscillations of the HRV at very different frequencies. The high frequency (HF=0.15–0.4 Hz) component is parasympathetically mediated and reflects primarily respiration-mediated HRV. Below HF, low frequencies (LF=0.04–0.15 Hz) are modulated by both branches of ANS and strongly affected by the oscillatory rhythm of the baroreceptor system. Furthermore, very low frequencies (VLF=0.003–0.04 Hz) may represent the influence of the peripheral vasomotor and renin-angiotensin systems and, finally, ultra low frequencies (ULF= 1.15×10^{-5}–0.4 Hz) that encompasses all variations in HR with a period of more than 5 min to 24 hours, and reflects primarily circadian rhythm. In addition to frequency domain, time domain, non-linearity based methods and higher order statistics have been exploited when studying HRV [37, 10].

Regardless of the success of linear parameters in predicting patients susceptible to SCD in long-term follow-up studies [37], the results are controversial in demonstrating the causal relationship between abnormalities in HRV and the onset of VTAs

[55]. Huikuri et al. [28] found significant changes in multiple frequency and time domain HRV parameters occurring in the 1 hour period before the onset of a VTA distinguishing sustained from non-sustained VT. These findings were confirmed by Shusterman et al. [63] using Holter recordings and by Pruvot et al. [52] and Lombardi et al. [36] with data from implantable cardiac defibrillators (ICDs). Despite these promising findings, subsequent and some contemporary studies have failed to repeat the results, see e.g. [79, 26, 44, 43, 80, 57]. Both Wessel et al. [80], Zhuang et al. [86] and Meyerfeldt et al. [43] found no significant difference in linear HRV parameters between pre-VTA and normal control periods but found significant changes in non-linear parameters using data from ICDs. In addition, Mäkikallio et al. [44] obtained similar results using long-term ECG recordings and Huikuri et al. [26] found that the ratio of instantaneous to long-term beat-to-beat variability increased during 1 hour period preceding the onset. These findings strongly suggest that various non-linear parameters, including entropy measures [86], symbolic dynamics [43], finite growth rates [80], correlation exponent and power-law slope [44], could be used in short-term VTA prediction. The assessment of HRV by means of linear parameters, however, fails generally due to non-stationary character of the ECG signal prior to the onset of a VTA [26].

The effect on HRV parameters is heterogeneous and affected by individual patient characteristics, which may explain the conflicting evidence in the literature [55]. It is well known that clinical investigations should be controlled for drugs, age, gender, physical and mental activity, methods recording and analysing, and pre-existing conditions [10]. This is, however, usually impossible with the small patient populations used in the studies. For example, it has been suggested that decreased HRV identifies patients at risk for VF or unstable VT, but not patients with inducible or clinically stable monomorphic VT [37]. Since most of the studies do not discriminate these two groups, this can be a confusing factor. Furthermore, erratic sinus rhythm increases HRV and may confound its predictive value. Episodes of erratic sinus rhythm (ESR), assumed to be as a high-degree of non-respiratory sinus arrhythmia with normal P waves, are seen on Holter recordings in the elderly and cardiac patients [74, 16]. In addition, frequent PVCs ruin the measurement of HRV. Multiple acceptance ratios are used ranging from 10 PVCs per hour to up to 15% of all RR intervals (see [55]) and ectopy removal or replacement is shown to be essential regardless of the spectral estimation technique [11].

It has been suggested by Sachdev et al. [57] that prediction of imminent ventricular arrhythmias based on measures of autonomic function is applicable only in patients with normal baseline values. Furthermore, Anderson et al. [5] found that changes in HRV precede only VTAs that are initiated by a complex with similar morphology to subsequent complexes and Meyerfeldt et al. [43] found that fast VTAs (cycle length < 270 ms) are preceded by decreasing trend in HR and, respectively, slow VTAs are characterized increased HR. Shusterman et al. [64] have suggested that baseline levels of HRV may determine HRV changes in response to short-term autonomic perturbations prior to VTAs. These findings suggests that alterations of autonomic nervous system activity is not associated with all VTAs and more attention should be

paid to the patient group division. Furthermore, it has been suggested that merely a change in HRV, rather than the magnitude or nature of the change, facilitates the initiation of VTAs [55].

3.2.2 T Wave Alternans

T wave alternans (TWA) is defined as a beat-to-beat alternation in the magnitude of successive T waves that repeats every other beat [65] and is thought to manifest the temporal heterogeneity of repolarization. Furthermore, it has been suggested that TWA can be a marker of action potential duration (APD) alternation (e.g. caused by abnormal calcium handling), increased tone of sympathetic nervous system activity or impaired adaptation of the conduction system to faster heart rates may contribute to the emergence of alternans in the setting of heart failure [37]. The microvolt level measure of TWA is widely used as a measure of susceptibility to VTAs and SCD [37]. Recently, an increase in T wave alternans has been reported to precede an imminent onset of VTA in several animal models and animal studies of ischemia induced VF [47]. In addition, TWA has been mechanistically linked to the onset of VF in a mathematical model [21]. These findings have led to the conclusion that TWA might serve as a short-term predictor of these life-threatening events [37] and motivated to study T wave dynamics prior to the onset of VTA episodes.

Recently, multiple studies have been conducted to discover whether a spontaneous initiation of VTA and increased TWA have a causal relationship [66]. Shusterman et al. studied repolarization dynamics before spontaneous initiation of VTA using human ambulatory ECG recordings [65]. TWA was found to be increasing, peaking 10 minutes before the onset of VTA with a peak value of $23.6 \pm 11.7\ \mu V$. In addition, an upsurge in non-TWA repolarization instabilities (i.e. longer-period oscillations) and heart rate was found to precede an event. Interesting studies by Nearing et al. [47, 46] demonstrate, by using a canine model of acute ischemia, that an increase in TWA and other repolarization instabilities precede the imminent onset of VF episodes. Interestingly, the changes were found to occur predominantly in the early half of the T wave in both of these studies. The similarities in the findings of these two studies suggest that there may be the same electrophysiological mechanism linking TWA to the initiation of arrhythmias in acute ischemia and chronic structural heart disease [65]. Maury et al. [41] studied alternans in various T wave morphology parameters using data stored in ICDs prior to the onset of a VTA episode. In this study, increased TWA was observed to precede half of the episodes.

So far, the analysis has mainly focused on TWA alone ignoring other types of repolarization instability that has been shown to arise before the onset of VTA [66]. It is unclear, whether TWA is the only form of repolarization instability that arises before the onset of arrhythmia or whether it represents a larger class of instabilities that coexists minutes to hours before the event [65]. The multiform repolarization instabilities could also be a result of complex and profound changes in the pattern of cardiac rhythm that occurs in the studied population during the 1 to 2 hours before the onset on VTA [65, 62]. Consequently, it is suggested by Shusterman et al. [66]

that the assessment of TWA needs to be dynamic and personalized to take into account the time evolution of risk and individual history and at least 120 minutes of continuous data is needed to draw any reliable conclusions.

3.2.3 Characteristics of the Rhythm Preceding VTAs

Occasional findings from individual recordings have motivated the search of precursors of VTA episodes from beat-to-beat analysis of ECG recordings. The episodes are usually preceded by a complex and changing pattern of abnormal heart beats including, e.g., single PVCs, segments of bigeminy and trigeminy [34], short PVS runs, escape beats, short-long-short sequences, early coupling (R on T phenomena) etc. Resent large-scale studies, however, suggest that frequent premature complexes or episodes of "warning" arrhythmias do not provide independent prognostic information in patients with heart failure and such arrhythmias are present, for example, in as many uncomplicated myocardial infarctions as in infarctions complicated by VF [9]. However, VTA episodes or PVCs that alter the hemodynamic stability are known to be more dangerous [25]. Furthermore, increased frequency of PVCs, i.e. increased ventricular automaticity or triggered activity, may be a manifestation of, e.g., enhanced sympathetic and/or decreased parasympathetic tone, acidosis or hypoxia [58]. Consequently, changes in the predominant rhythm may reflect arrhythmogenic changes.

3.3 Conclusions of Review

In general, current research on precursors of VTAs can be characterised by small sizes of databases that are not publicly available, findings are not reproduced by independent investigators and methods are not clearly documented and standardised. Because of these limitations, even the most promising results must be evaluated critically.

In essence, every parameter is both failed and succeeded in the prediction of forthcoming VTA episode. It seems that variation in patient population size, history, medication, diagnosis etc., methods used and inclusion criteria confound the results. This is a manifestation of the complexity that is included and not taken into account. Given that the results show such a high degree of variability for all the parameters, it appears unlikely that an ECG arrhythmia predictor with high sensitivity and specificity would emerge.

All the studies try to identify general changes on group level. However, due to variability between patients, it is likely that this can not be done by using only ECG. Moreover, statistically significant results in clinical studies do not give a clear insight into the mechanisms of arrhythmias in individual patients [34]. Thus, it may be possible to identify some changes that have useful prognostic value even though they fail to correlate with initiation of an event on group level.

4 Materials and Methods

As concluded in the previous section, it is unlikely that one could predict a forthcoming VTA episode with good sensitivity and specificity by trending a single ECG based parameter. However, less has been studied how parameters change with respect to each other and as a function of changing heart rate and if there are any changes in these relations prior to an event. Based on these poorly studied phenomena, a new idea of arrhythmia prediction is presented.

In this chapter the methods used in this thesis to extract useful features from ECG signal are presented together with detailed description of our arrhythmia prediction algorithm. In addition, the arrhythmia databases used for development and validation are characterised.

4.1 ECG as a Measure of Cardiac State

The state of the heart is determined by the states of all the cell constituting it. Findings in autopsies strongly suggest that the primary cause of arrhythmias arises as a result of pathological changes affecting the working ventricular myocardium, making ECG an attractive measure of the cardiac state. Unfortunately, ECG gives highly non -specific information about these states. The main factor masking the information about the true cardiac state as measured by surface ECG is ill-posedness of the inverse problem of ECG [39]. This means that surface ECG has an inherent limitation as a diagnostic tool: given a distribution of body surface potentials one can not know the distribution of potential in the heart. In addition, ECG signal may change independently of changes in the cardiac state, e.g., due to changes in electrode contact or patient movement. These changes may be inseparable from true changes. Despite these limitations, ECG is a very useful clinical tool when its limitation are properly taken into account when analyzing results and developing new algorithms.

When a change takes place in the cardiac state, it can be observed as a change in ECG parameters or as a change in relationship between the parameters. For example, all morphology parameters depend on heart rate and change as a function of changing RR interval and this heart rate dependency may change when the cardiac state is altered. Consequently, ventricular arrhythmia is predicted in this thesis by detecting both types of changes.

4.2 Algorithm for Arrhythmia Prediction

An algorithm was developed to measure various parameters from an ECG signal to be used in arrhythmia prediction. The algorithm consists of both existing and tailor-made subroutines (see Fig. 15 for an overview).

4.2.1 Structure of the Algorithm

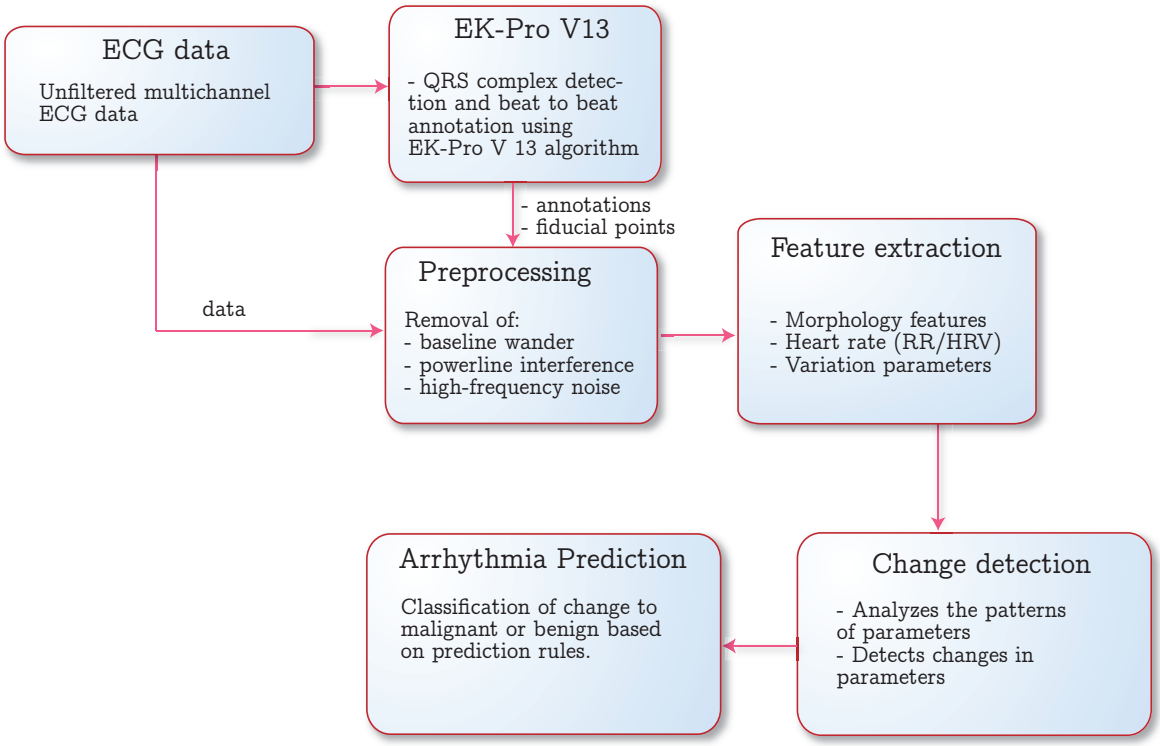

Figure 15: *The overview of the prediction algorithm.*

Measured ECG signal is processed using GE's EK-Pro version 13 algorithm [1]. The algorithm classifies every beat and detects various arrhythmias. The annotation file given by EK-Pro contains beat classifications, fiducial points and arrhythmia onset and offset times. The annotation file is used in the preprocessing and feature extraction routines of our prediction algorithm.

Preprocessing removes high-frequency and powerline interferences using linear filtering and baseline wandering using polynomial fitting. The feature extraction procedure is responsible for extraction of all the parameters from the preprocessed ECG signal.

Change detection routine analyzes the time series of parameters that are stored in the feature extraction. The routine makes alerts if it detects changes that predict imminent arrhythmias. Finally, the alerts are handled in the arrhythmia prediction, which contains decision rules and threshold values.

4.2.2 Preprocessing

The analysis of a biosignal requires a great deal of signal preprocessing and ECG makes no exception. Robust preprocessing is an essential step in more advanced phases of ECG signal processing.

QRS detection

Robust detection of QRS complexes is essential for any successful analysis of ECG signal. In our work detection is done using GE's EK-Pro version 13 algorithm [1]. This algorithm is also running in the latest GE monitors used in hospital throughout the world. Details of QRS detection are not given here.

Removal of baseline wander and high-frequency noise

Preprocessing removes high-frequency noise by using linear FIR-filtering with Chebychew window and cut-off frequency of 45 Hz. FIR-filtering is favoured over IIR to prevent any morphology distortions due to a nonlinear phase response.

Low-frequency baseline wander is removed by searching the isoelectric level of each signal in the PQ segment and removing the approximated baseline error, see Fig. 16. The error is estimated using a nonlinear cubic spline approximation (polynomial fit) as suggested in [10, 73]. The procedure includes search of the isoelectric level preceding each QRS complex (see Algorithm A1 in Appendix for details). The algorithm assumes PQ segment to remain stable throughout the recording. If this requirement is not met with all recordings, erroneous measurements of other parameters will occur since they are measured using the isoelectric point as a reference point. Since certain conditions, such as atrial arrhythmias and some conduction abnormalities, can destabilize the PQ segment, all recordings are manually verified and such cases are excluded from the study.

Vector ECG

In order to compare signals measured using different subsets of channels of 12-lead ECG, they are mapped to the Cartesian coordinate system by estimating the x,y and z components of the signal. These signals approximate vector-ECG.

In the simplest forward model of ECG, a patient is assumed to be homogenous spherical conductor with a single dipole in the centre (a heart vector) [39]. In this model, the measured signals are just projections of the heart vector with corresponding lead vectors (see Fig. 17). The data used in this thesis contains four channels of ECG (I,II,III and V1/V2). Thus, we have the following projections:

$$\mathbf{a}_I \cdot \mathbf{s} = s_I,\ \mathbf{a}_{II} \cdot \mathbf{s} = s_{II},\ \mathbf{a}_{III} \cdot \mathbf{s} = s_{III},\ \text{and}\ \mathbf{a}_V \cdot \mathbf{s} = s_V. \tag{1}$$

Here, $\mathbf{s} \in \mathbb{R}^3$ is representation of the signal in the Cartesian coordinate system, $\mathbf{a}_\mathrm{i} \in \mathbb{R}^3$ is the projection vector of lead i and $s_\mathrm{i} \in \mathbb{R}$ is the signal in lead i. This can be written as overdetermined linear system

$$\mathbf{s}_{12} = \begin{bmatrix} s_\mathrm{I} \\ s_\mathrm{II} \\ s_\mathrm{III} \\ s_\mathrm{V} \end{bmatrix} = \begin{bmatrix} \mathbf{a}_\mathrm{I}^\mathrm{T} \\ \mathbf{a}_\mathrm{II}^\mathrm{T} \\ \mathbf{a}_\mathrm{III}^\mathrm{T} \\ \mathbf{a}_\mathrm{V}^\mathrm{T} \end{bmatrix} \begin{bmatrix} s_x \\ s_y \\ s_z \end{bmatrix} = \begin{bmatrix} 0 & 1 & 0 \\ 0 & \sin(\pi/6) & -\cos(\pi/6) \\ 0 & -\sin(\pi/6) & -\cos(\pi/6) \\ 1 & 0 & 0 \end{bmatrix} \begin{bmatrix} s_x \\ s_y \\ s_z \end{bmatrix} = \mathbf{A}\mathbf{s}. \tag{2}$$

The minimum mean square error (MMSE) estimate for $\mathbf{s}$ is obtained by using the

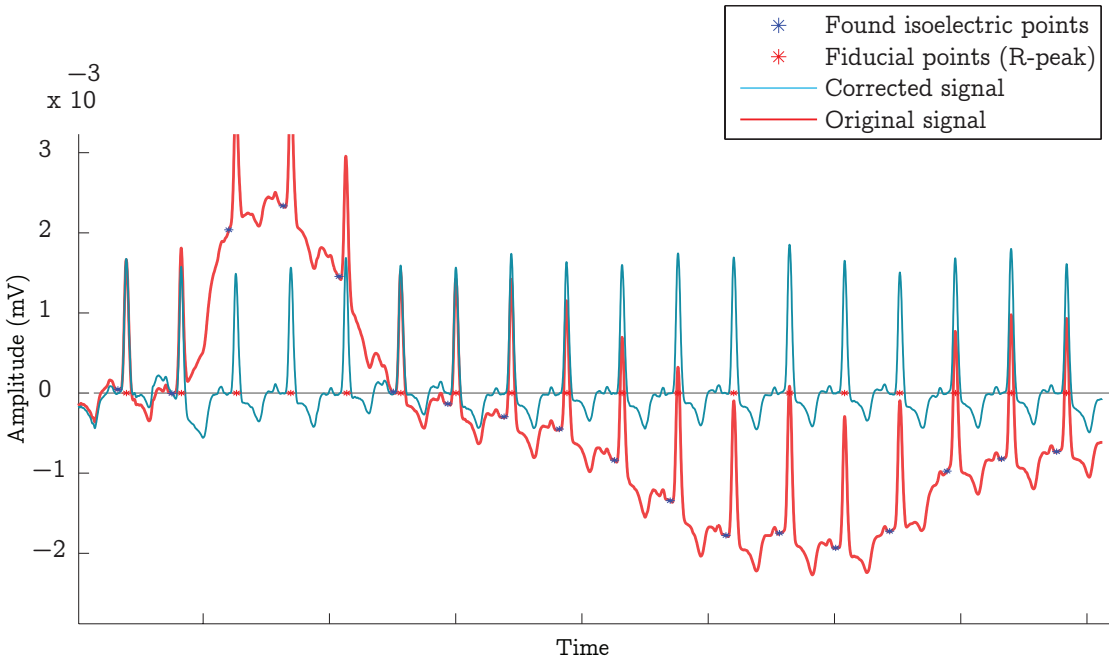

Figure 16: *Example of ECG baseline wander removal. Original (red) and corrected data (blue) are presented as a function of time. Red asterisks are fiducial points from the QRS detector and blue asterisks are found isoelectric positions that are used as nodes in the polynomial fitting.*

pseudoinverse of $\mathbf{A}$, denoted as $\mathbf{A}^{\dagger}$,

$$\mathbf{s} \approx (\mathbf{A}^{\mathrm{T}}\mathbf{A})^{-1}\mathbf{A}^{\mathrm{T}}\mathbf{s}_{12} = \mathbf{A}^{\dagger}\mathbf{s}_{12}. \tag{3}$$

The assumption of spherically symmetric conductor is, of course, a rough approximation and is known to be highly inaccurate [39, 6]. However, the transformation to the orthogonal space enables representation and comparison of redundant information of 12-lead system with varying measurement configuration.

4.2.3 Feature Extraction

After the steps presented above, the data is ready for more advanced feature extraction. The ECG signal is analysed segment by segment. For each segment a dominant beat morphology is calculated using a template matching procedure (see Fig. 19). The obtained dominant beat morphology in the segment is used for morphology feature calculation. In addition, beats accepted in the template matching procedure are used to obtain the variational parameters for the segment. See Fig. 18 for illustration of the feature extraction process.

Template matching and estimation of dominant beat morphology

The method of template matching is used to detect QRS complexes representing

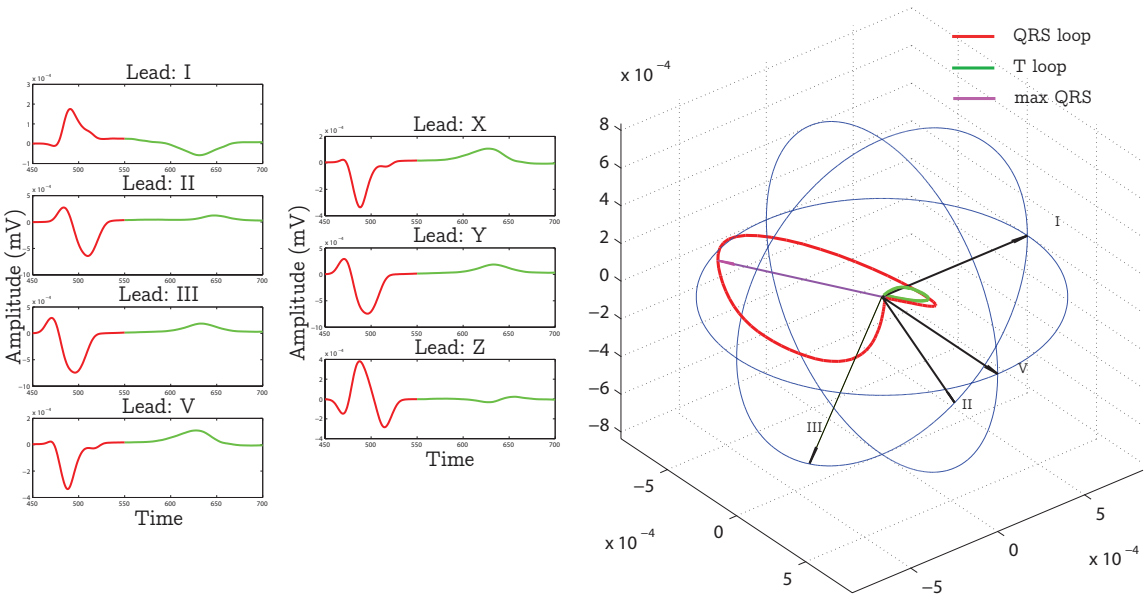

Figure 17: *Transformation of standard ECG leads to vector ECG representation.*

beats with ectopic origin and align accepted ones (see Fig. 19). The template matching is initiated by finding the dominant beat morphology from the beginning of the signal. The dominant beat is then used as the first template.

After initialisation, beats are processed sequentially by aligning them with the template beat and computing correlation and difference (error) in ST segments. If both correlation and ST-error are within predefined acceptance threshold values, the beat is accepted and stored. Using these two inclusion criteria, it is possible to measure ST-segment parameters robustly from the template. After storing the beat, the template is updated, which increases the acceptance ratio as the beat morphology is transiently changing. If the dominant morphology changes suddenly, e.g. when the direction of depolarization changes, the algorithm estimates the template from the near history of rejected beats.

The beats accepted in the template matching process are saved and morphology parameters are extracted from these beats.Extraction of the variation parameters, e.g. HRV and QTV, requires beat-to-beat analysis of the signal. As a side product of template matching, a beat history is saved and these beats are used to estimate variabilities.

4.2.4 Parameters

The parameters chosen to be measures of the state of heart in this thesis have demonstrated to possess some predictive potential or are related to the mechanisms of arrhythmias (see literature review in Ch.3). Parameter are classified as morphology and variation parameter depending on which characteristics they measure and

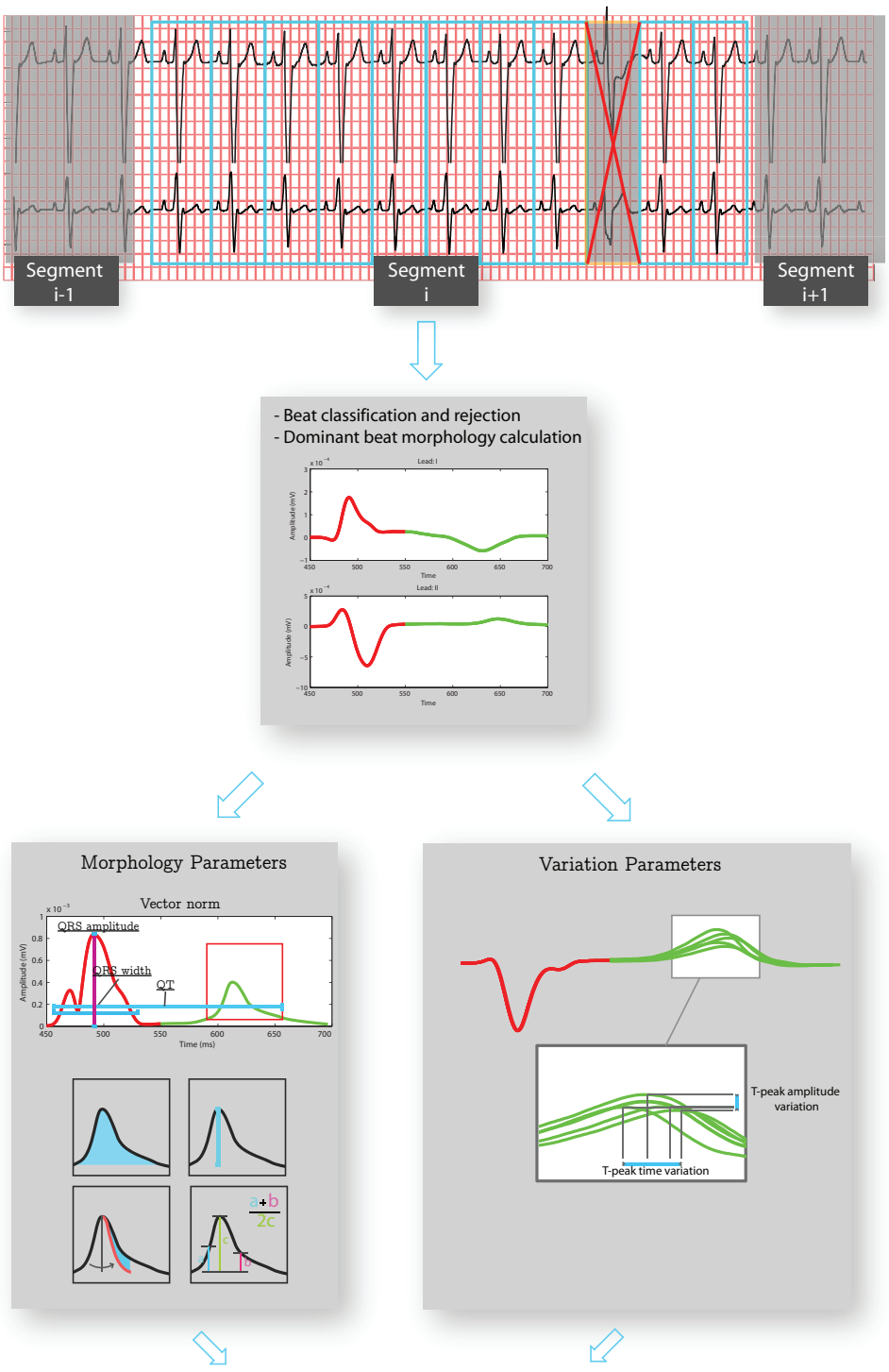

Figure 18: *Extraction of morphology and variation parameters from a segment of ECG signal.*

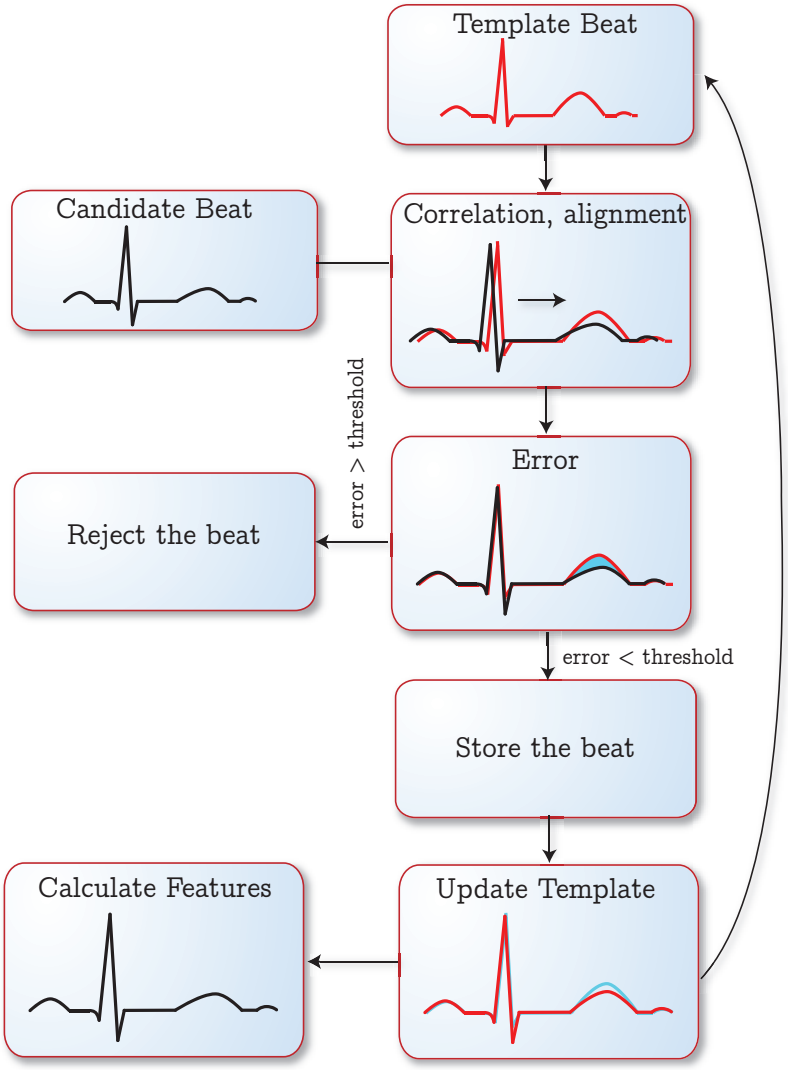

Figure 19: *Procedure of template matching to classify beats to usable and unusable.*

how they are measured from the signal.

Morphology parameters

Morphology parameters are features measured from a beat representing a dominant morphology in a segment of ECG signal. To measure both depolarization and repolarization processes robustly, all the signal are transformed to vector ECG before analysing. Using vector representation of the signal one can separate the analysis of morphology from direction of de- or repolarization and monitor morphology parameters continuously.

Parameters describing depolarization are QRS complex duration, maximal vector magnitude and polar coordinates of QRS complex. The ST segment of the signal is characterized by two parameters. ST level is mean signal amplitude in this segment and ST slope is the slope of linear fit to the samples of the segment. Repolariza-

tion descriptors include maximal vector magnitude, position and polar coordinates, angle between maximal re- and depolarization vectors (QRS-T angle). In addition, area, symmetry and flatness of the vector ECG describing repolarization process are measured. Symmetry is defined as a sum of difference between left and right sections of T wave and flatness is defined as a ratio of mean T wave amplitude to maximal T wave amplitude. To measure duration of one cardiac cycle QT time is included to the parameters. See Fig. 20 for illustration of the morphology parameters and the calculation process. To enable patient-by-patient comparison, parameters are normalised to average maximal QRS deviation over the entire recording.

Variation parameters

Variational parameters are measured from a segment of ECG signal by aligning beats belonging to the segment and measuring their variation, see Fig. 21.

Variation in T wave is measured both in voltage and time. T peak amplitude variation is the variance of T wave amplitude measured at its peak and T peak time variation is variance of T wave peaks position in time. In addition maximal variation in the ST-segment, i.e. ST lability, is measured.

Rhythm parameters

Changes in the rhythm preceding VTA episodes are frequently observed. To measure these changes the rhythm is analysed segment by segment. The parameters selected are average heart rate between consecutive sinus beats, heart rate variability (HRV) and ratio of PVC to normal beats, i.e. PVC ratio.

Control parameters

A few of the above-mentioned parameters are used as control parameters. The purpose of these is to detect changes that affect repolarization but are not related to real changes in the cardiac state or myocardial repolarization. Stability of depolarization is measured using QRS amplitude, QRS-T angle and position of QRS maxima. In addition, abrupt change in the position of T wave maxima can cause unwanted discontinuity in the measurement of morphology parameters. Thus, the position of T wave maxima is used as a control parameter. To prevent noisy segments from causing false prediction alarms, rejection ratio is used as a control parameter. Rejection ratio is the ratio of accepted to rejected beats in a segments.

4.2.5 Fast Change Detection

There are various possibilities for sources of change in ECG. A change can be very fast, occurring between adjacent beats, or it can take up to hours to occur. Furthermore, it can be seen as altered relationship between the parameters or directly in parameter trends. In order to detect both fast and transient changes two different strategies are used.

A segment i of the ECG signal, beginning at t_i, is used for the extraction of a feature vector $\mathbf{x}_i \in \mathbb{R}^N$, where N is the number of features extracted. By writing these vectors as columns of a matrix $\mathbf{X} \in \mathbb{R}^{N \times M}$, one obtains (with M segments)

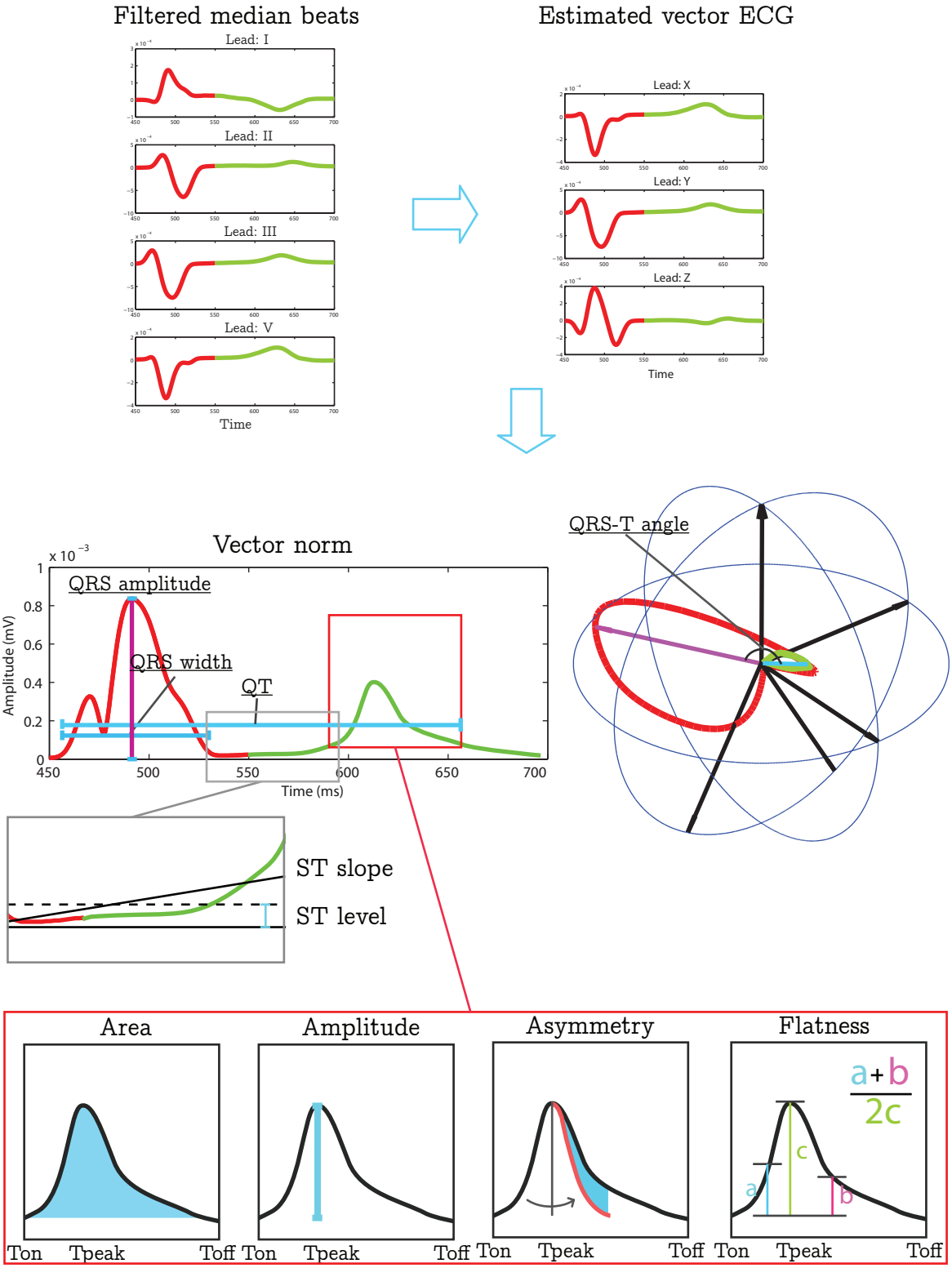

Figure 20: *T wave morphology parameters.*

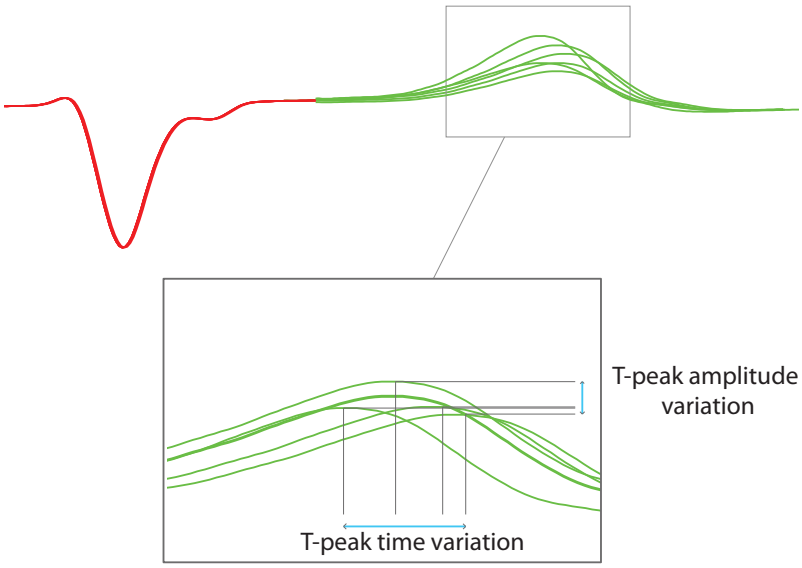

Figure 21: *Measurement of T wave variation parameters.*

$$\mathbf{X} = \begin{bmatrix} \mathbf{x}_1 & \mathbf{x}_2 & \dots & \mathbf{x}_M \end{bmatrix}. \tag{4}$$

In order to detect fast changes in parameter values two different measures are used. Mahalanobis distance (MD) is a measure of distance between adjacent segments of parameters, i.e. x_i and x_{i-1}. Unlike regular Euclidean norm, however, Mahalanobis distance is scale invariant and takes into account the correlation between parameters.

Rationale for utilization of Mahalanobis distance in change detection lies in the fact that measured parameters correlate with HR and with each other. Correlation between parameters can be presented as a correlation matrix, which can be estimated from the data. This way the Mahalanobis distance is insensitive to a normal oscillation and change predictable by earlier data, but larger distance is measured if the parameters do not "fit in the picture" of previously measured covariance matrix. Mahalanobis distance, $d(\mathbf{x_i}, \mathbf{x_{i-1}}) \in \mathbb{R}$, between adjacent segments is

$$d(\mathbf{x_i}, \mathbf{x_{i-1}}) = \sqrt{(\mathbf{x_i} - \mathbf{x_{i-1}})^T \mathbf{C}^{-1} (\mathbf{x_i} - \mathbf{x_{i-1}})}, \tag{5}$$

where $\mathbf{C}$ is the estimated covariance matrix.

For a limited range of HR all parameters x can be approximated by using some mapping $x = f(HR) : \mathbb{R} \to \mathbb{R}$. The same applies to the dependencies between all parameters. As an example, HR is known to modulate QT time. Thus, QT time alone is not relevant measure but function QT(HR) is. Moreover, if value of QT changes a way not predictable by the function QT(HR) the change can be regarded as a change in underlying cardiac state, not just manifestation of changing heart rate (see Fig. 22 for a schematic illustration). Since the true mapping between

a parameter and heart rate is not known in general, we use first and second order polynomials to approximate this relationship locally. Resulting polynomials are then used to calculate fitting error ratio, which is the ratio between residual error of data used for fitting and error of future samples (not used in the fitting) as predicted by the model.

Let us say, we have a parameter vector $\mathbf{x}$ measured over time and corresponding RR interval values stored in vector $\mathbf{y}$. In order to calculate the fitting error ratio, a predefined number of segments is used to fit the first and second order polynomial to data. In general, fitting can be done by solving the following overdetermined system for $\mathbf{p}$

$$\mathbf{y} = \mathbf{A}\mathbf{p}, \tag{6}$$

where $\mathbf{p}$ contains polynomial coefficients and $\mathbf{A}$ is linear mapping between the coefficients and the measurements $\mathbf{y}$. The LMSE estimate for $\mathbf{p}$ is calculated using the Moore-Penrose pseudoinverse:

$$\tilde{\mathbf{p}} = \mathbf{A}^{\dagger}\mathbf{y}. \tag{7}$$

Next, the goodness of fit is evaluated by calculating model predicted values for the data used in fitting and for unseen future data $\mathbf{x}_{fut}$. For fitted data $\tilde{\mathbf{y}} = \mathbf{A}\tilde{\mathbf{p}}$ and for the future data $\tilde{\mathbf{y}}_{fut} = \mathbf{A}_{fut}\tilde{\mathbf{p}}$. Finally, fitting error ratio (FER) is calculated as follows

$$FER = \frac{||\mathbf{y}_{fut} - \tilde{\mathbf{y}}_{fut}||_2}{||\mathbf{y} - \tilde{\mathbf{y}}||_2}. \tag{8}$$

The fitting error ratio is calculated for various parameter pairs and, finally, the value used for ventricular tachyarrhythmia (VTA) prediction is obtained as a sum over the parameter pair FERs.

The idea of the two measures of fast change described above is illustrated in Fig. 22. The green samples are measured parameter and heart rate values that are used to estimate both covariance and linear estimate of the heart rate dependency of the parameter (green dashed line). Red solid line is the true relationship between the parameter and heart rate. Furthermore, blue and red samples represent two possible changes occurring after the green samples. As can be seen in the image, Euclidean distance is not very good measure of change since distance $d2$ is significantly greater than $d1$ in spite of blue samples are just normal values for the parameter at slower heart rates. The equidistant lines of the Mahalanobis distance measure are illustrated as ellipsoids around the sample mean. Thus, Mahalanobis distance gives approximately the same distance for the two possible sample sets. For the fitting error ratio, however, the red samples are notably further from the estimated linear map than blue ones. Consequently, a significant change is detected when progressing from green samples to red ones but not when blue samples are detected.

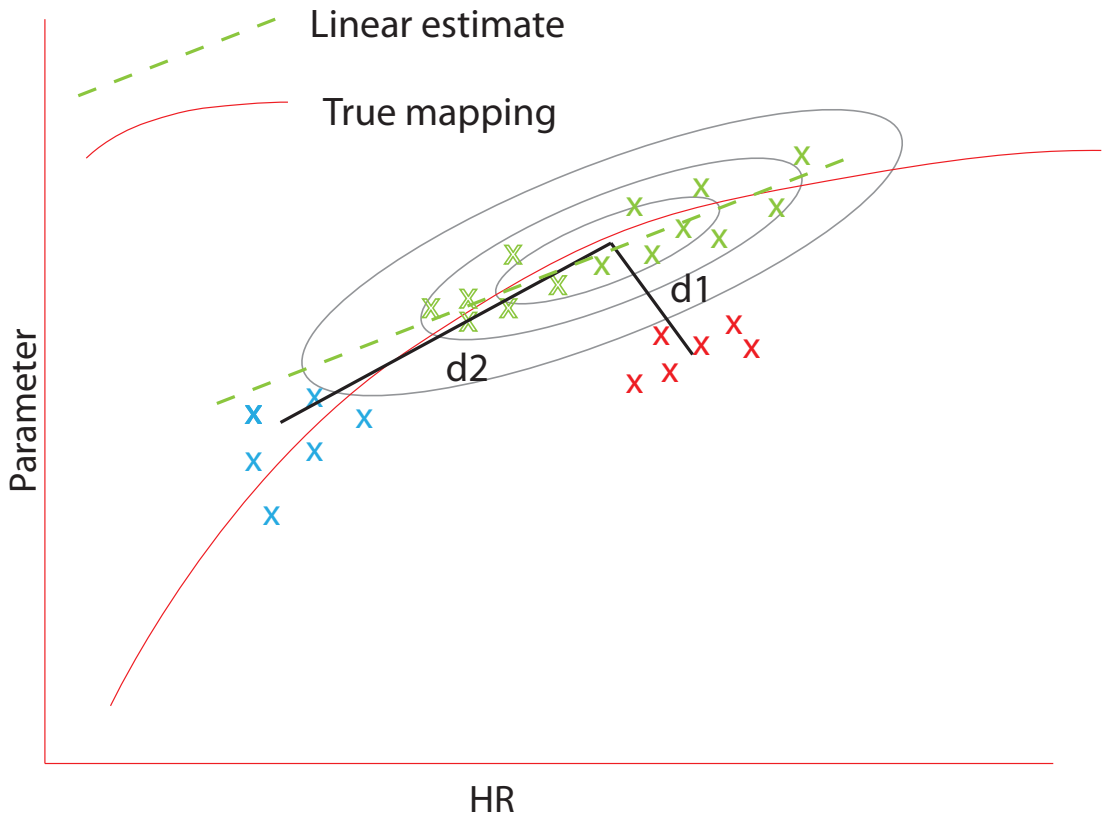

Figure 22: *Green samples are used to calculate the covariance matrix and linear estimate of dependency between two parameters. Red samples are closer to the samples mean than blue ones in Euclidian distance but the distance is approximately the same when Mahalanobis distance is used. The fitting error of the blue samples to the linear estimate is substantially smaler than the fitting error of red samples, thus fitting error ratio is potentially a good measure of change of the state of the heart.*

4.2.6 Transient Change Detection

Slow changes can not be detected easily using Mahalanobis distance or the fitting error ratio (FER), thus, in order to detect these slow changes, an alternative strategy is used. Based on findings in the group level trends in the development data, a subset of parameters is selected and a linear combination of them is calculated to obtain an optimal linear combination (OLC). It may be possible that some linear combination of the measured parameters is better predictor than any parameter

alone. To assess applicability of such a combination, coefficients of the linear projection where optimized to maximize the increase of the linear combination in the training arrhythmia data while minimizing the change among the control cases, see Fig. 23).

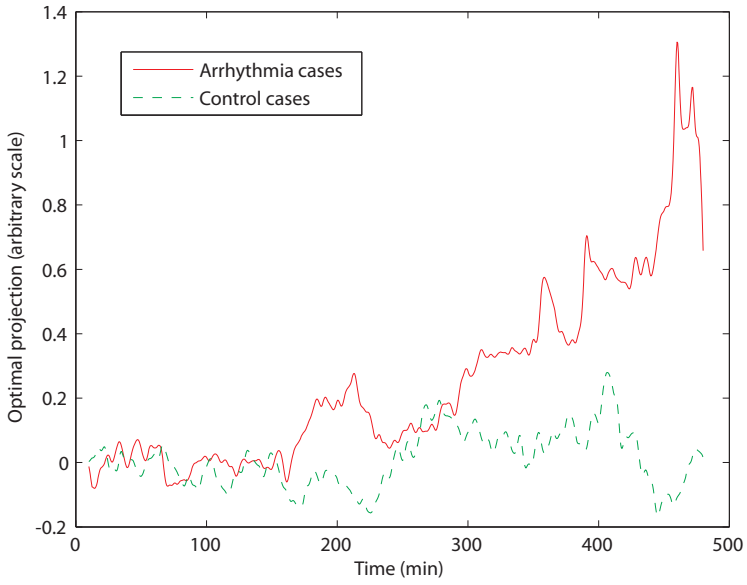

Figure 23: *Time evolution of optimal linear combination (OLC) over arrhythmia and control development data.*

Linear combination signal is calculated for selected parameters with coefficients $\mathbf{a} \in \mathbb{R}^N$ (with N parameters) as follows

$$\mathbf{z} = \begin{bmatrix} z(1) & z(2) & \dots & z(T) \end{bmatrix} = \mathbf{a}^T \begin{bmatrix} \mathbf{x}(1) & \mathbf{x}(2) & \dots & \mathbf{x}(T) \end{bmatrix} = \mathbf{a}^T \mathbf{X}, \tag{9}$$

where $z(t)$ is the linear combination at t and $\mathbf{x}(t) \in \mathbb{R}^N$ is the parameter vector measured at time t.

Mean linear combination signal over a group of M patients is calculated simply by averaging

$$\bar{\mathbf{z}} = \frac{1}{M}(\mathbf{a}^T\mathbf{X}_1 + \mathbf{a}^T\mathbf{X}_2 + \dots \mathbf{a}^T\mathbf{X}_M). \tag{10}$$

Next, we optimize $\mathbf{a}$ so that linear fit to $\bar{\mathbf{z}}$ has maximal slope. The problem is solved by finding the minimizer of the following problem (see Fig. 23 for illustration)

$$\underset{\mathbf{a}}{\operatorname{argmin}} \begin{bmatrix} 0 & -1 \end{bmatrix} \mathbf{A}^\dagger(\mathbf{a}^T\mathbf{X}) - (||\mathbf{a}||_2 - N)^2. \tag{11}$$

Here the first two-element row matrix is just used to select the second term, which corresponds to fitted slope. The last term just constrains norm of the solution to N.

In order to find the minimum, we use Matlab optimization routine *fminsearch*, which finds the minimum of an unconstrained multivariable function using a derivative-free method. The minimizer is

$$\mathbf{a} = \begin{bmatrix} 1.3173 \\ 0.7524 \\ 1.0142 \\ 1.0176 \\ 0.7965 \end{bmatrix}, \tag{12}$$

where the coefficients are for T wave amplitude, asymmetry, area, ST-level and ST slope, respectively.

4.2.7 Arrhythmia Prediction

All the methods presented above aim to one goal, which is prediction of a forthcoming VTA episode. A set of features are extracted from the ECG signal representing current cardiac state. The arrhythmia prediction routine uses this multi-dimensional parameter vector stored at every segment. The idea is to detect certain changes that are manifestations of imminent VTA.

The arrhythmia prediction routine goes through the parameters (Fig. 24) and compares Mahalanobis distance (MD) (Eq. 5), fitting error ratio (FER) (Eq. 8) and optimal linear combination (OLC) (Eq. 9) to respective threshold values. If threshold in d or D is exceeded, control signals are used to ensure that the detection is not caused by an abrupt change in depolarization, classified as secondary repolarization change, T wave measurement position or lead-off resulting to discontinuity in parameter values. If triggered change is not found to be caused by an artifact, or the value selective sum z exceed its threshold value alarm of increased risk of VTA is given.

The threshold values are optimized to give minimally false positives in the training database used in this study. See Section 5.3 for details and illustration of threshold selection.

4.3 Arrhythmia Database

In order to investigate parameter changes hours prior to an arrhythmia, a large long-term ECG database is needed. The reported incidence of IHCA is low, 0.175 events/bed annually including all hospital areas [60, 68], which makes collecting very time consuming and expensive. Fortunately, however, access to a relatively large high-quality database was available for this study. The database used is a subset of the data used in a study by Sachdev et al. [57].

The database was recorded at the CCU of Johns Hopkins University Hospital and Good Samaritan Hospital in Baltimore. Patients with a minimum of 8 hours of ECG data before an event constituted the study group. Patients with atrial arrhythmias,

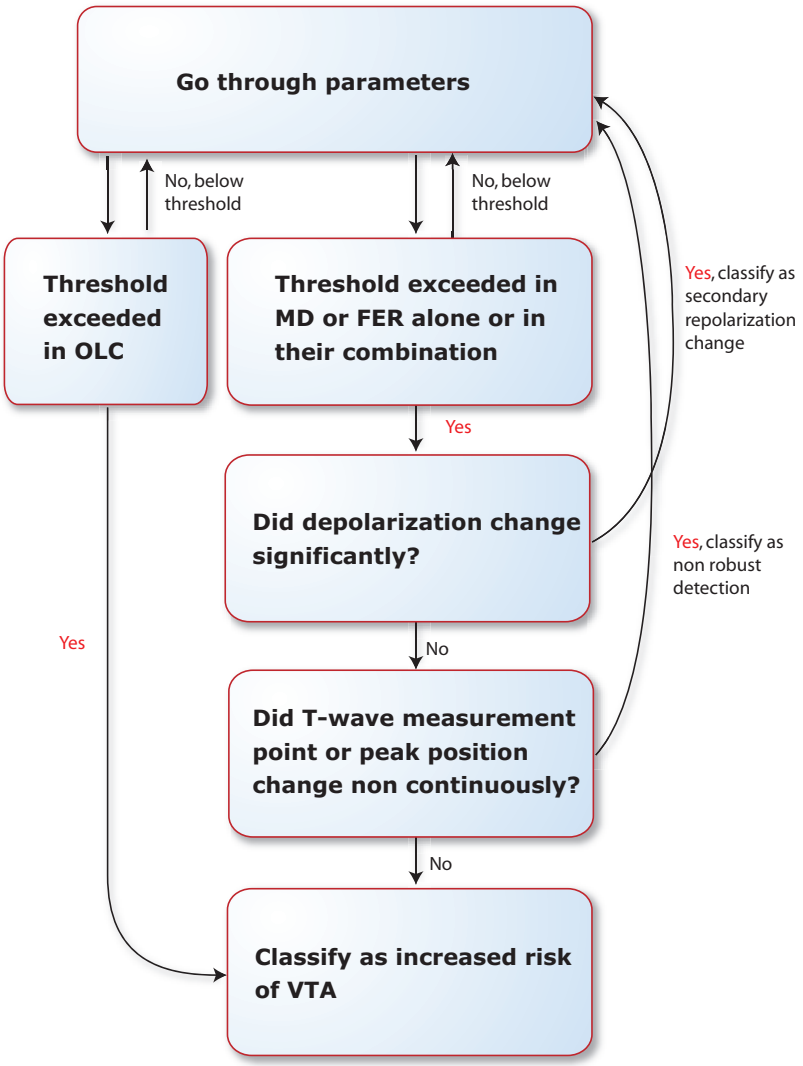

Figure 24: *Overview of the arrhythmia prediction. MD = Mahalanobis distance, OLC = optimal linear combination and FER = fitting error ratio. If the threshold is exceeded in MD, FER or their combination, validity of the prediction is guaranteed by using control signals.*

paced rhythm, frequent PVCs, low signal quality or a conduction block were excluded. Description of the included 60 patient cases is presented in Table 1 and B1 in Appendix B. For further details see the original article by Sachdev et al. [57].

The database was divided into three groups according to an event seen at the end of the recording. "Sustained VT/VF" group consist of patients with ventricular tachyarrhythmia lasting 30 seconds or more, patients in "non-sustained VT/VF" group have an episode with duration between 5 to 30 seconds, and patients in "no event" group are used as controls.

Total of 14 sustained, 9 non-sustained and 37 control patient cases were used in this

study. All cases were used to study the performance of Mahalanbis distance (MD) and fitting error ratio (FER) measures of changes in prediction of VTA episodes. In addition, the data was divided randomly into development and validation data in order to study the performance of optimal linear combination (OLC). The development data consist of 7 sustained, 4 non-sustained and 15 control recordings and validation data consist of 7 sustained, 5 non-sustained and 22 control cases.

Arrhythmia	Sustained	Nonsust	No Event	Total:
Diagnosis				
CAD + AMI	2/1	3/3	5/5	**10/9**
CAD + AP	0/0	0/0	3/3	**3/3**
Ischemic DCM	2/4	0/1	4/2	**6/7**
Non-Isch. DCM	0/1	0/1	1/2	**1/2**
Prim. Electrophys. Ev.	0/0	1/0	1/0	**2/0**
Unknown	3/1	0/0	1/0	**4/1**
Total:	**7/7**	**4/5**	**15/22**	
Demographic info				
Males	43/43 %	80/100 %	53/64 %	
White	57/57 %	50/60 %	60/64 %	
African American	29/29 %	50/40 %	27/27 %	
Other	14/14 %	0/0 %	13/9 %	
Age	67	64	61	
Medication				
Beta-blocker	14/14 %	50/40 %	47/64 %	
Antiarrhythmics	29/43 %	75/60 %	27/41 %	

Table 1: *Demographic description of the data in development/validation databases.*

4.4 Algorithm Development and Validation

To demonstrate the applicability of suggested methods for VTA prediction, some example cases are shown. These examples, however, illustrate the methods for individual patients only and group level conclusions can not be made. Predictive performance of all used methods, i.e. Mahalanobis distance (MD) and fitting error ratio (FER) is evaluated for both sustained VTA and non sustained VTA cases using all the data to tune the respective threshold parameters. Optimal linear combination (OLC) is first optimized in the training data and validated using the validation

data. The performance assessment of each method is calculated by determining the specificity and sensitivity in the training group with varying threshold values. Furthermore, the threshold value for the control signals is optimized to minimize false alarms among the control patients of the training data. Finally, the performance of the algorithm using alarm rules and combination of the individual change detectors is assessed. This is done simply by calculating the number of true/false positives and negatives.

5 Results

In order to observe group level trends, ECG morphology and variation parameters are plotted as a function of time before a VTA episode and the trends are compared to arrhythmia free controls. To demonstrate feasibility of our methods, three patient examples are shown. The examples illustrate our change detection strategy and usefulness of the control parameters in false positive rejection at patient level. The goodness of the change detection methods is evaluated by plotting sensitivity and specificity separately for all change detectors as a function of time. In addition, performance of the arrhythmia prediction algorithm is assessed in sustained and non sustained groups.

5.1 Parameter Trends in Arrhythmia Groups

Mean RR interval is approximately 100 ms faster in sustained group than in non-sustained and control groups (see Fig. 25). Heart rate does not change significantly in any of the groups. Width of the QRS complex, representing depolarization time, is longest in the sustained group suggesting slower conduction speed in this group. This difference is emphasized when higher HR, which increases conduction in normal heart, in the arrhythmia group is taken into account. Differences in the mean ST-level values are relatively small among the groups. However, variation of ST-levels is largest in the sustained group.

The morphology parameters are measured from the magnitude of transformed vector ECG signal and they are plotted in Fig. 25. The mean amplitude and area of T wave demonstrate significant increase in the sustained group compared to others initiating up to 2 hours prior to an event. Flatness of T wave magnitude remains unchanged throughout the measurement in the control group, increases slightly in the sustained group and as an abrupt drop in the non-sustained group. Asymmetry of T wave magnitude increases in the sustained group around 2 hours and in non-sustained group around 1 hour prior to an episode and remains unaltered in the control group.

Observable trends cannot be seen either in T wave amplitude variation or time variation values, Fig. 26. However, amplitude variation peaks just before an arrhythmic event in both arrhythmia groups. Similar findings can be seen in ST lability. Both QT time and Fridericia corrected QT time (QTcF) fail to demonstrate any noticeable trends. Ratio of PVC beats is only slightly increased in the non-sustained group and increases just before an event in both arrhythmia groups.

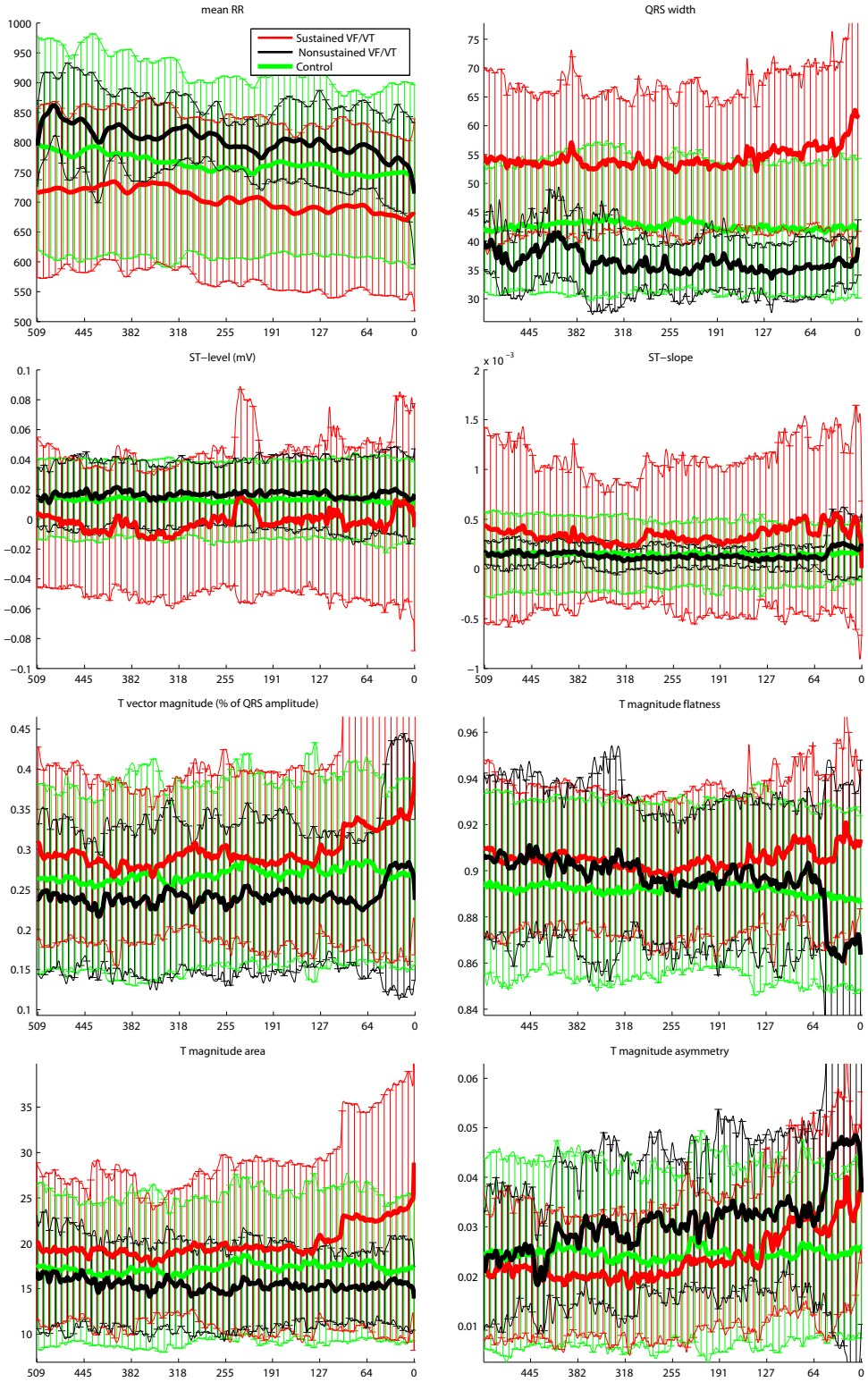

Figure 25: *Trends and variation of RR interval and ECG morphology parameters in different arrhythmia groups before VTA episode.*

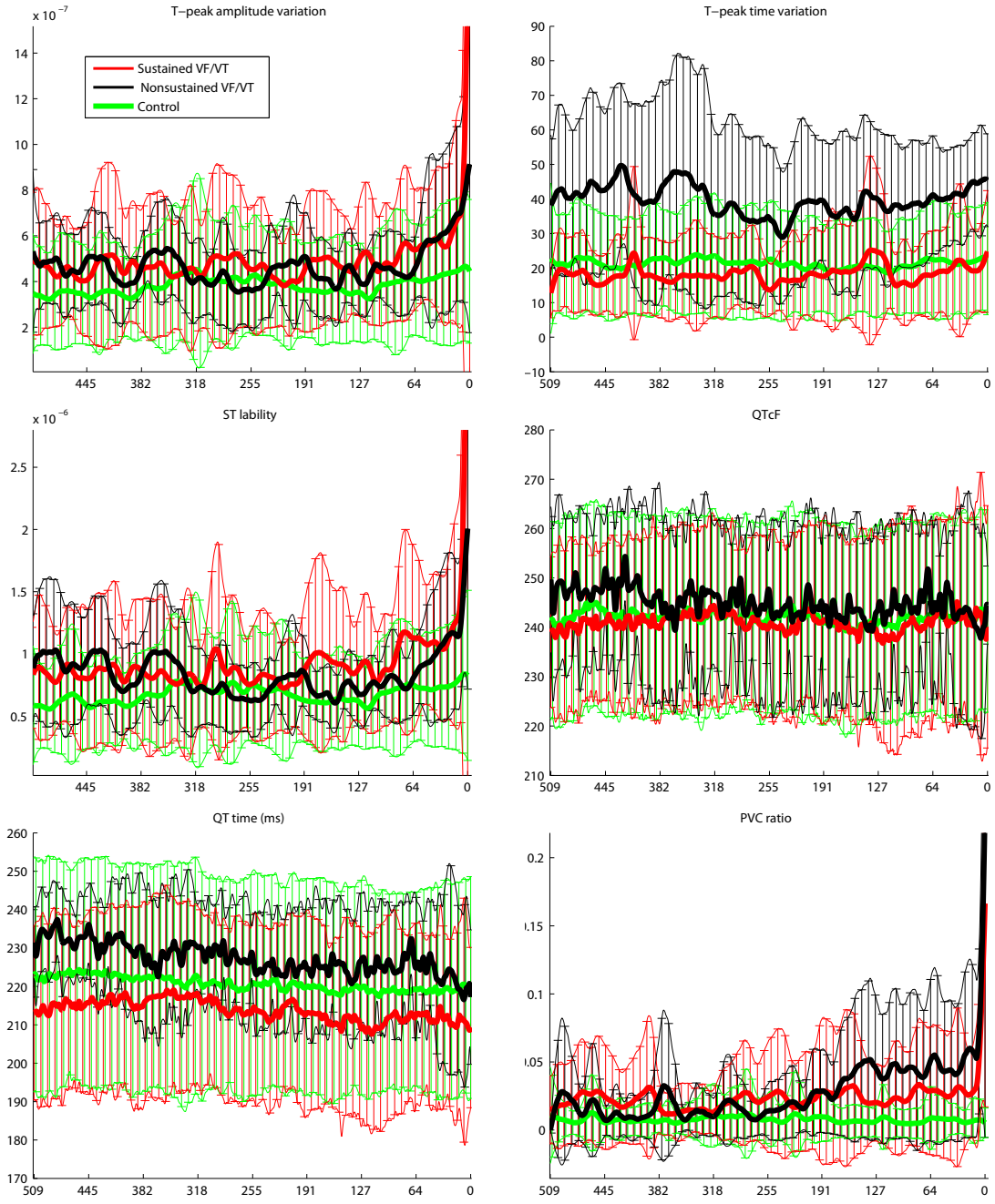

Figure 26: *Trends and variation of variability parameters of repolarization, QT time and PVC ratio in different arrhythmia groups before VTA episode.*

5.2 Characterizing Changes at Patient Level

The group averaged plots presented above do not tell very well what happens to individual patients before ventricular tachyarrhythmia (VTA) episodes. To characterize typical changes, some example cases are presented here in Fig. 27, 28 and 29.

Patients JH191 had ventricular fibrillation at the end of the recording. Two typical relatively fast changes can be seen in Fig. 27. The latter occurs just before 400 minutes has passed from the beginning. Mahalanobis distance is used to detect this step like change and changes in the control signals are within the threshold values. Thus prediction of coming arrhythmia is given about one hour before the episode.

Patient JH120 had a VTA episode at the end of the recording. About 2 hours prior to the onset of the event, the mapping between RR interval and T wave area changes. Fitting error ratio is used to detect this change and prediction of approaching arrhythmia is given up to 2 hours before the event.

To illustrate the importance of control signals, thirds example is given in Fig. 29. Patient JH128 belongs to the control group and does not have any arrhythmia during the monitoring. 350 minutes after initiation of the monitoring a spike in the Mahalanobis distance is detected. This would cause a false alarm if control signals were not taken into account. One can see that the ratio of rejected to accepted complexes spikes simultaneously with the Mahalanobis and the position of T wave maximum changes abruptly, which causes rejection of the prediction.

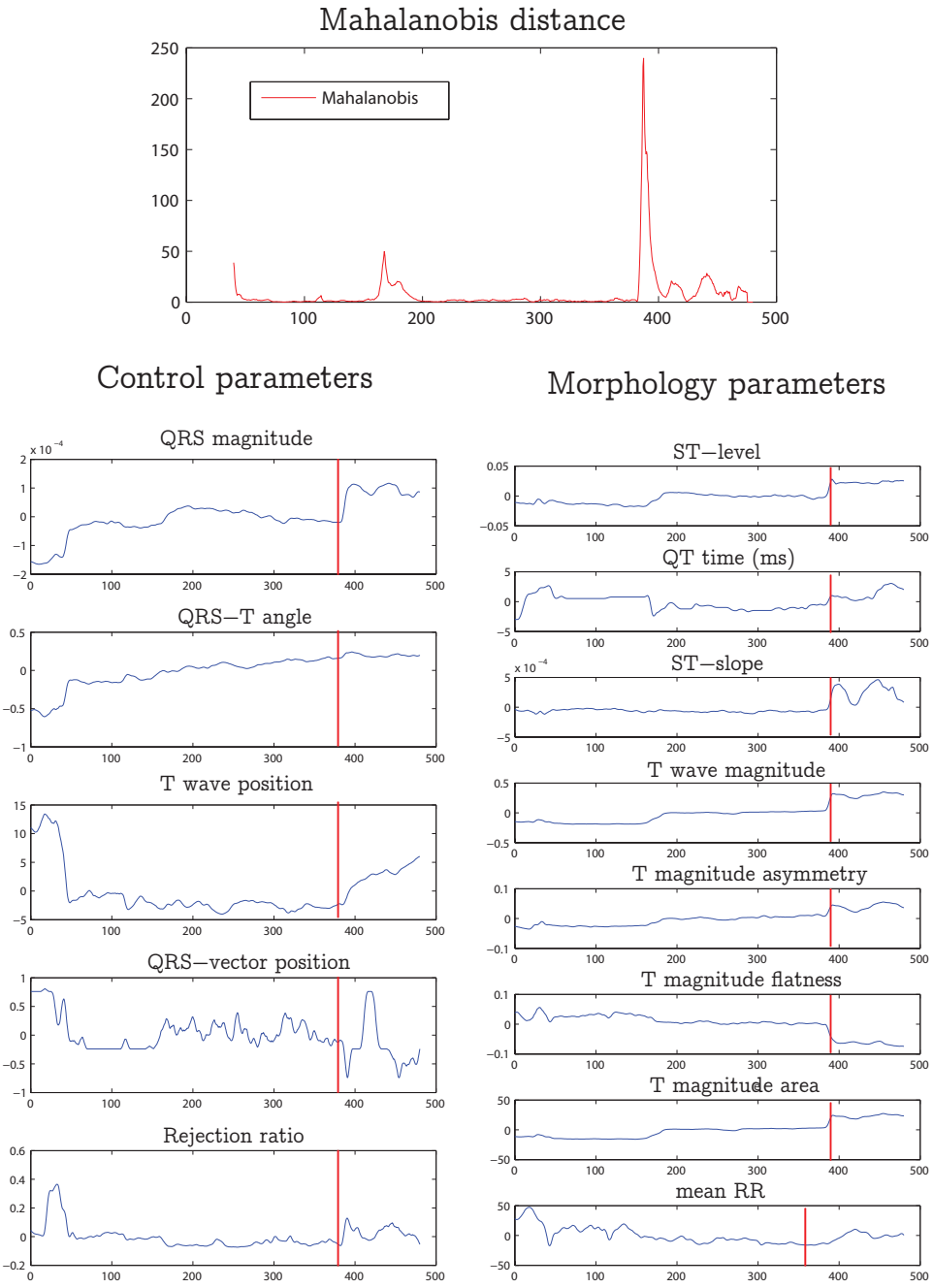

Figure 27: *An example of change in patient JH191 before an arrhythmia detected by sliding window Mahalanobis distance (see Eq. 5). No major discontinuity can be observed in control signal and prediction is not rejected.*

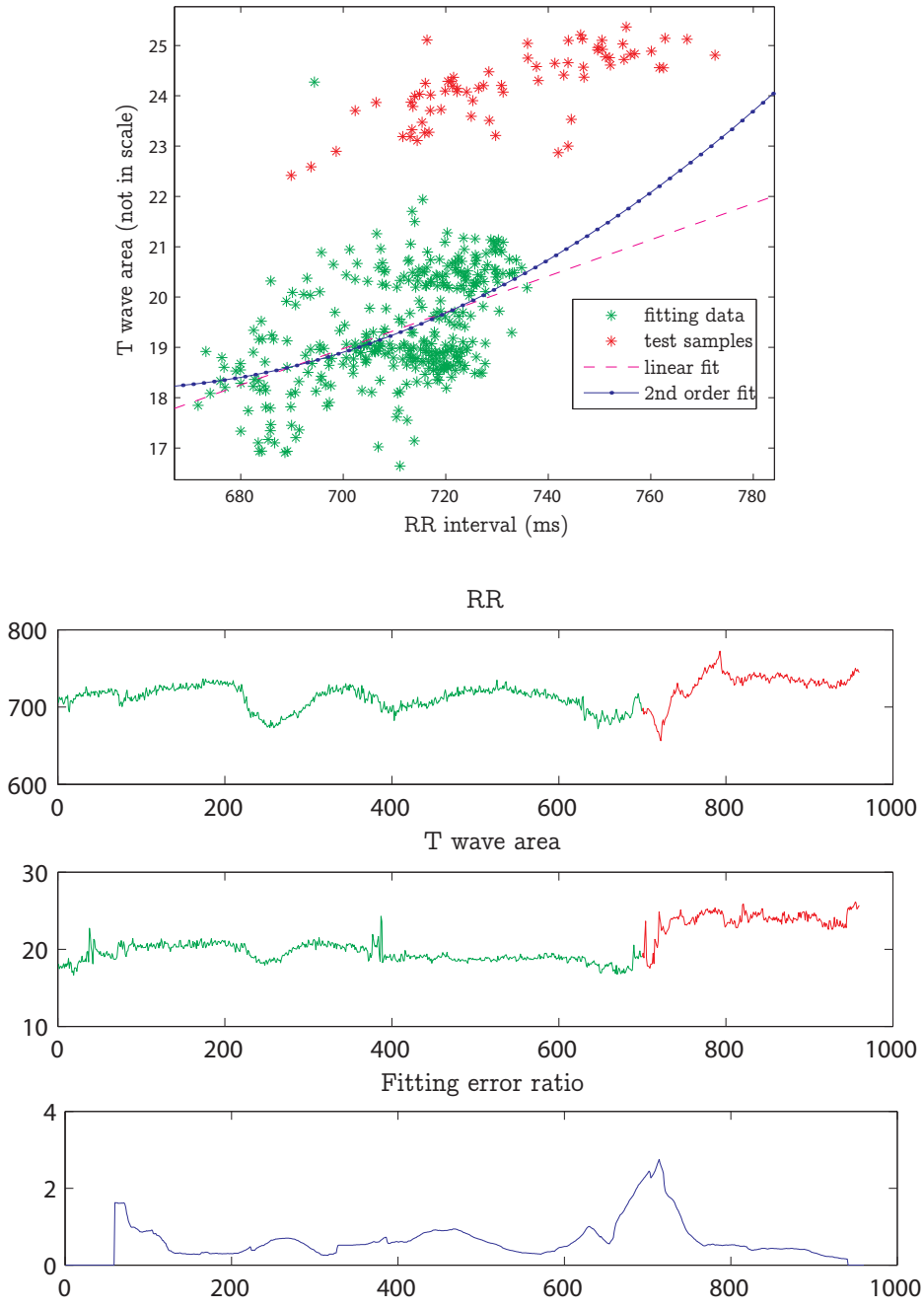

Figure 28: *An example of change in patient JH120 before an arrhythmia detected by fitting error ration (FER) (see Eq. 8).*

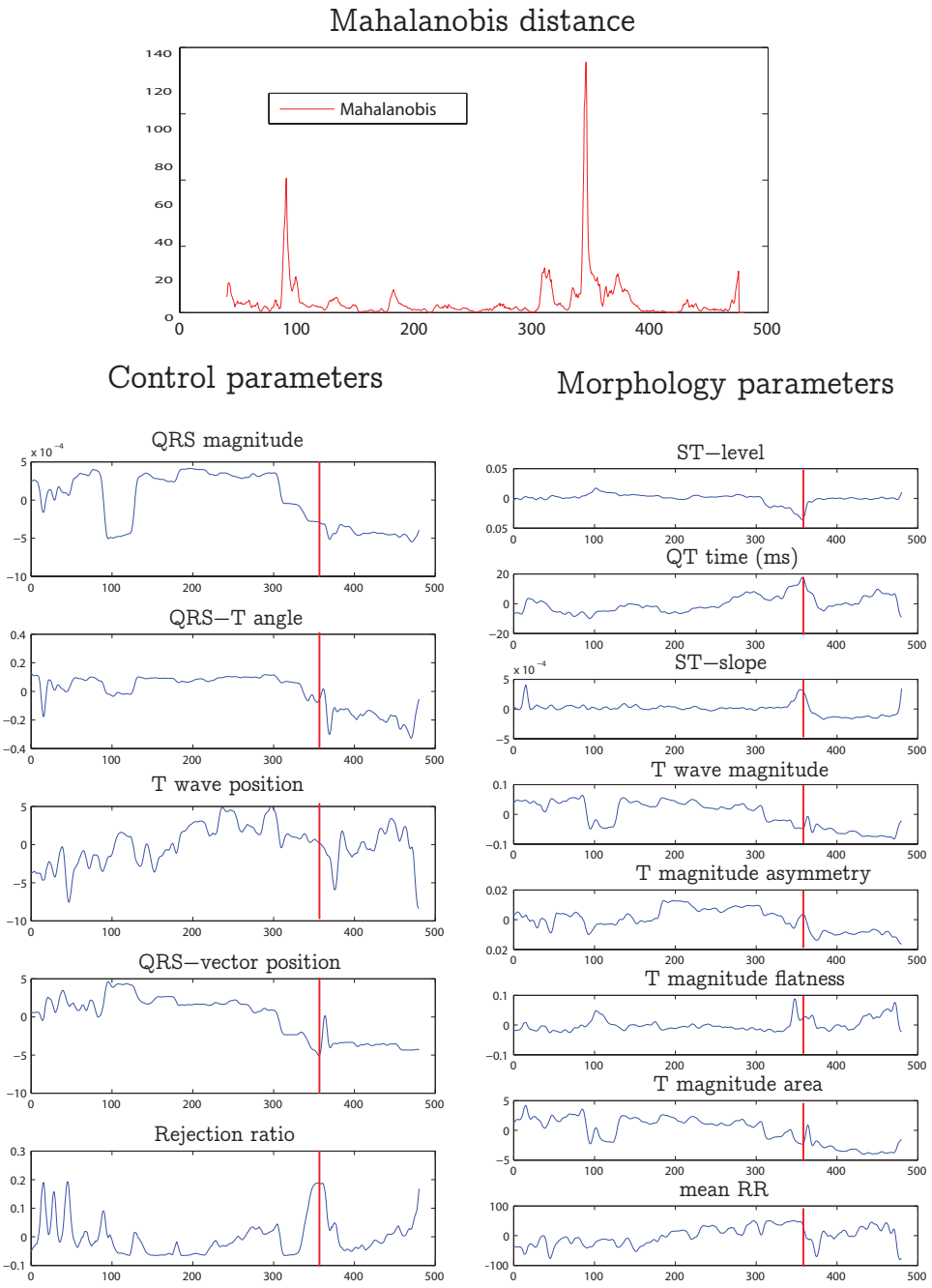

Figure 29: *Example of sudden change in patient JH128 related to changed depolarization detected by sliding window Mahalanobis distance function (see Eq. 5). Control signal can be used to identify false detection.*

5.3 Predictive Performance of the Change Detectors

The performance of the measures of change were evaluated using all the data for Mahalanobis distance (MD) and fitting error ratio (FER) and threshold values for them were tuned to minimize false negatives in this patient population (see Fig. 30 and 31). In addition, development data was used to find optimal linear combination of parameters and validation data was used to assess the usefulness of optimal linear combination (OLC) measure in VTA episode prediction.

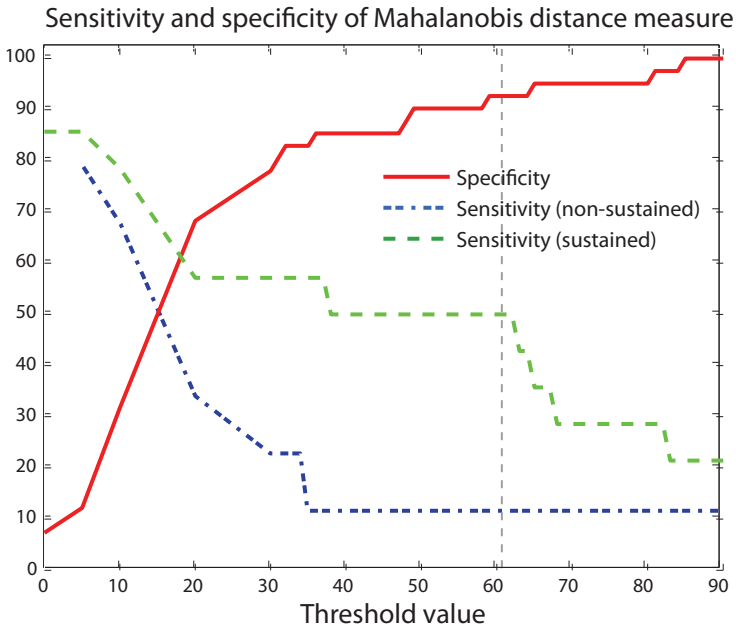

Figure 30: *Sensitivity and specificity as a function of a threshold value for Mahalanobis distance (MD) and optimized linear combination (OLC). Threshold values are drawn as dashed vertical lines.*

According to our results, Mahalanobis distance seems to be the best predictor of imminent VTA episodes while maintaining acceptable specificity. In our data it can predict approximately 50 % of the sustained cases with 93 % specificity whereas optimal linear combination and fitting error ratios achieve sensitivity of approximately 20 % each without false positive predictions. OLC was able to predict 44 % of the sustained cases in the development data but only 15 % in validation data.

For non sustained cases all the predictors seem to give disappointingly low sensitivity. MD is able to predict only 10 % of the VTA in this group. Both FER-based triggers fail to predict any arrhythmia while maintaining acceptable sensitivity.

Combination of MD and first order FER requires both measures to be above predefined threshold values. Specificity and sensitivity of this rule as a function of threshold value is illustrated for both measures separately in Fig. 33. Threshold values are defined to give around 30 % sensitivity and 95 % specificity.

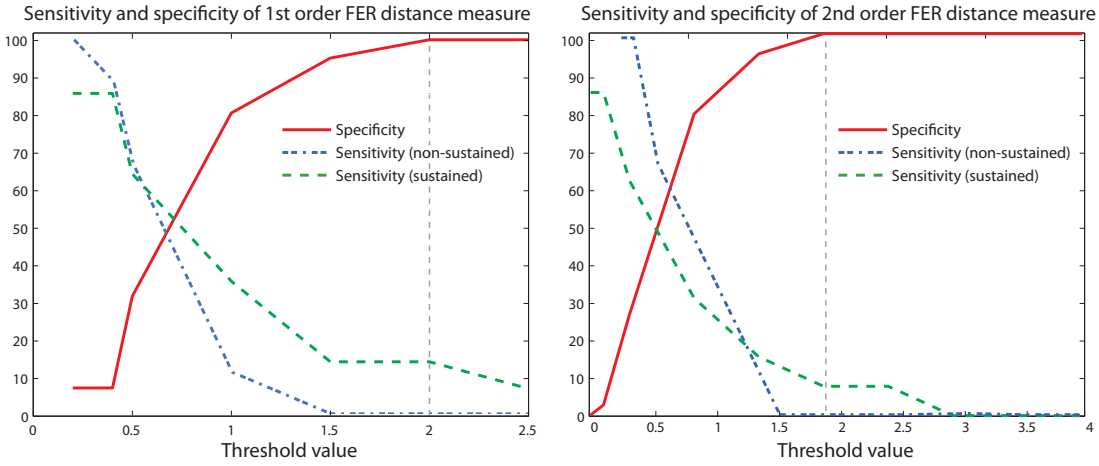

Figure 31: *Sensitivity and specificity as a function of a threshold value for 1st and 2nd order polynomial local fit based detectors, i.e. fitting error ratio (FER). Threshold values are denoted as dashed vertical lines.*

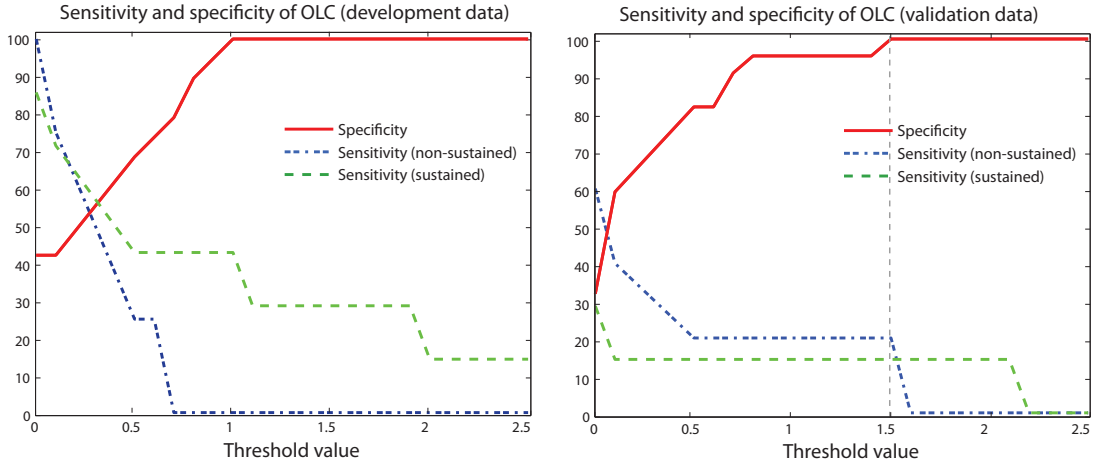

Figure 32: *Sensitivity and specificity as a function of a threshold value for optimal linear combination (OLC) in training and validation data.*

5.4 Predictive Performance

The performance of the arrhythmia prediction algorithm is evaluated using the database of 60 patients (14 sustained, 9 non sustained and 37 controls). Only three of the 37 arrhythmia free signals were classified as arrhythmia resulting to 3 false positive and 34 true negatives. Thus, specificity of the algorithm is around 0.93. Seven cases in the sustained arrhythmia group of 14 cases were classified correctly giving 9 false negatives and, consequently, sensitivity of 0.50. Positive and negative predictive values are 0.70 and 0.85, respectively, see Tab. 2. In non sustained arrhythmia group the algorithm detected only one cases out of 9 true events. This suggests that

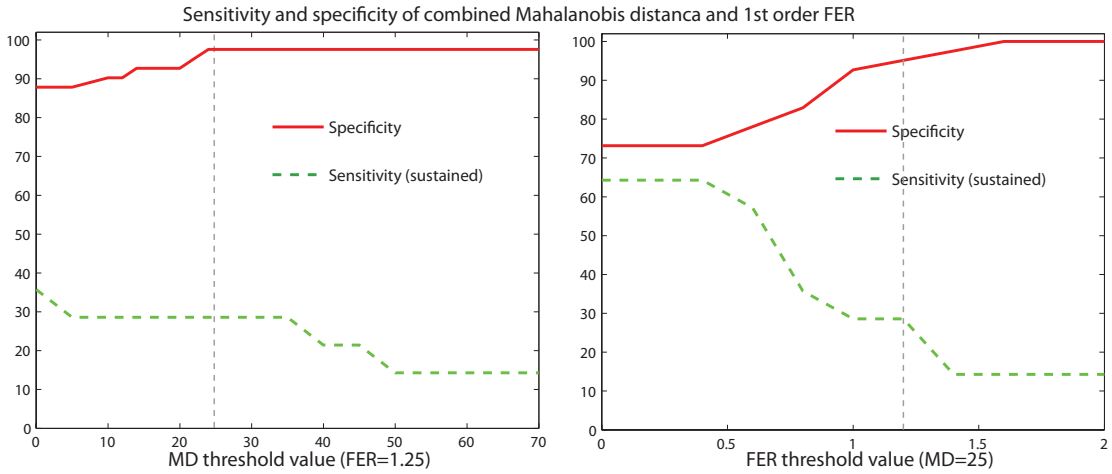

Figure 33: *Sensitivity and specificity as a function of a threshold value for combination rule of Mahalanobis distance (MD) and fitting error ratio (FER). Left: FER threshold value is fixed to 1.25 and on right MD threshold value is fixed to 25.*

sensitivity of the algorithm in the non sustained group is approximately 11 % and specificity is 93 %, see Tab. 3. The mean time from the alarm to the initiation of an episode is 275 minutes (see Fig. 34).

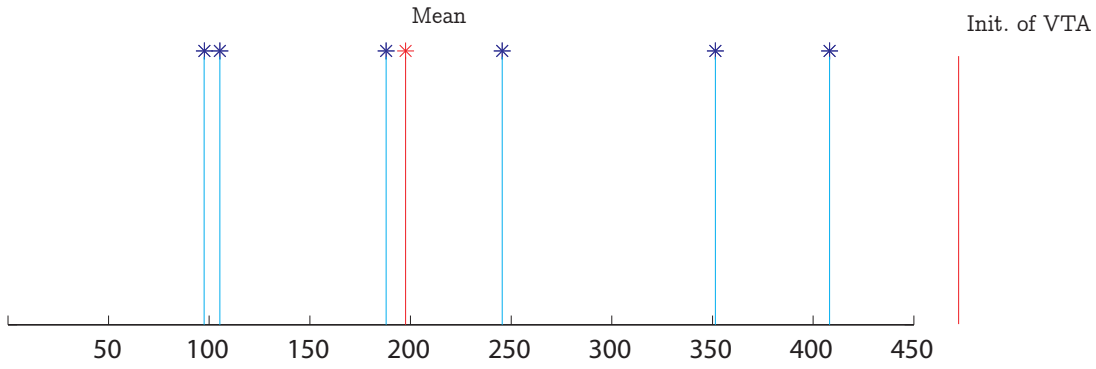

Figure 34: *Alarm times.*

These measures alone are inadequate in assessing the performance of the algorithm. The usefulness of the algorithm can be evaluated by considering sensitivity and specificity in relation to the true incidence of episodes. As mentioned earlier the incidence of VTA episodes in CCU is around 1-5 % [29]. Let's assume, for example, an incidence rate of 1 %. If average time in CCU was 48 hours and there were 5 beds in the unit, 9 patients out of 900 would experience an episode of VTA annually. On

average, VTA would be predicted in 4.5 cases. Based on the results, our algorithm gives one false alarm during 176 hours of monitoring. Thus, one monitor would give 49 false alarms annually, about one per week.

	Patient			
Result	**Arrhythmia**	**Control**		
Detection	**7**	**3**	0.70	PPV
No detection	**7**	**41**	0.85	NPV
	0.50	0.93		
	Sensitivity	Specificity		

Table 2: *Predictive performance of the algorithm for sustained VTA patients.*

	Patient			
Result	**Arrhythmia**	**Control**		
Detection	**1**	**3**	0.25	PPV
No detection	**8**	**41**	0.84	NPV
	0.11	0.93		
	Sensitivity	Specificity		

Table 3: *Predictive performance of the algorithm for non sustained VTA patients.*

6 Conclusions

6.1 Conclusions of the Results

6.1.1 Group Trends

The most common finding in the literature prior to ventricular tachyarrhythmias is an increase of heart rate (HR). The change in HR may cause the change of other parameters. However, HR does not change significantly in either of the arrhythmia groups and can not explain the observed trends in this study. Furthermore, changes in the ST segment of ECG are known to be sensitive of ischemic conditions in the myocardium. All three groups contain approximately same proportion of ischemia related conditions. Thus, it is unlikely that the differences can be explained only by properties of the study groups. However, variance in all parameters is high, which is a result of high inter-subject variability and reduces statistical power of the results. Furthermore, due to small study population, differences in the group means can not be considered statistically significant and the impact of a single outlier in the group can be significant.

Based on our results, the most relevant morphology parameters distinguishing the arrhythmia cases from the controls are T wave magnitude, area, asymmetry and ST-slope. Among variational parameters, both T peak amplitude variation and maximal variation in ST segment, i.e. ST lability, demonstrate slight increase in both arrhythmia groups compared to the control group. These changes could be a manifestation of increased spatio-temporal repolarization.

It was concluded in our review in chapter 3 that it is unlikely that VTA prediction succeeds when one uses parameter trends as a sole input to a prediction algorithm. Indeed, our results confirm this conclusion.

6.1.2 Prediction Performance

There were three false positive in our study and, consequently, our estimate of the specificity of the algorithm, 0.93, is surprisingly good. The size of the control group is only 37 cases (296 hours), which decreases reliability of our estimate. In order to get more reliable estimate of specificity, a much larger database of control recordings would be needed.

In the study, 7 out of 14 patients in the sustained group triggered alarm whereas only one out of 5 patients was classified as arrhythmia in the non sustained group. This gives relatively good estimate of sensitivity for sustained VTA group and poor for non-sustained group, 50 % and 0.11 %, respectively. Thus, it seems that with our algorithm, sustained arrhythmias are predictable whereas non sustained arrhythmias are not. This finding supports the idea that short VT/VF episodes may be just random whereas for an arrhythmia to persist detectable changes in the heart must take place.

The mean time from alarm to initiation of an episode was around 275 minutes. Even the shortest time, 10 minutes, is reasonably long time if one planned to use some preventive strategies or just increase the alertness of the staff.

Mahalanobis distance (MD) and fitting error ratio (FER) measures are based purely on change detection. The database was too small to facilitate the usage of any more intelligent classification methods to classify the change. It can be assumed, however, that common characteristics could be found from changes and they cold be used to decrease false alarms.

Optimal linear combination demonstrated promising trend in training data and was able to detect 30 % of the cases. In validation data, however, only one case was detected both in sustained and non sustained data. This suggests that our method was unable to learn anything general from the training set that could be used for prediction in general.

6.2 Issues with the Data

Difficulties in obtaining noise-free electrocardiographic data immediately preceding a lethal arrhythmia is a major disadvantage in development of predictive algorithms. Analysis of implantable cardioverter defibrillator (ICD) data is limited by the storage capacity of the devices, and the advantages of Holter data are offset by the low probability of capturing such events in an ambulatory population. In addition, this study demonstrates that the duration of the recordings should be at least 4 hours in order to be usable in predictive algorithm development.

Due to above-mentioned problems the size of database used is usually very limited and there is a lack of high quality ECG databases with lethal arrhythmias. In addition, heterogeneity of the population (medication, diseases) and measurement setup (channels used) is a major problem. To conclude, current databases are often noisy and as predictive algorithms require high signal to noise ratio, this provides extra challenges for algorithm development.

6.3 On Building an Automatic Arrhythmia Prediction Algorithm

The ultimate goal of this thesis was to build an automatic algorithm capable of estimating the risk of lethal arrhythmias. Here are some suggestions what to take into account when implementing such an algorithm. Firstly, no stationarity assumptions can be made due to the unstationary nature of ECG preceding VTA episodes. This means that most of the traditional and trendy measures will fail to measure anything useful from the ECG that is not even approximately stationary. Secondly, one needs to consider intra-subject variability more carefully and it may be necessary to distinguish patients with different medication, illness, current state and history. To conclude, the risk of VTA/SCD evolves over time with changes in

electrophysiologic substrate, environmental and physiologic triggers, and the impact of other physiologic (e.g. circadian) rhythmicity [66]. Thus, the parameters per se are highly non-specific and should be investigated with relation to other parameters, patient state and history.

Based on the findings from this study an abnormal change in the heart seems to trigger arrhythmias. Thus, it may be that change in cardiac state itself, not its direction, is essential in the initiation. Furthermore, it seems that both fast and slow changes are relevant but may require different methods for detection. The inconsistencies most likely arise from the differences in the underlying physiologic mechanisms driving the instabilities in different settings, leading to a common end point from a multitude of subcellular, intracellular, and multicellular processes. In real-life setting, electrophysiologic data are usually collected at the time when at least some of the covariates exhibit simultaneous changes. Thus, algorithms are needed to differentiate the respective impacts and weights of each participating covariate. The practical implementation of the algorithm requires continuous tracking of individual repolarization dynamics, along with other electrophysiologic parameters, including changes in heart rate, QRS duration (i.e. conduction), circadian variability, physical activity, and physiological status. Improvements can also be achieved by tracking the changes against individual baseline and using "personalized" pattern recognition analysis. [66]

6.4 Potential Benefits in Clinical Settings

An algorithm that predicts lethal ventricular arrhythmias will reduces delay of resuscitation by increasing alertness of the staff and enabling preventive means. Arrhythmias that are defibrillable, decreased delay before initiation of CPR is known to increase likelihood of survival and reduce disabling neurological damage. It is likely that some preventable episodes could be avoided if predictive algorithm was used for hight risk patients, e.g. in CCU. Furthermore, continuous monitoring of vital signals using simple, cost-effective and wireless monitoring in the general ward areas would enable observation of the slow deterioration, would support decision making, reduce the work load of nurses and other healthcare professionals and increases alertness.

6.5 Future Development and Suggestions

It is obvious that to confirm the findings presented in this thesis, one would need to repeat the analysis using much larger amount of data with separate training and learning data. The original idea in this thesis was to learn patterns of features preceding episodes and to test if these patterns are present in the validation data. Because of scarcity of data this remains to be done, however. Furthermore, it would be interesting to test which parameters work for different patient classes, like morphology for ischemia and alternans for myopathy.

An interesting topic in future research would be exploitation of multi-parameter

monitoring already frequent in intensive and coronal care units. For example, monitoring electrical and mechanical properties simultaneously, e.g. ECG and arterial blood pressure, would enable evaluation of any changes in the electromechanical coupling of the myocardial cells, which is assumed to cause arrhythmias [56].

Current trend in monitoring is toward continuous around a clock monitoring and telemetry, wireless, low-power consuming invasive sensors. This opens new possibilities for predictive algorithms, too. Ubiquitous monitoring could mean numerous people would benefit from arrhythmia prediction algorithms. However, even though we know which ECG or other cardiovascular changes precede ventricular arrhythmias and SCD, we have no idea who to monitor. This results from the fact that the majority of sudden deaths occur out-of-hospital in apparently healthy individuals who show little clinical evidence of latent heart disease during their life [58]. This question remains to be unanswered.

In order to make research in the field more efficient it is important to identify the patient groups that would benefit the most from prevention and for which it is possible to prevent the onset in the first place. Then, target the algorithm development for these patients.

References

[1] General Electric Healthcare EK-Pro whitepaper. `http://clinicalview.gehealthcare.com/download.php?obj_id=207&browser=true`, 2011.

[2] J. G. Akar and F. G. Akar. Mapping arrhythmias in the failing heart: from Langendorff to patient. *Journal of Electrocardiology*, 39:19–23, 2006.

[3] M. P. Andersen, J. Q. Xue, C. Graff, T. B. Hardahl, E. Toft, J. K. Kanters, M. Christiansen, H. K. Jensen, and J. J. Struijk. A robust method for quantification of IKr-related T-wave morphology abnormalities. *Computers in Cardiology*, 34:341–344, 2007.

[4] M. P. Andersen, J. Q. Xue, C. G. Graff, J. K. Kanters, E. Toft, and J. J. Struijk. New descriptors of T-wave morphology are independent of heart rate. *Journal of Electrocardiology*, 41:557–561, 2008.

[5] K. P. Anderson, V. Shusterman, B. Aysin, R. Weiss, S. Brode, and V. Gottipaty. Distinctive RR dynamics preceding two modes of onset of spontaneous sustained ventricular tachycardia. (ESVEM) Investigators. Electrophysiologic Study Versus Electrocardiographic Monitoring. *Journal of Cardiovascular Electrophysiology*, 10:897–904, 1999.

[6] J. A. Belloch, M. S. Guillem, A. Climent, J. Miller, D. Husser, and A. Bollman. Comparison of Different Methods for the Derivation of the Vectocardiaogram from the ECG and Morphology Descriptors. *Computers in Cardiology*, 34:435–438, 2007.

[7] G. Berlot, A. Pangher, L. Petrucci, and R. Bussani. Anticipating events of in-hospital cardiac arrest. *European Journal of Emergency Medicine*, 11:24–28, 2004.

[8] W. E. Cascio, H. Yang, B. J. Muller-Borer, and T. A. Johnson. Ischemia-induced arrhythmia: the role of connexins, gap junctions, and attendant changes in impulse propagation. *Journal of Electrocardiology*, 38:55–59, 2005.

[9] G. D. Clifford. *Mechanisms and Management of Cardiac Arrhythmias*. BMJ Publishing Group, 1st edition, 2001.

[10] G. D. Clifford, F. Azuaje, and P. McSharry. *Advanced Methods and Tools for ECG Data Analysis*. Artech House, 1st edition, 2006.

[11] G. D. Clifford and L. Tarassenko. Quantifying errors in spectral estimates of HRV due to beat replacement and resampling. *IEEE Transactions on Bio-Medical Engineering*, 52:630–638, 2005.

[12] J. P. Couderc, W. Zareba, X. Xia, M. Andrew, and A. J. Moss. T-wave morphology and arrhythmic events in patients with dilated cardiomyopathy. *Computers in Cardiology*, 30:149–152, 2003.

[13] D. di Bernardo, P. Langley, and A. Murray. Effect of changes in heart rate and in action potential duration on the electrocardiogram T wave shape. *Physiological Measurement*, 23:355–364, 2002.

[14] D. Di Bernardo and A. Murray. Modelling cardiac repolarisation for the study of the T wave: effect of repolarisation sequence. *Chaos, Solitons & Fractals*, 13:1743–1748, 2002.

[15] B. H. Diem, C. Stellbrink, M. Michel, P. Schauerte, and P. Hanrath. Temporary disturbances of the QT interval precede the onset of ventricular tachyarrhythmias in patients with structural heart diseases. *Pacing and Clinical Electrophysiology*, 25:1413–1418, 2002.

[16] P. P. Domitrovich and P. K. Stein. A new method to detect erratic sinus rhythm in RR-interval files generated from Holter recordings. *Computers in Cardiology*, pages 665–668, 2002.

[17] L. Fei. Shortening of the QT interval immediately preceding the onset of idiopathic spontaneous ventricular tachycardia. *American Heart Journal*, 130:915–917, 1995.

[18] H. Gombotz, B. Weh, W. Mitterndorfer, and P. Rehak. In-hospital cardiac resuscitation outside the ICU by nursing staff equipped with automated external defibrillators–the first 500 cases. *Resuscitation*, 70:416–422, 2006.

[19] C. Haarmark, C. G. Graff, M. P. Andersen, T. Hardahl, J. J. Struijk, E. Toft, J. Xue, G. I. Rowlandson, P. R. Hansen, and J. K. Kanters. Reference values of electrocardiogram repolarization variables in a healthy population. *Journal of Electrocardiology*, 43:31–39, 2010.

[20] G. Hanton and Y. Racaud. Temporal variability of QT interval and changes in T wave morphology in dogs as markers of clinical risk of drug-induced proarrhythmia. *Journal of Pharmacological and Toxicological Methods*, 57:194–201, 2008.

[21] H. M. Hastings, F. H. Fenton, S. J. Evans, O. Hotomaroglu, J. Geetha, K. Gittelson, J. Nilson, and A. Garfinkel. Alternans and the onset of ventricular fibrillation. *Physical review E*, 62:4043–4048, 2000.

[22] J. Heikkilä, H. Huikuri, K. Luomanmäki, M. Nieminen, and K. Peuhkurinen. *Kardiologia*. Duodecim, 1st edition, 2000.

[23] J. Heikkilä and M. Mäkijärvi. *EKG*. Duodecim, 1st edition, 2003.

[24] T. J. Hodgetts, G. Kenward, I. Vlackonikolis, S. Payne, N. Castle, R. Crouch, N. Ineson, and L. Shaikh. Incidence, location and reasons for avoidable in-hospital cardiac arrest in a district general hospital. *Resuscitation*, 54:115–123, 2002.

[25] H. Huikuri, A. Castellanos, and R. J. Myerburg. Sudden death due to cardiac arrhythmias. *New England Journal of Medicine*, 345:1473–1482, 2001.

[26] H. Huikuri, T. Seppänen, J. Koistinen, J. Airaksinen, M. J. Ikäheimo, A. Castellanos, and R. Myerburg. Abnormalities in beat-to-beat dynamics of heart rate before the spontaneous onset of life-threatening ventricular tachyarrhythmias in patients with prior myocardial infarction. *Circulation*, 93:1836–1844, 1996.

[27] H. Huikuri, J. Tapanainen, K. Lindgren, and P. Raatikainen. Prediction of sudden cardiac death after myocardial infarction in the beta-blocking era. *Journal of American College of Cardiology*, 42:652–658, 2003.

[28] H. Huikuri, J. Valkama, K. Airaksinen, T. Seppänen, K. M. Kessler, J. T. Takkunen, and R. J. Myerburg. Frequency domain measures of heart rate variability before the onset of nonsustained and sustained ventricular tachycardia in patients with coronary artery disease. *Circulation*, 87:1220–1228, 1993.

[29] J. Hulting. In-hospital ventricular fibrillation and its relation to serum potassium. *Acta Medica Scandinavica Supplementum*, 209:109–116, 1981.

[30] J. Jalife, M. Delmar, J. M. Davidenko, and J. Anumonwo. *Basic cardiac electrophysiology for the clinician*. Futura Publishing Company, 1st edition, 1999.

[31] H. Jin, A. R. Lyon, and F. G. Akar. Arrhythmia mechanisms in the failing heart. *Pacing and Clinical Electrophysiology*, 31:1048–1056, 2008.

[32] S. Kurokawa, S. Niwano, M. Kiryu, M. Murakami, S. Ishikawa, Y. Yumoto, N. Moriguchi, H. Niwano, T. Kosukegawa, and T. Izumi. Importance of morphological changes in T-U waves during bepridil therapy as a predictor of ventricular arrhythmic event. *Circulation Journal*, 74:876–884, 2010.

[33] G. Larkin, W. Copes, B. Nathanson, and W. Kaye. Pre-resuscitation factors associated with mortality in 49,130 cases of in-hospital cardiac arrest: a report from the National Registry for Cardiopulmonary Resuscitation. *Resuscitation*, 81:302–311, 2010.

[34] C. Lerma, N. Wessel, A. Schirdewan, J. Kurths, and L. Glass. Ventricular arrhythmias and changes in heart rate preceding ventricular tachycardia in patients with an implantable cardioverter defibrillator. *Medical & Biological Engineering & Computing*, 46:715–727, 2008.

[35] A. Lewicke, K. Bellor, K. Dillon, T. Kaib, S. Szymkiewicz, and S. Schuckers. Exploiting QT interval changes as a precursor to the onset of ventricular fibrillation/tachycardia. *Journal of Electrocardiology*, 42:374–379, 2009.

[36] F. Lombardi, A. Porta, M. Marzegalli, S. Favale, M. Santini, A. Vincenti, and A. De Rosa. Heart rate variability patterns before ventricular tachycardia onset in patients with an implantable cardioverter defibrillator. Participating Investigators of ICD-HRV Italian Study Group. *The American Journal of Cardiology*, 86:959–963, 2000.

[37] M. Malik. *Risk of Arrhythmia and Sudden Death*. BMJ Publishing Group, 1st edition, 2001.

[38] M. Malik, Y. Birnbaum, R. MacLeod, and V. Shusterman. Markers of impaired repolarization. *Journal of Electrocardiology*, 40:54–57, 2007.

[39] J. Malmivuo and R. Plonsey. *Bioelectromagnetism: Principles and Applications of Bioelectric and Biomagnetic Fields*. Oxford University Press, 1st edition, 1995.

[40] H. J. Marriot and M. B. Conover. *Advanced Concepts in Arrhythmias*. Mosby, 3rd edition, 1998.

[41] P. Maury, J. L. Pasquié, F. Raczka, L. Beck, J. Taieb, A. Duparc, B. Hallier, and et al. Feasibility of measurement of endocardial T wave alternans prior to onset of ventricular arrhythmias in ICDs (ETWAS study). *Archives of Cardiovascular Diseases Supplements*, 2:62, 2010.

[42] P. Maury, F. Raczka, J. L. Pasquie, L. Beck, and J. Taieb. Changes in T wave morphology prior to onset of ventricular arrhythmias in ICDs. *Archives of Cardiovascular Disease Supplements*, 2:64–65, 2010.

[43] U. Meyerfeldt, N. Wessel, H. Schütt, D. Selbig, A. Schumann, A. Voss, J. Kurths, C. Ziehmann, R. Dietz, and A. Schirdewan. Heart rate variability before the onset of ventricular tachycardia: differences between slow and fast arrhythmias. *International Journal of Cardiology*, 84:141–151, 2002.

[44] T. Mäkikallio, J. Koistinen, L. Jordaens, M. P. Tulppo, N. Wood, B. Golosarsky, C. K. Peng, A. L. Goldberger, and H. Huikuri. Heart rate dynamics before spontaneous onset of ventricular fibrillation in patients with healed myocardial infarcts. *The American Journal of Cardiology*, 83:880–884, 1999.

[45] M. Nakagawa, T. Ooie, B. Ou, M. Ichinose, N. Takahashi, M. Hara, H. Yonemochi, and T. Saikawa. Gender differences in autonomic modulation of ventricular repolarization in humans. *Journal of Cardiovascular Electrophysiology*, 16:278–284, 2005.

[46] B. Nearing. Analysis of complex T-wave oscillations for prediction of ventricular fibrillation. *Journal of Electrocardiology*, 36:199–203, 2003.

[47] B. Nearing and R. Verrier. Progressive increase in complexity of T-wave oscillations herald ischemia-induced ventricular fibrillation. *Circulation Research*, 91:727–732, 2002.

[48] J. P. Nolan. *Resuscitation Guidelines 2010*. Resuscitation Council (UK), 2010.

[49] J. P. Nolan, J. Soar, D. A. Zideman, D. Biarent, L. L. Bossaert, C. Deakin, R. W. Koster, J. Wyllie, and B. Böttiger. European Resuscitation Council Guidelines for Resuscitation 2010. *Resuscitation*, 81:1219–1451, 2010.

[50] M. A. Peberdy, J. P. Ornato, P. Reynolds, L. R. Thacker, and M. H. Weil. The first documented cardiac arrest rhythm in hospitalized patients with heart failure. *Resuscitation*, 80:1346–1350, 2009.

[51] K. Porthan, M. Viitasalo, A. Jula, and A. Reunanen. Predictive value of electrocardiographic QT interval and T-wave morphology parameters for all-cause and cardiovascular mortality in a general population sample. *Heart Rhythm*, 6:1202–1208, 2009.

[52] E. Pruvot, G. Thonet, J. M. Vesin, G. Van-Melle, K. Seidl, H. Schmidinger, J. Brachmann, W. Jung, E. Hoffmann, R. Tavernier, M. Block, A. Podczeck, and M. Fromer. Heart rate dynamics at the onset of ventricular tachyarrhythmias as retrieved from implantable cardioverter-defibrillators in patients with coronary artery disease. *Circulation*, 101:2398–2404, 2000.

[53] D. Rakić, Z. Rumboldt, V. Carević, J. Bagatin, S. Polić, N. Pivac, and R. Avelini-Perković. In-hospital cardiac arrest and resuscitation outcomes: rationale for sudden cardiac death approach. *Croatian Medical Journal*, 46:907–912, 2005.

[54] P. M. Rautaharju, B. Surawicz, and L. S. Gettes. AHA/ACCF/HRS Recommendations for the Standardization and Interpretation of the Electrocardiogram. Part IV: The ST Segment, T and U Waves, and the QT interval. *Journal of the American College of Cardiology*, 53:982–991, 2009.

[55] M. J. Reed, C. E. Robertson, and P. S. Addison. Heart rate variability measurements and the prediction of ventricular arrhythmias. *QJM : monthly journal of the Association of Physicians*, 98:87–95, 2005.

[56] M. Rubart and D. P. Zipes. Mechanisms of sudden cardiac death. *Journal of Clinical Investigation*, 115:2305–2315, 2005.

[57] M. Sachdev, B. J. Fetics, S. Lai, D. Dalal, J. Insel, and R. D. Berger. Failure in short-term prediction of ventricular tachycardia and ventricular fibrillation from continuous electrocardiogram in intensive care unit patients. *Journal of Electrocardiology*, 43:400–407, 2010.

[58] J. E. Saffitz. The pathology of sudden cardiac death in patients with ischemic heart disease–arrhythmology for anatomic pathologists. *Cardiovascular Pathology*, 14:195–203, 2005.

[59] C. Sandroni, G. Ferro, S. Santangelo, F. Tortora, L. Mistura, F. Cavallaro, A. Caricato, and M. Antonelli. In-hospital cardiac arrest: survival depends mainly on the effectiveness of the emergency response. *Resuscitation*, 62:291–297, 2004.

[60] C. Sandroni, J. Nolan, F. Cavallaro, and M. Antonelli. In-hospital cardiac arrest: incidence, prognosis and possible measures to improve survival. *Intensive Care Medicine*, 33:237–245, 2007.

[61] D. Sato, L-H. Xie, A. Sovari, D. X. Tran, N. Morita, H. Karagueuzian, A. Garfinkel, J. N. Weiss, and Z. Qu. Synchronization of chaotic early afterdepolarizations in the genesis of cardiac arrhythmias. *Proceedings of the National Academy of Sciences*, 106:2983–2988, 2009.

[62] V. Shusterman, B. Aysin, K. P. Anderson, and A. Beigel. Multidimensional rhythm disturbances as a precursor of sustained ventricular tachyarrhythmias. *Circulation Research*, 88:705–712, 2001.

[63] V. Shusterman, B. Aysin, V. Gottipaty, R. Weiss, S. Brode, D. Schwartzman, and K. P. Anderson. Autonomic nervous system activity and the spontaneous initiation of ventricular tachycardia. ESVEM Investigators. Electrophysiologic Study Versus Electrocardiographic Monitoring Trial. *Journal of the American College of Cardiology*, 32:1891–1899, 1998.

[64] V. Shusterman, B. Aysin, R. Weiss, S. Brode, V. Gottipaty, D. Schwartzman, and K. P. Anderson. Dynamics of low-frequency R-R interval oscillations preceding spontaneous ventricular tachycardia. *American Heart Journal*, 139:126–133, 2000.

[65] V. Shusterman, A. Goldberg, and B. London. Upsurge in T-wave alternans and nonalternating repolarization instability precedes spontaneous initiation of ventricular tachyarrhythmias in humans. *Circulation*, 113:2880–2887, 2006.

[66] V. Shusterman, R. Lampert, and B. London. The many faces of repolarization instability: which one is prognostic? *Journal of Electrocardiology*, 42:511–516, 2009.

[67] S. Sicouri and C. Antzelevitch. Sudden cardiac death secondary to antidepressant and antipsychotic drugs. *Expert Opinion on Drug Safety*, 7:181–194, 2008.

[68] E. Skogvoll and T. Nordseth. The early minutes of in-hospital cardiac arrest: shock or CPR? A population based prospective study. *Scandinavian Journal of Trauma, Resuscitation and Emergency Medicine*, 16:1–11, 2008.

[69] G. B. Smith. In-hospital cardiac arrest: Is it time for an 'in-hospital chain of prevention'? *Resuscitation*, 81:1209–1211, 2010.

[70] T. W. Smith and M. E. Cain. Sudden cardiac death: epidemiologic and financial worldwide perspective. *Journal of Interventional Cardiac Electrophysiology*, 17:199–203, 2006.

[71] K. G. Spearpoint, C. P. McLean, and D. A. Zideman. Early defibrillation and the chain of survival in 'in-hospital' adult cardiac arrest; minutes count. *Resuscitation*, 44:165–169, 2000.

[72] A. Sridhar, Y. Nishijima, D. Terentyev, R. Terentyeva, R. Uelmen, M. Kukielka, I. M. Bonilla, G. A. Robertson, S. Györke, G. E. Billman, and C. A. Carnes. Repolarization abnormalities and afterdepolarizations in a canine model of sudden cardiac death. *American Journal of Physiology Regulatory, Integrative and Comparative Physiology*, 295:1463–1472, 2008.

[73] L. Sörnmo and P. Laguna. *Bioelectrical Signal Processing in Cardiac and Neurological Applications*. Elsevier, 2005.

[74] P. K. Stein, D. Yanez, P. P. Domitrovich, J. Gottdiener, R. Kronmal, and P. Rautaharju. Heart rate variability is confounded by the presence of erratic sinus rhythm. *Computers in Cardiology*, 29:669–672, 2002.

[75] S. Suraseranivongse, T. Chawaruechai, P. Saengsung, and C. Komoltri. Outcome of cardiopulmonary resuscitation in a 2300-bed hospital in a developing country. *Resuscitation*, 71:188–193, 2006.

[76] G. F. Tomaselli and D. P. Zipes. What causes sudden death in heart failure? *Circulation Research*, 95:754–763, 2004.

[77] G. J. Tortora and B. H. Derrickson. *Principles of Anatomy and Physiology*. John Wiley and Sons, 11th edition, 2006.

[78] B. H. Van Huysduynen, C. A. Swenne, H. M. Draisma, M. L. Antoni, H. Van De Vooren, E. E. Van Der Wall, and M. J. Schalij. Validation of ECG indices of ventricular repolarization heterogeneity: a computer simulation study. *Journal of Cardiovascular Electrophysiology*, 16:1097–1103, 2005.

[79] T. Vybiral, D. H. Glaeser, and A. L. Goldberger. Conventional heart rate variability analysis of ambulatory electrocardiographic recordings fails to predict imminent ventricular fibrillation. *The American Journal of Cardiology*, 22:557–565, 1993.

[80] N. Wessel, C. Ziehmann, J. Kurths, U. Meyerfeldt, A. Schirdewan, and A. Voss. Short-term forecasting of life-threatening cardiac arrhythmias based on symbolic dynamics and finite-time growth rates. *Physical Review E*, 61:733–739, 2000.

[81] J. Xue, W. Gao, Y. Chen, and X. Han. Study of repolarization heterogeneity and electrocardiographic morphology with modeling approach. *Journal of Electrocardiology*, 41:581–587, 2008.

[82] J. Xue, W. Gao, Y. Chen, and X. Han. Identify drug-induced T wave morphology changes by a cell.to-electrocardiogram model and validation with clinical trial data. *Journal of Electrocardiology*, 42:534–542, 2009.

[83] J. Xue, C. Graff, J.K. Kanters, E. Toft, and J. J. Struijk. New descriptors of T-wave morphology are independent of heart rate. *Journal of Electrocardiology*, 41:557–561, 2008.

[84] F. Yap and K. Lam. In-hospital arrest. `http://www.aic.cuhk.edu.hk/web8/Cardiac\%20arrest\%20in\%20hospital.htm`, 2006.

[85] W. Zareba and A. De Luna. QT dynamics and variability. *Annals of Noninvasive Electrocardiology*, 10:256–262, 2005.

[86] J. J. Zhuang, X. B. Ning, S. Du, Z. Wang, C. Huo, X. Yang, and A. Fan. Nonlinear short-term heart rate variability prediction of spontaneous ventricular tachyarrhythmia. *Chinese Science Bulletin*, 53:2446–2453, 2008.

Appendix A: Algorithms

Isoelectric point search and removal of baseline wandering are the most essential parts in the preprocessing of an ECG signal. Moreover, the performance of the baseline removal algorithm is critically dependent on the accuracy of the isoelectric point determination. In this appendix, the algorithms responsible of these crucial preprocessing steps are described and derived.

The isoelectric point search algorithm (see Alg. A1) uses the fiducial points (locations of QRS complexes) calculated using the GE EK-Pro software [1]. Since the QRS complex detector finds the position of each complex around maximal signals amplitude, the found QRS complex positions are good starting points in isoelectric position search. Our algorithm goes through one channel of ECG at a time (input parameter x) locating the isoelectric position preceding each fiducial point (input parameter fp). The algorithm has the following two step search strategy: try to find position where the sign of derivative of the signal changes in interval to search for Q peak (determined by the parameter QS). The second step starts at Q wave or, if not found, at QS samples before the fiducial point. In this step, the algorithm goes back PQS samples calculating deviation from a flatness interval mean. Minimal deviation from the interval mean means maximally flat signal and central point of it is stored and used as an estimate for the isoelectric position.

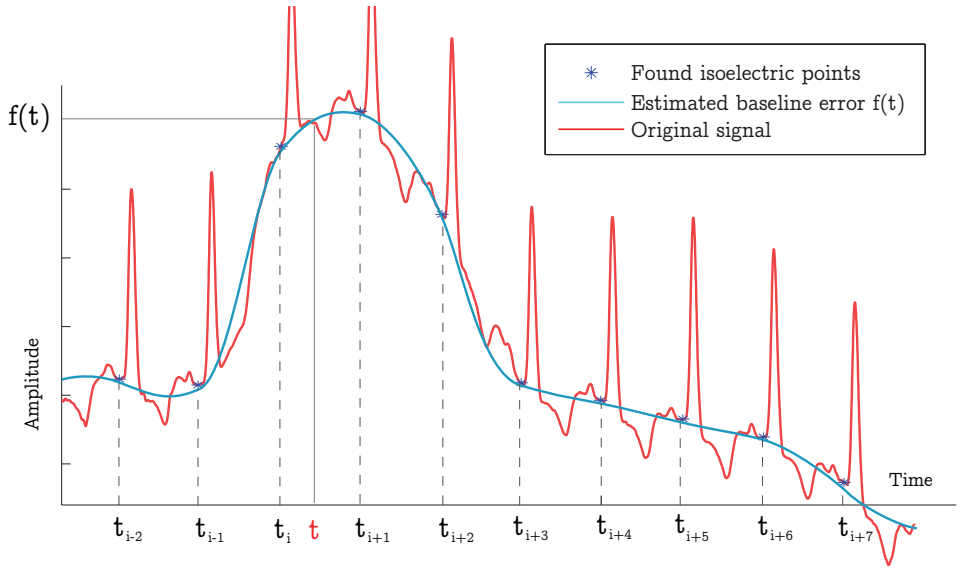

Figure A1: *Baseline wandering is removed from the ECG signal using cubic spline polynomial fitting.*

Removal of the baseline wander of the signal can be considered as a problem of finding the wandering signal from the raw ECG data. Since the isoelectric points can be assumed to have zero amplitude, the baseline signal must pass these points. The found ith isoelectric positions is denoted as t_i and corresponding baseline wander value at that position is denoted by using the baseline wander signal $f(t_i)$ (see Fig.

Algorithm A1 Search of isoelectric point

procedure $[I,z]$ = FindIsoelectricPoint(x,fp)
    Constants:
    f_s: Sampling frequency
    $\Delta T = 1/f_s$: Time step
    T_Q: Interval to search for Q peak
    $QS = T_Q/\Delta T$: Samples to search for Q peak
    T_{PQ}: Interval to search for PQ sement
    $PQS = T_{PQ}/\Delta T$: Samples to search for PQ
    T_f: Flatness interval
    $L = T_f/\Delta T$: Samples for flatness interval
    Input:
    x: ECG data
    fp: Fiducial point
    Output:
    z: Estimated isoelectric level
    I: Position of the isoelectric level
    Code:
    $k = fp/\Delta T$;
    sp =sign$(x(k-2) - x(k))$;
    $k = k - 2$;
    s =sign$(x(k-1) - x(k))$;
    while $(s \neq 0)\&(s = sp)\&(fp/\Delta T - k < QS)$ **do**
        $sp = s$;
        $k = k - 1$;
        s =sign$(x(k-1) - x(k))$;
    end while
    $k = k - 2$;
    $z = \frac{1}{L}\sum_{l=-L/2}^{L/2} x(k+l)$;
    $I = \Delta T$;
    $minabsdev = \sum_{l=-L/2}^{L/2} |x(k+l) - z|$;
    for $m = k-1 : k - PQS + 2$ **do**
        $mean = \frac{1}{L}\sum_{l=-L/2}^{L/2} x(m+l)$;
        $absdev = \sum_{l=-L/2}^{L/2} |x(m+l) - mean|$;
        if $absdev < minabsdev$ **then**
            $z = mean$;
            $I = m\Delta T$;
            $minabsved = absdev$;
        end if
    end for
end procedure

A1. The next step is to use $f(t_i)$, $f(t_{i+1})$ and $f(t_{i+2})$ to estimate values of $f(t)$ in the interval $t \in [t_i\ t_{i+1}]$. The estimation is done by fitting a polynomial to pass the isoelectric points. Arbitrary shaped baseline wander can be expressed around t_i by using the Taylor approximation. When three derivatives is included we get the following formula

$$f(t_i + \delta t) = f(t) \approx f(t_i) + f'(t_i)(t - t_i) + \frac{f''(t_i)}{2}(t - t_i)^2 + \frac{f'''(t_i)}{6}(t - t_i)^3, \quad \text{(A1)}$$

Where $f(t_i) = x(t_i)$ is just the ECG signal value at the isoelectric point. The estimate for the first derivative is calculated as a linear slope between adjacent points

$$f'(t_i) = \frac{x(t_{i+1}) - x(t_i)}{t_{i+1} - t_i}. \quad \text{(A2)}$$

We still need the to know the second and third derivatives before we can compute Eq. A1. In order to get these values we need to consider the following Taylor approximations when $t = t_{i+1}$. Thus, we get

$$f(t_{i+1}) \approx f(t_i) + f'(t_i)(t_{i+1} - t_i) + \frac{f''(t_i)}{2}(t_{i+1} - t_i)^2 + \frac{f'''(t_i)}{6}(t_{i+1} - t_i)^3, \quad \text{(A3)}$$

and

$$f'(t_{i+1}) \approx f'(t_i) + f''(t_i)(t_{i+1} - t_i) + \frac{f'''(t_i)}{2}(t_{i+1} - t_i)^2. \quad \text{(A4)}$$

Again, $f(t_{i+1}) = x(t_{i+1})$ and the first derivative is

$$f'(t_{i+1}) = \frac{x(t_{i+2}) - x(t_{i+1})}{t_{i+2} - t_{i+1}}. \quad \text{(A5)}$$

Now, one can solve $f''(t_i)$ and $f'''(t_i)$ from Eq. A3 and A4. The formulae are

$$f''(t_i) = \frac{6(f(t_{i+1}) - f(t_i))}{\Delta t_{i1}^2} - \frac{2(2f'(t_i) + (f(t_{i+2}) - f(t_i))/(\Delta t_{i2}))}{\Delta t_{i1}} \quad \text{(A6)}$$

and

$$f'''(t_i) = \frac{12(f(t_{i+1}) - f(t_i))}{\Delta t_{i1}^3} - \frac{6(f'(t_i) + (f(t_{i+2}) - f(t_i))/(\Delta t_{i2}))}{\Delta t_{i1}^2}, \quad \text{(A7)}$$

where $\Delta t_{ij} = t_{i+j} - ti$. Now values for $f(t)$ can be calculated and the procedure can be applied for the next interval.

Appendix B: Database

This appendix contains detailed information of the database used in this study. See Tab. B1 to see a complete list of patients constituting the study groups, B2 to decode the abbreviated words in the list and the original study by Sahdev et.al [57] where the database is described.

Patients who were admitted to the cardiac intensive care unit (CCU) of either the Johns Hopkins Hospital or Good Samaritan Hospital in Baltimore were candidates for the study. Patients in coronary care unit (CCU) who experienced an event of sustained (30 seconds) monomorphic ventricular tachycardia (MVT), polymorphic ventricular tachycardia (PVT), or ventricular fibrillation (VF) were identified. Patients with a minimum of 8 hours of ECG data before the event constituted the study group. In addition, a group of patients who did not experience any arrhythmic event while in the CCU was identified at random to serve as a control population. For controls, a random point in time was taken as the "event": and 8 hours of ECG leading up to this time point was used for analysis. Specific demographic information including presenting diagnosis, administration of β-blockers or other antiarrhythmic drugs during the monitored period, and other related conditions were obtained by chart review.

Electrocardiographic tracings were downloaded from the specialized intensive care unit MARS telemetry system (GE Medical Systems, Milwaukee, WI) that is capable of retaining up to 28 hours of multi-lead ECG tracings, filtered between 0.3 and 50 Hz and sampled at 120 Hz, and transferred to a computer for analysis. Each tracing was considered by event type – MVT, PVT, VF, or control. Noisy ECG recordings due to motion artifact or electrical noise were excluded from analysis. Patients with intermittent bundle-branch block, atrial fibrillation, or excessive background noise (N10% of record) were excluded because of difficulty in analyzing their data. Patients with more than one major event during the 12-hour period were also excluded to avoid ambiguity in the time of end point.

Pat	gend/race	age	event	disease	B-blocker	antiarrhy.	valid	group
JH 50	w/m	57	3	1a	0	0	0	1
JH 80	b/f	49	2m	5	0	0	0	1
JH 120	b/f	73	2m	2a	0	0	1	1
JH 128	w/f	87	2m	1a	0	1	1	1
JH 167	w/m	66	2p	5	0	1	0	1
JH 191	o/f	72	2m	?	0	0	0	1
JH 69	w/m	48	2m	2a	0	0	0	1
JH 84	w/f	76	2m	1a	0	1	0	1
GS 5	w/f	74	3	2a	0	0	1	1
gs 24	b/f	78	-	-	0	0	1	1
JH 78	b/f	67	-	2a	1	0	0	1
JH 14	a/f	70	-	2a	0	1	1	1
jh 141	w/m	40	-	2b	0	0	1	1
jh 184	w/m	53	-	2a	1	1	1	1
JH 29	b/m	65	1m	1a	1	1	0	2
JH 42	w/m	60	1m	1a	0	0	0	2
JH 66	w/m	80	1m	1a	0	1	1	2
JH 77	w/m	64	1p	1a	0	1	0	2
JH 153	w/m	69	1m	1a	1	0	1	2
GS 4	b/f	47	1p	4	1	1	0	2
gs 6	b/m	69	1p	2a			1	2
gs 1	b/m	63	1p	2b	0	1	1	2
JH 118	w/m	53	1p	1a	1	1	1	2
JH 24	b/f	73	0	2a	1	1	0	3
JH 25	w/m	55	0	1a	0	1	0	3
JH 28	w/m	36	0	2b	0	0	0	3
JH 39	b/m	48	0	2a	0	0	0	3
JH 45	w/m	59	0	1a	1	0	0	3
JH 57	u/f	80	0	1a	1	0	0	3
JH 58	w/m	66	0	1b	1	0	0	3
JH 59	b/f	47	0	1b	1	0	0	3
JH 62	w/m	83	0	1a	0	1	0	3
JH 76	w/m	51	0	1a	1	0	0	3
JH 91	w/f	56	0	4	0	0	0	3
JH1 03	w/f	60	0	2a	1	0	0	3
JH 107	w/f	83	0	2a	0	1	0	3
JH 140	a/f	76	0	1b	0	0	0	3
JH 169	b/m	43	0	5	0	0	0	3

Pat	gend/race	age	event	disease	B-blocker	antiarrhy.	valid	group
jh 195	w/f	70	0	1a	0	0	1	3
gs 28	w/m	79	0	1a	0	1	1	3
jh 198	w/m	56	0	1a	0	0	1	3
jh 171	b/f	42	0	1a	1	0	1	3
jh 165	o/m	38	0	1a	1	0	1	3
jh 151	w/m	65	0	1a	0	0	1	3
jh 144	b/m	23	0	2b	1	0	1	3
JH 119	w/m	40	0	1a	0	0	1	3
JH 117	w/m	71	0	1a	1	0	1	3
JH 111	w/f	45	0	1a	0	1	1	3
JH 94	w/f	73	0	1a	0	1	1	3
JH 86	b/m	55	0	2a	1	0	1	3
JH 72	b/f	65	0	1b	1	0	1	3
JH 51	w/m	56	0	1a	1	1	1	3
JH 47	w/m	64	0	1b	0	0	1	3
JH 23	a/f	60	0	1a	1	0	1	3
jh 190	b/m	68	0	1a	1	1	1	3
JH 45	w/m	59	0	1a	1	1	1	3
JH 93	b/m	37	0	2b	1	1	1	3
JH 98	w/m	66	0	2a	1	0	1	3
JH 122	w/f	78	0	1b	1	1	1	3
JH 124	w/f	65	0	1a	1	1	1	3

Table B1: *Details of the database used in this thesis. See Tab. B2 for description of the codes.*

Code	Explanation
Disease	
1a	CAD+AMI
1b	CAD+Angina Pectoris
1c	CAD+OMI
2a	Ischemic Dilated Cardiomyopathy
2b	Non-ischemic Dilated Cardiomyopathy
2c	Hypertrophic Carediomyopathy
3	Valve Disease
4	Primary Electrophysiological Event
5	Unknown
Rhythm	
0	No arrhythmia
1m	NSVT (< 30 sec) , monomorphic
1p	NSVT, poly
2m	Sustained VT, monomorphic
2p	Sustained VT, polymorphic
3	VF
4	Arrest
5	Other
Group	
1	Sustained VT/VF
2	Non sustained VT/VF
3	Control
Race/Gender	
w	White
b	African American
a	Asian
o	Other
u	Unknown
m	Male
f	Female

Table B2: *Codes of the Tab. B1. CAD=coronary artery disease, AMI=acute myocardial infarction, OMI=oclusive myocardial infarction, NSVT=non sustained ventricular tachycardia, VT=ventricular tachycardia, VF=ventricular fibrillation.*